Tampere University

Arttu Halonen

NUMERICAL MODELLING OF HEAT LOSSES AND ECONOMIC OPTIMISATION OF INSULATION THICKNESS IN PROCESS INDUSTRY PIPELINES

Faculty of Engineering and Natural Sciences
Master of Science Thesis
February 2020

ABSTRACT

Arttu Halonen: Numerical modelling of heat losses and economic optimisation of insulation thickness in process industry pipelines
Master of Science Thesis
Tampere University
Environmental and Energy Engineering
February 2020

All over the world, fluids at varying temperatures are transported in process industry plants using pipes. The temperature difference between the fluid and its surroundings drives heat transfer, causing heat loss in the fluid. To maintain the desired temperature and phase of the fluid, as specified by the process, the heat loss can be counteracted by providing additional heating or cooling using a heat exchanger, and by mitigating the rate of heat transfer using pipe insulation made of materials with low thermal conductivity. The capital costs of the heat exchangers and insulation as well as the operational costs of heating or cooling can be minimised by optimising the insulation thickness of pipelines, leading to cost savings over the lifetime of the plant.

In this thesis, a fast, computer-assisted method of evaluating heat loss and economically optimising insulation thickness in process industry pipes is presented. The method is implemented as a computer program as part of an existing plant design software solution, Vertex G4Plant. The calculation program evaluates the heat loss in a pipe, based on parameters acquired from user input, using a numerical, iterative, and implicit form of an analytical solution for heat loss in a pipe. Based on the price of energy, the price of insulation, and economic parameters provided as user input, the program calculates and minimises the annual cost caused by the heat loss and the annuity of the investment cost of insulation.

The heat loss calculation model is constructed from a control volume approach, discretising an analytical solution into a series of shorter sections, which are then consecutively solved numerically. For each section, the analytical solution is applied using re-evaluated material properties and surface temperatures. For increased accuracy and stability, an implicit form of the analytical solution is used, where the outlet temperature of the calculation section affects the solution, and the numerical solution is iteratively continued until the outlet temperature converges to a stable result. The conductive heat transfer through the pipe wall and the insulation, and the radiative heat transfer on the exterior are evaluated using analytical solutions, whereas well-established correlations presented in the literature are used for evaluating the convective heat transfer on the interior and exterior surfaces. The insulation thickness is economically optimised by evaluating the total annual costs of the energy and the annuity of the capital cost of insulation as a function of the insulation thickness. The lone local and global minimum of the total cost function is numerically solved using a simple gradient-descent method, solving the optimal value of the variable insulation thickness.

The insulation thicknesses optimised with the calculation program are compared with insulation thicknesses suggested by the Finnish standard SFS 3977. The comparison suggests that in certain cases, lower total costs over the lifetime of a pipeline could be achieved by using the insulation thickness suggested by the calculation program presented in this thesis, instead of the insulation thickness suggested by the standard. Potential cost savings of up to 7% of the total heating and insulation costs of the pipeline are demonstrated through case examples, which compare the insulation thickness suggested by SFS 3977 with the optimal economical insulation thickness optimised using the calculation program developed as part of this thesis.

Keywords: heat loss, pipes, insulation, economic optimisation, numerical modelling

The originality of this thesis has been checked using the Turnitin OriginalityCheck service.

TIIVISTELMÄ

Arttu Halonen: Prosessiteollisuuden putkilinjojen lämpöhäviön numeerinen mallinnus ja eristepaksuuden taloudellinen optimointi
Diplomityö
Tampereen yliopisto
Ympäristö- ja energiatekniikka
Helmikuu 2020

Kaikkialla maailmassa eri lämpötiloissa olevia fluideja kuljetetaan putkilla prosessiteollisuuden laitoksissa. Fluidin ja ympäristön välinen lämpötilaero johtaa lämmönsiirtoon, aiheuttaen lämpöhäviötä fluidissa. Prosessin määrittelemien fluidin halutun lämpötilan ja olomuodon ylläpitämiseksi lämpöhäviötä voidaan korvata järjestämällä ylimääräistä lämmitystä tai jäähdytystä käyttämällä lämmönvaihtimia ja heikentämällä lämmönsiirtoa käyttämällä alhaisen lämmönjohtavuuden materiaaleja putkieristeenä. Lämmönvaihtimien ja eristyksen pääomakustannuksia sekä lisälämmityksen tai -jäähdytyksen käyttökustannuksia voidaan minimoida optimoimalla putkilinjojen eristepaksuutta, jolloin saavutetaan kustannussäästöjä laitoksen eliniän ajalta.

Tässä opinnäytetyössä esitellään nopea, tietokoneavusteinen menetelmä prosessiteollisuuden putkilinjojen lämpöhäviön laskemiseen ja eristepaksuuden taloudelliseen optimointiin. Menetelmä on toteutettu tietokoneohjelmana osana olemassa olevaa laitossuunnitteluohjelmistoa Vertex G4Plant. Laskentaohjelma arvioi käyttäjän syöttämien arvojen pohjalta putkessa tapahtuvan lämpöhäviön käyttäen putken lämpöhäviön analyyttisen ratkaisun numeerista, iteratiivista ja implisiittistä muotoa. Energian hinnan, eristeen hinnan sekä käyttäjän syöttämien taloudellisten arvojen perusteella ohjelma laskee ja minimoi lämpöhäviöstä ja eristyksen investointikustannuksen annuiteetista koostuvat vuosittaiset kokonaiskustannukset.

Lämpöhäviölaskentamalli on rakennettu kontrollitilavuusmenetelmän pohjalta diskretoimalla analyyttinen ratkaisu sarjaksi lyhyempiä osioita, jotka ratkaistaan numeerisesti järjestyksessä. Jokaiselle osiolle sovelletaan analyyttistä ratkaisua käyttäen uudelleen arvioituja aineominaisuuksia ja pintalämpötiloja. Tarkkuuden ja vakauden lisäämiseksi laskennassa käytetään analyyttisen ratkaisun implisiittistä muotoa, jossa laskentaosion ulostulolämpötila vaikuttaa ratkaisuun, ja numeerista laskentaa jatketaan iteratiivisesti, kunnes ulostulolämpötila vakiintuu vakaaseen tulokseen. Lämmönsiirto johtumalla putkiseinämän ja eristemateriaalin läpi sekä säteilemällä putken ulkopinnalla arvioidaan käyttäen analyyttisiä ratkaisuja, kun taas putken sisä- ja ulkopintojen konvektiivisen lämmönsiirron ratkaisemiseen käytetään kirjallisuudessa esitettyjä yleisesti hyväksyttyjä korrelaatioita. Eristepaksuus optimoidaan taloudellisesti arvioimalla energian vuosikustannuksen ja eristyksen pääomakustannuksen annuiteetin vuosittaisia kokonaiskustannuksia eristepaksuuden funktiona. Kokonaiskustannusfunktion ainoa paikallinen ja globaali minimikohta ratkaistaan numeerisesti käyttäen yksinkertaista gradienttilaskeutumismenetelmää, jolla ratkaistaan muuttujana toimivan eristepaksuuden optimiarvo.

Laskentaohjelmalla optimoituja eristepaksuuksia verrataan suomalaisen standardin SFS 3977 suosittelemiin eristepaksuuksiin. Vertailun mukaan tietyissä tapauksissa voidaan saavuttaa pienempiä kokonaiskustannuksia putkilinjan eliniän ajalta käyttämällä tässä opinnäytetyössä esitellyn laskentaohjelman suosittelemaa eristepaksuutta standardissa suositellun eristepaksuuden sijaan. Saavutettavissa olevia jopa 7% kustannussäästöjä putkilinjan lämmityksen ja eristyksen kokonaiskustannuksissa esitellään esimerkkitapauksilla, joissa verrataan standardissa SFS 3977 suositeltua eristepaksuutta tässä opinnäytetyössä kehitetyllä laskentaohjelmalla taloudellisesti optimoituun eristepaksuuteen.

Avainsanat: lämpöhäviö, putket, eristys, taloudellinen optimointi, numeerinen mallinnus

Tämän julkaisun alkuperäisyys on tarkastettu Turnitin OriginalityCheck -ohjelmalla.

PREFACE

This Master of Science thesis was written in cooperation with and under the employment of Vertex Systems. I wish to express my sincerest gratitude to Timo Tulisalmi from Vertex Systems, for providing me with the opportunity to work on my thesis at the company. I also wish to give my thanks to my thesis supervisor from Vertex Systems, Mikko Rupponen, for his support and encouragement throughout the work. I am extremely grateful for the supportive low-pressure environment in which I was allowed to work on my thesis. For this I wish to extend my thanks to the Plant team and all my other co-workers at Vertex Systems.

I am also deeply grateful to my thesis supervisor from Tampere University, Niko Niemelä, for the continued support and insightful feedback through regular meetings, amidst their busy schedule. I also wish to sincerely thank Dr. Henrik Tolvanen for asking hard questions and helping me keep sight of the main objective of the thesis. Their combined support has been immeasurably valuable throughout the process of working on this thesis.

Finally, I want to give my thanks to my parents for their endless love and support, and to my friends for their support and encouragement. Lastly, I want to give my heartfelt thanks to Essi, for being there for me, and for helping me take my mind off work at times.

Tampere, 28th February 2020

Arttu Halonen

CONTENTS

LIST OF FIGURES

LIST OF TABLES

LIST OF SYMBOLS AND ABBREVIATIONS

Acronyms		
CIWH	condensation induced water hammer	
DN	nominal diameter	
SFS	Suomen Standardoimisliitto, Finnish Standards Association	
VDI	Verein Deutscher Ingenieure, The Association of German Engineers	
Greek symbols		**Unit**
α	thermal diffusivity	m^2/s
β	thermal volume coefficient	$1/\mathrm{K}$
ϵ	emissivity	$-$
μ	dynamic viscosity	$\mathrm{Pa} \cdot \mathrm{s}$
ν	kinematic viscosity	m^2/s
π	ratio of the perimeter and diameter of a circle	$-$
ρ	density	kg/m^3
σ	Stefan-Boltzmann constant	$\mathrm{W}/(\mathrm{m}^2 \cdot \mathrm{K}^4)$
Latin symbols		**Unit**
A	area	m^2
dA	infinitesimally small area	m^2
$A_{c,f}$	cross-sectional area of pipe flow	m^2
$a_{n/i}$	annuity factor	$-$
c_p	specific heat at constant pressure	$\mathrm{J}/(\mathrm{kg} \cdot \mathrm{K})$
C_a	annual payment	€
C_e	annual energy cost	€/m
$C_{e,th}$	price of thermal energy	€/MWh
C_f	future payment	€
C_i	initial investment	€
C_{ins}	insulation cost	€/m
C_p	present day value	€

$C_{tot,a}$	total annual costs	€
D	outer diameter	m
D_h	hydraulic diameter	m
d	inner diameter	m
$\mathcal{F}$	transfer factor	$-$
f	Darcy friction factor	$-$
Gr	Grashof number	$-$
g	gravitational acceleration	$\mathrm{m/s^2}$
h	convective heat transfer coefficient	$\mathrm{W/(m^2 \cdot K)}$
$h_{conv,o}$	heat transfer coefficient of external convection	$\mathrm{W/(m^2 \cdot K)}$
h_i	heat transfer coefficient at pipe interior surface	$\mathrm{W/(m^2 \cdot K)}$
h_o	heat transfer coefficient at exterior surface of pipe or insulation	$\mathrm{W/(m^2 \cdot K)}$
h_{rad}	radiative heat transfer coefficient	$\mathrm{W/(m^2 \cdot K)}$
i	rate of interest	$-$
k	insulation factor of equipment	$-$
k	thermal conductivity	$\mathrm{W/(m \cdot K)}$
k_f	thermal conductivity of fluid	$\mathrm{W/(m \cdot K)}$
k_{ins}	thermal conductivity of insulation	$\mathrm{W/(m \cdot K)}$
k_{pipe}	thermal conductivity of pipe wall	$\mathrm{W/(m \cdot K)}$
L	length	m
L_c	characteristic length	m
$\dot{m}$	mass flow	$\mathrm{kg/s}$
Nu	Nusselt number	$-$
Nu_d	Nusselt number with pipe inner diameter as characteristic length	$-$
$\mathrm{Nu}_{laminar}$	Nusselt number in the laminar regime	$-$
$\mathrm{Nu}_{transitional}$	Nusselt number in the transitional regime	$-$
$\mathrm{Nu}_{turbulent}$	Nusselt number in the turbulent regime	$-$
$\overline{\mathrm{Nu}}$	average Nusselt number	$-$
n	lifetime	a
P	perimeter	m

P_w	wetted perimeter	m
Pr	Prandtl number	$-$
p	pressure	Pa
p	annual increase of thermal energy price	$-$
$\dot{Q}$	heat flow	W
$\dot{Q}_{tot,L}$	heat loss flow per unit length	$\mathrm{W/m}$
q	heat flux	$\mathrm{W/m^2}$
R	heat transfer resistance	$\mathrm{K/W}$
R_{cond}	conductive heat transfer resistance	$\mathrm{K/W}$
R_{conv}	convective heat transfer resistance	$\mathrm{K/W}$
R_{rad}	radiative heat transfer resistance	$\mathrm{K/W}$
R_{tot}	total heat transfer resistance	$\mathrm{K/W}$
$R_{o,tot}$	total heat transfer resistance between pipeline exterior surface and surroundings	$\mathrm{K/W}$
Ra	Rayleigh number	$-$
Ra_d	Rayleigh number with pipe inner diameter as characteristic length	$-$
Ra_{max}	upper limit of Rayleigh number for transitional flow	$-$
Ra_{min}	lower limit of Rayleigh number for transitional flow	$-$
Re	Reynolds number	$-$
Re_d	Reynolds number with pipe inner diameter as characteristic length	$-$
r	radius	m
r_i	radius of pipe inner surface	m
r_{ins}	exterior radius of insulation	m
r_o	radius of pipe outer surface	m
T	temperature	K
ΔT	temperature difference	K
dT	infinitesimally small temperature difference	K
T_f	temperature of bulk fluid	K
T_i	temperature at pipe inner surface	K

T_{in}	temperature at pipe inlet	K
T_{inf}	temperature of surroundings	K
T_m	mean temperature	K
T_o	temperature at pipe outer surface	K
T_{out}	temperature at pipe outlet	K
T_s	surface temperature	K
t	insulation thickness	mm
U	overall heat transfer coefficient	$\mathrm{W}/(\mathrm{m}^2 \cdot \mathrm{K})$
u	thermal energy price factor	$-$
V	mean velocity of internal flow	m/s
V_{ext}	mean velocity of external flow	m/s
x	generic coordinate	m
dx	infinitesimally short length	m

1 INTRODUCTION

The process industry plays a key role as a part of the global infrastructure, enabling countless other industries, services, and products to function by providing fuels, chemicals and other materials necessary in their continuous operation [9]. Everywhere in the process industry, numerous fluid species at vastly different temperatures are transported over short and long distances by pumping them through pipes and pipelines [34]. In order to ensure that the hot fluids remain hot, the cold fluids remain cold, and that steam and vapour flows do not condense, pipes are covered with insulating materials, such as mineral wool, in varying thicknesses [31][33]. In addition to the technical requirements for the properties and condition of the fluid, the investment cost of insulation is justified by the reduction in other costs, mainly those related to counteracting heat loss by reheating or re-cooling the fluid [31].

The selection of the insulation thickness is an optimisation problem, where the total costs of the investment of the insulation and the energy cost of the heat loss are minimised [31]. With the ubiquity of pipes in the process industry, even small improvements in the total lifetime cost of a pipeline can become significant over the lifetime of the process plant, through the combined effect of all the insulated pipes in the plant. In addition to economical motivations, the optimisation of pipe insulation serves environmental purposes as well. As the industry strives to conserve energy and reduce emissions, reducing heat loss to an economically optimal level is a financially safe, and even profitable, method of pursuing environmental goals and following regulations.

In the industry, a common way of determining pipe insulation thickness is by utilising standards and pre-calculated tables, such as the tables of the Finnish standard SFS 3977 [31]. While such standards do provide simple and easy-to-use tools for the different insulation cases mentioned earlier, static, pre-calculated tables are always based on certain assumptions for parameters, such as insulation emissivity, the ambient temperature, and the cost of insulation. Thus, when working with a real-life case that does not fully match the assumptions of the standard table, the designer is forced to either accept the results that may or may not be valid for the task at hand, or to calculate the appropriate insulation thickness themselves. For this purpose, the standard SFS 3977 does also suggest an iterative method for calculating the heat loss and the total cost for the pipe system, including simple correlations for heat transfer coefficients [31].

For determining the economically optimal thickness of pipe insulation, several methods are presented in the literature, as demonstrated by the review article of Kaynakli [18]. Certain works, such as those by Bahadori and Vuthaluru [1][2], favour correlations with non-physical parameters fitted to reported data, instead of calculations based directly on heat transfer theory. A similar trend towards leaning away from heat transfer theory can be seen in the work by Čarnogurská et al. [6] on modelling heat loss in central heat distribution pipe networks. Some more recently published works on the evaluation of economically optimal thickness of pipe insulation, such as Daşdemir et al. [8], do still utilise iterative methods based on heat transfer theory. In addition to simply minimising the total cost of the pipe system over its lifetime, some works, such as Öztürk et al. [30], also consider the loss of exergy in the pipe system as part of the analysis.

In this thesis, an approach to pipe insulation optimisation is proposed where the heat loss in the pipeline and the economically optimal insulation thickness are numerically evaluated using a computer program. As part of this thesis, such a computer program was created and programmed using the C++ programming language. To improve the usability of the optimisation program, the program was implemented into an existing plant design software solution, Vertex G4Plant. The heat loss calculation, on which the insulation thickness optimisation is based, is performed iteratively, such that an implicit form of an analytical solution for the heat loss in the pipe is solved for a short section of pipe at a time, progressing through the whole pipeline.

The overall heat transfer coefficient is evaluated based on convective heat transfer on the interior and exterior of the pipe, heat conduction through the pipe wall and insulation, and radiative heat transfer on the exterior of the pipe. For heat conduction, a simple analytical solution is utilised. Heat radiation is also modelled using an analytical solution, where the pipe or insulation surface is assumed to be a small grey object in a large black environment. For convective heat transfer, due to its complex nature, well-established empirical correlations presented in the literature are used in the absence of analytical solutions. The correlations for internal forced convection are largely based on the work of Gnielinski [12] [14], whereas correlations by Churchill and Chu [7][26] are used for natural external convection.

Pipe insulation thickness is optimised by calculating the heat loss in a pipeline using varying insulation thicknesses, and comparing the total annual costs of the pipeline. The total costs are calculated from the magnitude of the heat loss and the cost of thermal energy, and from the thickness and price of the insulation. The initial investment cost of insulation is converted into an annual cost using an annuity factor, which takes into account the lifetime of the pipeline and the assumed rate of interest.

The calculation program developed as part of this thesis is presented as an alternative to using insulation thickness tables presented in standards such as SFS 3977. To demonstrate the motivations behind this work, case examples are presented, showcasing the potential cost savings brought by using the insulation thickness optimised with the calculation program, instead of the insulation thickness suggested by the standard.

Additionally, the goal of the calculation program is to make it easier for users to take into account the various conditions and variables related to the pipeline when determining the optimal insulation thickness than what is possible with pre-calculated tables in a standard.

The objective of this thesis is to provide answers to the following questions:

1. Which phenomena significantly affect the heat transfer process in fluid flow in a pipe?
2. What methods are most effective in:
    - evaluating the heat loss in a process industry pipeline?
    - optimising pipe insulation from an economic standpoint over its lifetime?
3. How significant cost savings can be achieved by optimising insulation thickness using a software solution compared to standard insulation tables?

2 HEAT TRANSFER IN PIPES

Pipes are ubiquitous in the process industry, where they are used for transporting a great variety of liquid and gaseous fluids over varying distances both indoors and outdoors [34]. Various processes require certain properties and behaviour from the fluids, creating requirements for the temperature of the fluids [34]. Regardless whether the pipe is transporting a fluid hotter or colder than the environment, the fluid will undergo heat transfer with the surroundings, provided that a temperature difference exists between them [35]. In processes with specific requirements for the temperature of the fluid, the heat transfer, often referred to as heat loss, creates undesirable deviation from the specified conditions of the process. In order to design suitable countermeasures against heat loss, such as adding pipe insulation, it is crucial to understand the phenomena that contribute to heat loss in pipes.

On a general level, heat transfer phenomena follow simple and well-understood principles of heat transfer theory, which have been extensively studied and described in literature. Heat transfer is typically divided into three distinct modes: heat conduction, heat convection and heat radiation [26][35]. While heat transfer related to heat conduction and radiation is typically modelled with sufficient accuracy using analytically derived equations, modelling heat convection and its relation to fluid flow often relies on equations derived empirically from experimental test results [35].

This chapter presents the laws and equations of heat transfer theory that are relevant for modelling heat losses in pipes, going into further detail on the three aforementioned modes of heat transfer and how they can be modelled together in the context of a pipeline. Additionally, this chapter discusses the technical and financial consequences of heat losses in an industrial context, and how these consequences can be mitigated using insulation.

2.1 Modes of heat transfer

In this section, different modes of heat transfer are discussed in the context of fluid flows in pipes. Sections 2.1.1, 2.1.2, and 2.1.3 discuss individual modes of heat transfer and present relevant mathematical models, whereas Section 2.1.4 discusses a model with which the combined effect of the different modes of heat transfer can be evaluated.

2.1.1 Heat conduction

Process industry pipe materials are typically metals, due to their vast range of operating temperatures, and high strength against the stress created from internal fluid pressure [15]. Many fluids used in the process industry are also corrosive, and thus special metal grades with high resistance against chemical corrosion are used [24]. However, due to the nature of the metal lattice on the molecular level, metals have characteristically high thermal conductivities compared to other pipe materials [35], such as plastics, which are commonly used in less challenging operating conditions [37]. In order to reduce the rate of heat transfer between the transported fluid and the environment, thermal insulation is commonly used in process industry piping [31]. In pipe insulation, materials with low thermal conductivity, such as mineral wool [33], are used not only to reduce heat loss, but also to protect plant personnel from pipe surfaces of extreme temperatures [31].

On a fundamental level, heat conduction means the transfer of kinetic energy in the form of thermal translational, rotational or vibrational energy on the molecular level in or between solids or fluids [35]. Thus, heat conduction always requires a medium through which heat is transferred, but does not require mass transfer. In the interactions between atoms, molecules, or free electrons in a metal lattice, energy is transferred from higher-energy particles to particles with lower energy [35]. This is in agreement with the second law of thermodynamics, which states that heat is transferred in the direction of decreasing temperature [26].

At a macroscopic scale, one-dimensional heat conduction can be simplified into a mathematical model, where the heat flux q is directly proportional to the negative of the local temperature gradient $\partial T/\partial x$, or in mathematical notation [26][35]

$$q \propto -\frac{\partial T}{\partial x}, \tag{2.1}$$

where heat flux q is defined as the heat flow $\dot{Q}$ over a unit area A, or

$$q = \frac{\dot{Q}}{A}. \tag{2.2}$$

Relation (2.1) is commonly known as Fourier's law of heat conduction, after Jean Baptiste Joseph Fourier, who published the relation in the early 19th century [28][35]. The negative sign on the right-hand side of Relation (2.1) enforces the second law of thermodynamics, so that there is a positive heat flux in the direction of decreasing temperature.

The proportionality between heat flux and the temperature gradient depends on a non-negative material property of the medium, known as thermal conductivity k. With the thermal conductivity, Relation (2.1) can be written as [26][35]

$$q = -k\frac{\partial T}{\partial x} \tag{2.3}$$

for a temperature gradient in the direction of the x coordinate. In the context of cylindrical pipes, it is most often sensible to consider one-dimensional heat conduction radially. Thus, Equation (2.3) can be written as [35]

$$q = -k\frac{\partial T}{\partial r}, \tag{2.4}$$

where r is the radius of the cylindrical pipe. Integrating Equation (2.4), a new equation can be written for the heat flux through the pipe wall with the temperature T and radius r at the inner (subscript i) and outer (subscript o) surfaces of the pipe, such that [35]

$$q = k\frac{T_i - T_o}{\ln(r_o/r_i)}. \tag{2.5}$$

Combining Equations (2.5) and (2.2) gives a heat flow of

$$\dot{Q} = k2\pi L\frac{T_i - T_o}{\ln(r_o/r_i)} \tag{2.6}$$

through the pipe wall for a pipe section of length L.

2.1.2 Heat convection

As the purpose of process industry pipelines is to transport fluids by directing the pressure-gradient-driven flow of the fluid, understanding heat convection on the interior surface of the pipe is an important part in modelling the heat loss in a pipeline. Additionally, the exterior surface of the pipe or the insulation is typically exposed to air, providing another fluid-surface-interface where convective heat transfer can occur between the pipeline and the environment.

Technically heat convection refers to heat transfer through mass transfer, where energy stored in a medium is transported by the movement of the medium [26][35]. Typically heat convection is understood through the flow of a fluid, but a moving solid can also be considered to convect heat [26]. In a larger and more practical context, however, heat convection is also considered to include heat transfer between a solid surface and a flowing fluid, even though such convective heat transfer between a fluid and a surface largely relies also on conduction and radiation in the boundary layer at the interface between the surface and the fluid [26].

As mentioned previously, convective heat transfer is heavily related to fluid flow, which by its very nature is a complex phenomenon. On an abstract level, convective heat transfer can be modelled using an equation known as Newton's law of cooling, which states that [26][35]

$$q = h(T_s - T_f), \tag{2.7}$$

where $h > 0$ is the convective heat transfer coefficient, T_s the temperature of the surface and T_f the temperature of the bulk fluid. The name of the Equation (2.7) suggests the

cooling of the surface, such that the positive direction of the heat flux q is from the surface to the fluid. Thus, heat flux q is positive when the surface temperature T_s is greater than the fluid temperature T_f, and the heat flux is negative in the opposite case. Furthermore, there is no heat flux when the temperatures of the surface and the fluid are equal, showing that the driving force behind the convective heat flux is a temperature difference, similarly to how the driving force behind conductive heat flux is a temperature gradient, or in other words, a temperature difference in a coordinate direction, as presented in Equation (2.3).

The deceptively simple Equation (2.7) models complex fluid flow phenomena using the convective heat transfer coefficient h, the correct evaluation of which is often the most challenging part of a convective heat transfer problem. Due to the complex nature of fluid flow, the convective heat transfer coefficient h is typically solved using a dimensionless group known as the Nusselt number Nu, which in turn is typically solved using empirically derived correlations involving other dimensionless groups [35]. The Nusselt number Nu is defined as [29, see 35]

$$\mathrm{Nu} = \frac{hL_c}{k_f}, \tag{2.8}$$

where h is the convective heat transfer coefficient, L_c is the characteristic length of the system and k_f is the thermal conductivity of the fluid. In the context of cylindrical pipes, the characteristic length is the hydraulic diameter D_h, or [26]

$$L_c = D_h = \frac{4A_{c,f}}{P_w}, \tag{2.9}$$

where $A_{c,f}$ is the cross-sectional area of the flow and P_w is the wetted perimeter of the cross-section. If the flow fully envelops the cylindrical pipe,

$$D_h = \frac{4A_{c,f}}{P_w} = \frac{4\pi r^2}{2\pi r} = 2r = d, \tag{2.10}$$

where r and d are the inner radius and the inner diameter of the pipe, respectively.

Depending on the nature of the fluid flow in the vicinity of the surface, convection is typically divided into two distinct types: forced convection and natural convection [26][35]. Forced convection refers to a situation where the fluid flow is propagated by some external force or factor, such as a pump, blower or wind [35]. In natural convection, sometimes also referred to as free convection, the fluid flow is induced in the otherwise stationary fluid by buoyancy effects created typically by temperature differences in the bulk fluid and the boundary layer [26][35]. Process industry pipes typically feature both forced and natural convection. The internal flow of the process medium promotes forced convective heat transfer at the inside surface of the pipe, whereas the typically mostly stationary air surrounding the outside of the pipe or its insulation promotes natural convective heat transfer. In the case of heavy air conditioning for indoor pipes or wind for pipes outdoors, the convective heat transfer on the pipe exterior can also have properties of forced convection.

As mentioned earlier, evaluating the Nusselt number for a specific case relies on empirically derived correlations. These correlations typically utilise additional dimensionless groups, some of which are specific to either forced or natural convection. On a conceptual level, forced convection correlations for the Nusselt number typically depend on the Reynolds number Re and the Prandtl number Pr, whereas natural convection correlations depend on the Grashof number Gr as well as the Prandtl number Pr [35]. More concisely, this can be expressed as [35]

$$\begin{aligned} \mathrm{Nu}_{forced} &= f_1(\mathrm{Re}, \mathrm{Pr}) \\ \mathrm{Nu}_{natural} &= f_2(\mathrm{Gr}, \mathrm{Pr}). \end{aligned} \tag{2.11}$$

In both cases there is one dimensionless group, the Reynolds number or the Grashof number, that represents the characteristics and behaviour of the flow of the fluid, and another dimensionless group, the Prandtl number, that represents the material properties of the fluid. The exact form of the correlation equation can depend on the geometry of the system, the scale of the dimensionless groups, or other such factors.

For forced convection, the Reynolds number represents the degree of turbulence in the flow. The Reynolds number for flow in cylindrical pipes is defined as [26][35]

$$\mathrm{Re} = \frac{\rho V d}{\mu}, \tag{2.12}$$

where ρ is the density of the fluid, V is the mean velocity of the flow, d is the inner diameter of the pipe, and μ is the dynamic viscosity of the fluid. Thus, the Reynolds number is affected by the properties of the fluid, as well as the flow velocity and system geometry. The Reynolds number can be applied to other geometries by altering the characteristic length, which for cylindrical pipes is the inner diameter, in the case of internal flow, and the outer diameter in the case of external cross-flow [26].

The exact boundary values of the Reynolds number that limit the laminar and turbulent flow regimes, and the transition regime between them, depend on the geometry of the system. For cylindrical pipes, the generally accepted values are $\mathrm{Re} < 2000...2300$ for laminar flow [14][26] and $\mathrm{Re} > 4000...5000$ for turbulent flow [20], although it is argued that turbulence becomes fully established only for $\mathrm{Re} > 10000$ [14][26]. These boundary values are not exact, as, for example, turbulent flow can occur at lower values of the Reynolds number if the flow is disturbed sufficiently.

For natural convection, the dimensionless group describing the flow characteristics, the Reynolds number, is replaced by the Grashof number, which is defined as [26][35]

$$\mathrm{Gr} = \frac{g\beta\Delta T L_c^3}{\nu^2}, \tag{2.13}$$

where g is the gravitational acceleration, β is the thermal volume coefficient of the fluid, ΔT is the temperature difference between the fluid and the surface, L_c is the characteristic length of the system, and ν is the kinematic viscosity of the fluid. For

natural convection on the outside of a cylindrical pipe, the characteristic length of the system is the outer diameter of the pipe or the insulation around the pipe.

For both forced and natural convection, fluid properties are characterised using the Prandtl number, defined as [35]

$$\mathrm{Pr} = \frac{\nu}{\alpha}, \tag{2.14}$$

where the thermal diffusivity α of the fluid is defined as [35]

$$\alpha = \frac{k_f}{\rho c_p}, \tag{2.15}$$

where c_p is the specific heat of the fluid at constant pressure. Certain correlations for natural convection feature the Rayleigh number, another dimensionless group, which can be defined based on the Grashof and Prandtl numbers as [36]

$$\mathrm{Ra} = \mathrm{GrPr}. \tag{2.16}$$

In the context of cylindrical pipes, the simplest type of convective heat transfer for which to evaluate the Nusselt number, is forced convection caused by a laminar, hydrodynamically and thermally fully developed flow inside the pipe. For this case, a constant value of Nusselt number can be found, depending on the boundary conditions. For a uniform pipe wall temperature, the Nusselt number reaches a constant value of [26]

$$\mathrm{Nu}_d = 3.66, \tag{2.17}$$

where the subscript d denotes that the characteristic length of the system is the inner diameter d of the pipe. For a uniform heat flux through the pipe wall, the Nusselt number reaches a value of [26]

$$\mathrm{Nu}_d = \frac{48}{11} \approx 4.364. \tag{2.18}$$

Both Equations (2.17) and (2.18) assume that the flow is both hydrodynamically and thermally fully developed. This means that both the velocity profile and the temperature profile of the flow have reached a constant state. At the entrance of a pipe, so-called entrance effects generally increase the rate of heat transfer, before the velocity and temperature profiles are fully developed [26]. For a laminar flow that is not yet fully thermally developed, the average Nusselt number for a pipe length L with uniform wall temperature can be evaluated with [26]

$$\overline{\mathrm{Nu}}_d = 3.66 + \frac{0.065(d/L)\mathrm{Re}_d\mathrm{Pr}}{1 + 0.04\big((d/L)\mathrm{Re}_d\mathrm{Pr}\big)^{2/3}}. \tag{2.19}$$

As the flow advances in the pipe and $d/L \to 0$, the flow approaches a fully developed flow, and thus the Nusselt number approaches the constant value for a fully developed flow, as given by Equation (2.17).

For fully developed turbulent flow, there are several power law correlations presented in literature, which differ slightly in the constants used in exponents and the valid ranges for the relevant dimensionless groups. The typical form for turbulent flow correlations in smooth pipes is

$$\mathrm{Nu} = C\ \mathrm{Re}^{a}\mathrm{Pr}^{b}, \tag{2.20}$$

where the constant C is often 0.023 [26] or 0.024 [35], and typically $a = 0.8$ [26][35]. The exponent b of the Prandtl number varies in the range of $0.3 < b < 0.4$ in some correlations based on whether the fluid is being cooled or heated. A more accurate correlation for smooth pipes often cited in the literature is the Petukhov correlation modified by Gnielinski, which states that for $2300 < \mathrm{Re}_d < 10^4$, which spans the transition from laminar flow to intermittent turbulence, [12]

$$\mathrm{Nu}_d = \frac{(f/8)(\mathrm{Re}_d - 1000)\mathrm{Pr}}{1 + 12.7(f/8)^{1/2}(\mathrm{Pr}^{2/3} - 1)}, \tag{2.21}$$

where f is the Darcy friction factor of the pipe. The Darcy friction factor for a smooth pipe can be solved using Petukhov's equation [26]

$$f = \big(0.790\ \ln(\mathrm{Re}_d) - 1.64\big)^{-2} \tag{2.22}$$

for a Reynolds number range $\mathrm{Re}_d < 5 \cdot 10^6$. For the flow regime of full turbulence, $10^4 \leq \mathrm{Re}_d \leq 10^6$, and for $0.1 \leq \mathrm{Pr} \leq 1000$, Equation (2.21) can be modified into the form [14]

$$\mathrm{Nu}_d = \frac{(f/8)\mathrm{Re}_d\mathrm{Pr}}{1 + 12.7(f/8)^{1/2}(\mathrm{Pr}^{2/3} - 1)}, \tag{2.23}$$

where the friction factor f can be calculated from [14]

$$f = \big(1.8\ \log_{10}(\mathrm{Re}_d) - 1.5\big)^{-2}, \tag{2.24}$$

as suggested by Konakov [19, see 14]. In its full form, where the development length of the flow is considered, Equation (2.23) by Gnielinski for full turbulence states that [14]

$$\mathrm{Nu}_d = \frac{(f/8)\mathrm{Re}_d\mathrm{Pr}}{1 + 12.7(f/8)^{1/2}(\mathrm{Pr}^{2/3} - 1)}\left(1 + \big(d/l\big)^{2/3}\right), \tag{2.25}$$

where d is the inner diameter of the pipe and l is the travelled length in the pipe.

On the exterior of the pipe, or the insulation around it, if the surrounding fluid is mostly stationary, convective heat transfer on the exterior is driven by natural convection. The Nusselt number for natural convection depends on the characteristics of the buoyancy-driven flow, as characterised by the Rayleigh number, the properties of the fluid, as characterised by the Prandtl number, and the geometry of the system. For horizontal cylindrical pipes, which are a common occurrence in the industry, the correlation presented by Churchill and Chu [7] states that the average Nusselt number for laminar

flow, in the range $10^{-6} < \mathrm{Ra} \lesssim 10^9$, where $\mathrm{Ra}_d = \mathrm{Gr}_d\mathrm{Pr}$, can be calculated from

$$\overline{\mathrm{Nu}}_d = 0.36 + \frac{0.518\mathrm{Ra}_d^{1/4}}{\left(1 + (0.559/\mathrm{Pr})^{9/16}\right)^{4/9}}. \tag{2.26}$$

For turbulent natural convection, or $\mathrm{Ra}_d \gtrsim 10^9$, Churchill and Chu [7] suggest

$$\overline{\mathrm{Nu}}_d = \left(0.60 + 0.387\left(\frac{\mathrm{Ra}_d}{\left(1 + (0.559/\mathrm{Pr})^{9/16}\right)^{16/9}}\right)^{1/6}\right)^2. \tag{2.27}$$

It is worth noting that the transition between Equation (2.26) for laminar flow and Equation (2.27) for turbulent flow is not continuous in the vicinity of $\mathrm{Ra}_d \sim 10^9$ [26]. Both Equations (2.26) and (2.27) are presented as valid for all values of Prandtl number $0 < \mathrm{Pr} < \infty$ [7]. The Finnish standard SFS 3977 presents a simpler correlation for natural convection on the exterior surface of a pipe, such that [31]

$$h_{conv,o} = 1.32 \cdot \left(\frac{T_s - T_{inf}}{D}\right)^{0.25}, \tag{2.28}$$

where $h_{conv,o}$ is the heat transfer coefficient of external convection, T_s is the temperature of the pipe or insulation surface, T_{inf} is the ambient temperature and D is the exterior diameter of the pipe or insulation.

2.1.3 Heat radiation

In processes where the fluid temperature, and thus the surface temperature of the pipe, is considerably high, the significance of an additional mode of heat transfer is increased, as heat can also be transferred via the emission and absorption of large-wavelength electromagnetic radiation [17]. All matter gives off heat radiation at a certain rate, which is dependent on its temperature [17][26]. A theoretical *black body* surface emits heat radiation at a heat flux of [35]

$$q = \sigma T^4, \tag{2.29}$$

where σ is the Stefan-Boltzmann constant of $\sigma \approx 5.67 \cdot 10^{-8}\ \mathrm{W/(m^2K^4)}$ [27], and T is the temperature of the body. Due to the fourth-power-dependence on temperature, the heat flux drastically grows as temperature increases. For real surfaces, the emitted heat flux is lessened by a material property known as emissivity ϵ [35]. Modifying Equation (2.29) with the emissivity ϵ of the surface, the emitted heat flux of a real surface can be expressed as [35]

$$q = \epsilon\sigma T^4, \tag{2.30}$$

where $0 < \epsilon \leq 1$, with $\epsilon = 1$ being the theoretical limit corresponding with a black body. While emissivity as a material property can depend on many factors, such as the temperature of the material and the wavelength of the radiation, it is common to

approximate surfaces as *grey bodies* with a constant emissivity with sufficient accuracy [26][17]. When considering the rate of radiative heat transfer between a body and its surroundings, it is necessary to evaluate the emission of heat radiation from the body to the surroundings, and the absorption of heat radiation from the surroundings to the body. For a black body (subscript 1) in black surroundings (subscript 2), the rate of heat transfer can be expressed as [26]

$$\dot{Q}_{1,2} = \sigma A_1 (T_1^4 - T_2^4), \tag{2.31}$$

where A_1 is the surface area of the body, and the positive direction of heat transfer is from the body to the surroundings.

The effect of surface emissivities, relative surface areas and the physical geometry of the surfaces can be evaluated using a dimensionless transfer factor $\mathcal{F}$ [26]. A relatively small grey body in a relatively large and nearly black environment, which is a decent approximation for a pipeline in a process industry plant, can be represented with a transfer factor of $\mathcal{F}_{1,2} \approx \epsilon_1$ [26], where ϵ_1 is the emissivity of the grey body. Thus, the rate of radiative heat transfer presented in Equation (2.31) becomes

$$\begin{aligned} \dot{Q}_{1,2} &= \sigma A_1 \mathcal{F}_{1,2} (T_1^4 - T_2^4) \\ &= \epsilon_1 \sigma A_1 (T_1^4 - T_2^4) \end{aligned} \tag{2.32}$$

for a grey pipeline in large and nearly black surroundings.

The emissivities of process industry pipes can vary greatly depending on the material of the pipe, the temperature of the surface, as well as the condition of the material [17]. For polished metal surfaces, emissivities at normal operating temperatures tend to be in the region of $\epsilon \lesssim 0.1$, but for oxidised metal surfaces the emissivities are considerably greater, in the region of $0.2 \lesssim \epsilon \lesssim 0.8$ [17]. For insulated pipes, insulation jacketing materials, such as steel sheet or aluminium foil, are used on top of the actual insulation materials to control the emissivity of the surface [32].

In most process industry settings, pipelines are typically surrounded by air at or near normal temperature and pressure. While gases can emit and absorb heat radiation, symmetrical gas molecules such as nitrogen N_2 and oxygen O_2, which represent essentially the entire composition of air, are largely transparent to heat radiation in the specified conditions [17]. Thus, air effectively does not absorb radiation in the part of the electromagnetic spectrum of heat radiation, and thus does not significantly affect radiation heat transfer in process industry pipes. [26]

2.1.4 Heat transfer resistance

Heat loss in industry pipelines features simultaneous heat conduction, convection, and radiation, and as such, a convenient method of considering them all is required for proper evaluation of heat loss. As discussed in relation to heat conduction and convection, the

driving force behind heat flux is a temperature difference, rather similarly to how voltage, a difference in electrical potential, is the driving force behind electrical current. An equation known as Ohm's law defines this relation using a concept of electrical resistance R_{el}, such that [35]

$$R_{el} = \frac{U}{I}, \tag{2.33}$$

where U is voltage, or the difference in electrical potential between two points, and I is electrical current. Analogously, the concept of heat transfer resistance R can be defined as [26][35]

$$R = \frac{\Delta T}{\dot{Q}}, \tag{2.34}$$

where ΔT is the temperature difference between two points, and $\dot{Q}$ is the rate of heat transfer. The unit of heat transfer resistance, $\mathrm{K/W}$, can be understood as the temperature difference in kelvins required to induce a certain heat flow in watts over a system with a heat transfer resistance of R.

Using this analogy between electricity and heat transfer, it is possible to model heat transfer systems in a similar fashion to electrical circuits. Rearranging Equation (2.6) to match Equation (2.34) gives

$$\frac{\ln(r_o/r_i)}{k2\pi L} = \frac{\Delta T}{\dot{Q}}, \tag{2.35}$$

from which heat conduction resistance can be defined as

$$R_{cond} = \frac{\ln(r_o/r_i)}{k2\pi L}. \tag{2.36}$$

Similarly, the heat transfer resistance for convection can be defined. Combining Equations (2.7) and (2.2) and rearranging to match Equation (2.34) gives

$$\frac{1}{hA} = \frac{\Delta T}{\dot{Q}}. \tag{2.37}$$

For a cylindrical pipe of length L, convective heat transfer resistance can be defined as

$$R_{conv} = \frac{1}{hA} = \frac{1}{h2\pi rL}. \tag{2.38}$$

In a similar way to Equation (2.37), it is also possible to define a radiation heat transfer coefficient h_{rad}, for which

$$\frac{1}{h_{rad}A} = \frac{\Delta T}{\dot{Q}_{rad}}. \tag{2.39}$$

While Equation (2.32) does not directly contain a first-power temperature difference term ΔT, the fourth-power temperature difference term can be rearranged to provide such a term. For a surface temperature T_s and environment temperature T_{inf}, the fourth-power

temperature difference term can be rearranged as

$$(T_s^4 - T_{inf}^4) = (T_s - T_{inf})(T_s^3 + T_s^2 T_{inf} + T_s T_{inf}^2 + T_{inf}^3). \tag{2.40}$$

Now, Equation (2.32) can be rearranged as

$$\frac{1}{\epsilon\sigma A(T_s^3 + T_s^2 T_{inf} + T_s T_{inf}^2 + T_{inf}^3)} = \frac{\Delta T}{\dot{Q}_{rad}}, \tag{2.41}$$

where $A = 2\pi r L$ for a pipe of length L with outer radius r. Thus, radiation heat transfer resistance can be defined as

$$R_{rad} = \frac{1}{\epsilon\sigma A(T_s^3 + T_s^2 T_{inf} + T_s T_{inf}^2 + T_{inf}^3)}. \tag{2.42}$$

The inclusion of temperature terms in the definition of R_{rad}, such that $R_{rad} = R_{rad}(T_s, T_{inf})$, does not deviate from the previous definitions of heat transfer resistances for heat conduction and convection, given how $R_{cond} = R_{cond}(k)$ and $R_{conv} = R_{conv}(\mathrm{Nu})$, where $k = k(T)$ and $\mathrm{Nu} = \mathrm{Nu}(T)$. Equation (2.42) can be simplified if T_s and T_{inf} are close. Given the temperature difference $\Delta T = T_s - T_{inf}$ and mean temperature $T_m = (T_s + T_{inf})/2$, if $\Delta T \ll T_m$, Equation (2.32) can be approximated as [20]

$$\begin{aligned} \dot{Q}_{1,2} &= \epsilon_1 \sigma A_1 (T_1^4 - T_2^4) \\ &\approx 4\sigma\epsilon_1 T_m^3 A \Delta T, \end{aligned} \tag{2.43}$$

from which a heat transfer coefficient for heat radiation can be defined as

$$h_{rad} = 4\sigma\epsilon_1 T_m^3. \tag{2.44}$$

Thus, the heat transfer resistance for radiation at the outer surface of a cylindrical pipe can be approximated with

$$R_{rad} = \frac{1}{h_{rad} A} = \frac{1}{(4\sigma\epsilon_1 T_m^3)(2\pi r_o L)}. \tag{2.45}$$

Considering a typical insulated process industry pipe, and disregarding heat radiation for now, the heat loss consists of four consecutive parts: forced convection on the interior of the pipe, heat conduction through the pipe wall, heat conduction through the insulation, and natural convection on the exterior of the pipe. In electrical circuits, consecutive resistances, where the same current flows through each of them, are referred to as resistances connected *in series*. For resistances connected in series, the total resistance equals the sum of all the resistances connected in series, or [35]

$$R_{tot} = \sum_i (R_i). \tag{2.46}$$

Using the analogy for the heat transfer system described before, the total heat transfer resistance can be calculated as the sum of the consecutive heat transfer resistances, or

$$\begin{aligned} R_{tot} &= R_{conv,i} + R_{cond,pipe} + R_{cond,ins} + R_{conv,o} \\ &= \frac{1}{h_i 2\pi r_i L} + \frac{\ln(r_o/r_i)}{k_{pipe} 2\pi L} + \frac{\ln(r_{ins}/r_o)}{k_{ins} 2\pi L} + \frac{1}{h_o 2\pi r_{ins} L}, \end{aligned} \tag{2.47}$$

where subscripts i, ins, and o refer to the inside surface of the pipe, the insulation and the outside surface of the pipe, respectively.

In the case of consecutive heat transfer resistances, the same heat flux or the same heat flow passes through each of the resistances. However, if radiation heat transfer on the exterior of the insulation is included in the model, the heat flow that passes through the first three heat resistances does not first pass through the exterior convective resistance and then through the radiation resistance. Instead, the heat flow that passes through the first three resistances is the sum of the heat flows through the convective and radiation resistances. In the terminology of electrical circuits, the exterior heat resistances are connected *in parallel*, instead of in series. For resistances in parallel, the total resistance R_{tot} can be calculated from [35]

$$\frac{1}{R_{tot}} = \sum_i \left(\frac{1}{R_i} \right). \tag{2.48}$$

Thus, including exterior heat radiation in the case discussed earlier, the total heat transfer resistance becomes

$$\begin{aligned} R_{tot} &= R_{conv,i} + R_{cond,pipe} + R_{cond,ins} + R_{o,tot} \\ &= R_{conv,i} + R_{cond,pipe} + R_{cond,ins} + \left(\frac{1}{R_{conv,o}} + \frac{1}{R_{rad,o}} \right)^{-1} \\ &= \frac{1}{h_i 2\pi r_i L} + \frac{\ln(r_o/r_i)}{k_{pipe} 2\pi L} + \frac{\ln(r_{ins}/r_o)}{k_{ins} 2\pi L} + \frac{1}{(h_o + h_{rad}) 2\pi r_{ins} L}. \end{aligned} \tag{2.49}$$

Circuits corresponding to Equations (2.47) and (2.49) are shown in Figure 2.1.

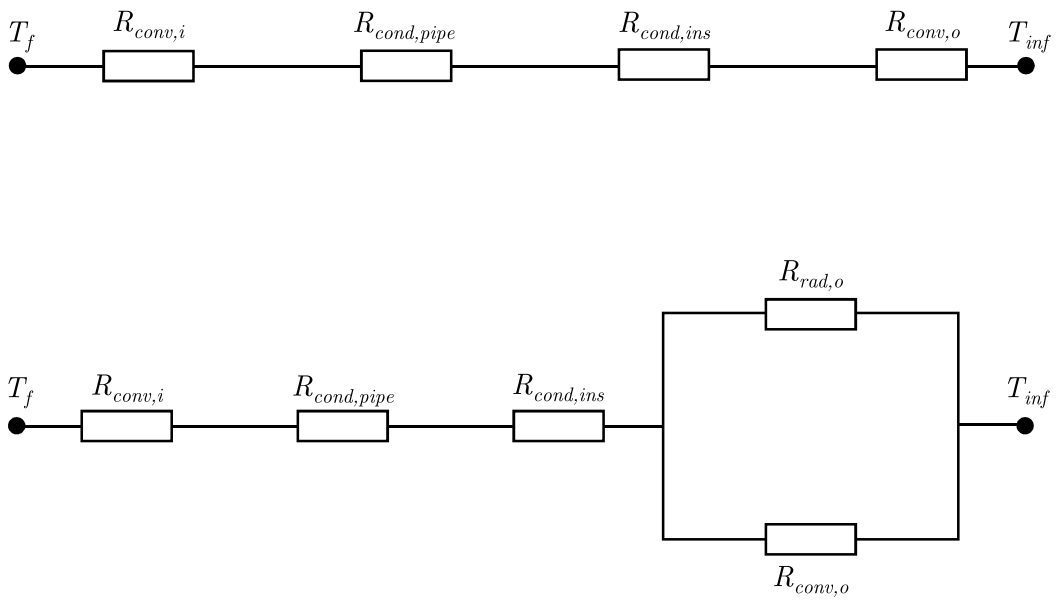

Figure 2.1. *Heat transfer resistances in series and in parallel.*

Based on the total heat transfer resistance, an *overall* heat transfer coefficient U for the system can be defined as [26][35]

$$U = \frac{1}{R_{tot}A}, \tag{2.50}$$

where the exact value of U depends on the definition of the heat transfer area A. For cylindrical pipes, a common choice for A is the cylindrical outer surface of the pipe or its insulation, due to being easier to determine [35]. Now, the heat flow $\dot{Q}$ through a certain heat transfer area A given a certain temperature difference ΔT between the fluid and the surroundings can be expressed as

$$\begin{aligned} \dot{Q} &= \frac{\Delta T}{R_{tot}} \\ \Leftrightarrow \dot{Q} &= UA\Delta T \\ \Leftrightarrow \dot{Q} &= UA(T_{inf} - T_f). \end{aligned} \tag{2.51}$$

The modes of heat transfer from the fluid to the surroundings are visualised in Figure 2.2, along with related solution methods discussed earlier.

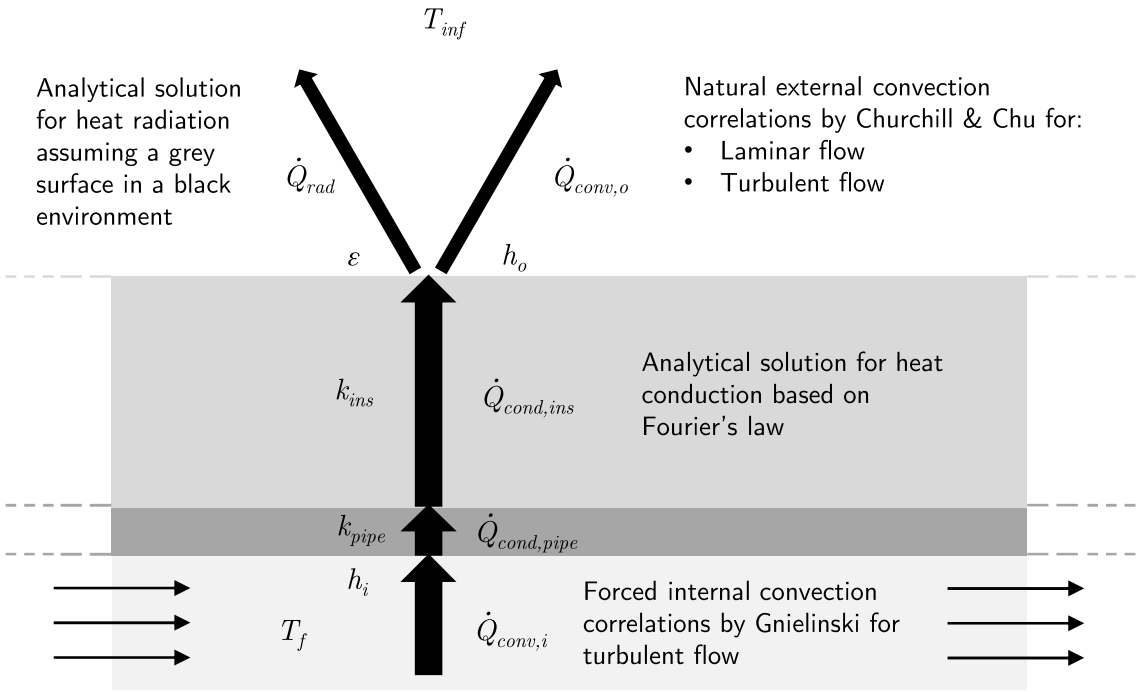

Figure 2.2. *Modes of heat transfer and related solution methods.*

Heat flow from or to the fluid causes either a change in temperature or a phase transition. The temperature change ΔT_f of the fluid can be calculated based on the mass flow $\dot{m}$ and the specific heat at constant pressure c_p from the expression

$$\dot{Q} = \dot{m} c_p \Delta T_f = \dot{m} c_p (T_{f,out} - T_{f,in}). \tag{2.52}$$

If the heat loss brings the fluid to its saturation temperature, the transfer of thermal energy causes a phase change in the fluid, instead of a change in temperature. A common, yet in certain conditions undesirable [25][38], phase change in the process industry, the condensation of steam to liquid water, is discussed in Section 2.2.1.

2.2 Heat losses and insulation

Loss implies something negative. While technically *heat loss* in a pipe would only refer to a situation where a higher-temperature fluid flow loses heat to lower-temperature surroundings, the opposite situation where a lower-temperature fluid flow gains heat from higher-temperature surroundings, being equally as undesirable, can also be referred to as heat loss.

2.2.1 Technical and financial consequences

As the fluids used in the process industry often have very specific operating temperatures or temperature ranges which are required by the process, heat loss causes undesired deviations from the specified conditions. Thus, additional heating or cooling of the fluid is required, which can be achieved with heat exchangers. Adding equipment, such as heat exchangers or valves, does however increase the investment cost of the pipeline, while often additionally increasing the operational costs by introducing pressure loss, increasing the pumping power required for the fluids involved.

Heat losses in steam pipes can also lead to condensation, as the cooling steam becomes saturated and begins to form liquid water. This is typically undesirable in steam pipes, and thus, *steam traps* are installed to remove the condensate. Condensate gathering in horizontal sections of steam pipes increases the effects of corrosion [15] and can cause *condensation induced water hammer* (CIWH) [25][38], which can drastically reduce the lifetime of the pipe and cause severe damage to the pipeline and its equipment, also introducing risk of personnel injury. In extreme cases, condensation induced water hammer can even cause large sections of steam pipelines to become completely dislodged and violently ejected over great distances, damaging nearby infrastructure [10]. Another negative effect of condensation in steam pipes is the erosion caused by entrained water particles in high-velocity steam flow [16]. This can be especially damaging and costly in steam turbines, where increased wetness in the steam can cause physical damage to the turbine rotor blades, significantly reducing their lifespan [16]. While condensation in steam pipes is often undesired, condensation of water and refrigerants in heat exchangers is commonly utilised in the process industry [22].

2.2.2 Purposes of pipe insulation

Insulation is used in pipes in the process industry for a number of different reasons, and the methods for determining the correct type and thickness of insulation vary accordingly [18]. The most straightforward goal of insulating a pipe is to reduce the rate of heat transfer through the pipe walls. Regardless of whether the fluid is at a higher or lower temperature than its surroundings, the appropriate insulation thickness can be determined using the same methods, based on the heat transfer phenomena discussed earlier. Depending on the context, the motivation behind reducing the rate of heat transfer may vary. In some cases, the insulation serves to reduce the total lifetime costs of the plant, by reducing the operational costs of extra heating or cooling required to compensate for the heat loss. In other cases, the insulation serves to maintain the temperature of the fluid in a range required by the process. In extreme cases, the purpose of the insulation may be to prevent a phase change in the fluid, such as a water pipe freezing in outdoors conditions in a cold climate, especially if the flow may temporarily come to a stop. [31]

An additional reason to insulate process industry pipes is to improve workplace safety. In places where plant personnel may come into contact with pipes with extreme surface temperatures, protective insulation is used to bring the surface temperature to a less hazardous range, thus reducing the risk of workplace injuries. Protective insulation can be used to protect personnel from either high or low temperature surfaces. In the case of low pipe surface temperatures, insulation can also be used to reduce the condensation of air humidity on the surface of the pipe, by reducing the temperature difference between the surface and the air. [31]

Typical insulation materials used in the industry are various fiber-based materials such as mineral wools, and rigid open-cell or closed-cell structures extruded or expanded from materials such as polystyrene and polyurethane [33]. As discussed in the Finnish standard SFS 3977, the thermal conductivity of insulation materials is typically a function of the mean temperature of the insulation material [31]. Additionally, the temperature difference between the interior and exterior surfaces of the insulation has an effect on the thermal conductivity of the material [31]. Thermal conductivities of insulation materials are typically available directly from the insulation provider, but such tables are also available in standards such as SFS 3976 [33].

3 NUMERICAL ANALYSIS AND OPTIMISATION

While analytical solutions for heat loss in pipes under certain conditions, such as with a constant wall temperature, can be derived, problems arise when attempting to apply these solutions to real-life problems. For a pipe flow where the temperature of the fluid changes due to heat loss, the wall temperature also changes as a function of the temperature of the fluid. Additionally, even if the wall temperature were to remain constant, the changing fluid temperature alters the material properties of the fluid, which affects the overall heat transfer coefficient U. Thus, numerical methods are implemented in order to overcome these problems, while still utilising the same underlying principles of heat transfer theory as with analytical solutions.

Once a reliable method for evaluating heat loss in the pipe system is established, the method can be utilised to find an optimal solution to a particular problem, such as determining the optimal insulation thickness. Since the concept of an optimal solution is a highly subjective matter, given the variety of variables to optimise, various tools for optimising such solutions have been developed to allow optimisation based on different goals, whether process-related, economic, or otherwise. This chapter presents numerical solution methods for applying the heat transfer theory results presented in Chapter 2 to process industry pipelines, as well as optimisation methods, which can be used in determining optimal insulation thickness from an economic standpoint.

3.1 Numerical solution methods for heat loss in pipes

As mentioned previously, while the results presented in the form of Equations (2.49), (2.51) and (2.52) would allow the calculation of heat loss in a pipeline and the fluid temperature change related to it, the change in fluid temperature alters the material properties of the fluid along the length of the pipe. Thus, a solution acquired with material properties evaluated at inlet conditions is inaccurate. One approach to the problem is to acquire the material properties at a mean temperature between inlet and outlet conditions. However, a problem arises as the outlet temperature is required in order to solve the outlet temperature, and thus iterative calculation is required. Another approach is to split the solution domain, or in this case the length of the pipe, into sufficiently small subdomains, so that the temperature change in any single subdomain is small enough to justify the assumption of approximately constant temperature, and thus constant material properties inside the subdomain.

3.1.1 Discrete piece-wise iteration of an analytical solution

An analytical solution for the outlet temperature of a fluid flow in a pipe with heat transfer between the fluid and the environment can be derived using a control volume approach. In a cylindrical pipe section of infinitesimally short length dx, the heat content of the fluid at the inlet of the control volume can be defined as $\dot{m}c_pT_m$, where T_m is the mean temperature of the fluid [26]. The heat transfer between the fluid and the environment through the infinitesimally small heat transfer area dA on the exterior of the pipe can be expressed using the overall heat transfer coefficient as $U(T_{inf} - T_m)dA$, where T_{inf} is the temperature of the environment, as in Equation (2.51). Considering the infinitesimally small temperature change dT_m of the fluid mean temperature, caused by the heat transfer, the heat content of the flow at the outlet becomes $\dot{m}c_p(T_m + dT_m)$.

The heat balance equation for the control volume can now be expressed as

$$\dot{m}c_pT_m + U(T_{inf} - T_m)dA = \dot{m}c_p(T_m + dT_m), \tag{3.1}$$

which can be converted to a function of the infinitesimally short control volume length dx by acknowledging that $dA = Pdx$, where $P = \pi \cdot D$, where D is the exterior diameter of the cylindrical geometry. Rearranging the balance Equation (3.1) gives an equation where each side of the equation can be integrated, for $T_m \in [T_{in}, T_{out}]$ and $x \in [0, L]$ respectively, where T_{in} is the inlet temperature of the fluid, T_{out} is the outlet temperature of the fluid and L is the length of pipe between the inlet and outlet:

$$\int_{T_{in}}^{T_{out}} \frac{1}{T_{inf} - T_m} dT_m = \int_0^L \frac{UP}{\dot{m}c_p} dx. \tag{3.2}$$

After the evaluation of the integrals, Equation (3.2) can be rearranged, giving the expression

$$T_{out} = T_{inf} + (T_{in} - T_{inf})\mathrm{e}^{\frac{-UPL}{\dot{m}c_p}} \tag{3.3}$$

to solve the outlet temperature T_{out}.

While technically a valid solution for the heat transfer problem, Equation (3.3) does not take into account that both U and c_p are functions of the fluid temperature. Thus, as the fluid temperature changes as the flow travels over the length L, a solution acquired with values of U and c_p evaluated at the inlet temperature T_{in} will not accurately represent the heat transfer for the system. To solve this issue, two different iterative approaches can be utilised. The first approach involves evaluating the properties at a mean temperature $T_m = (T_{in} + T_{out})/2$ to more accurately represent the changing values of the properties. However, as the value of T_{out} is required to solve the value of T_{out}, an initial approximation of T_{out} is required for the first calculation. The calculation can be iterated by replacing the approximated T_{out} with the calculated T_{out}, and continuing iteration until the solution converges, as is typical for an *implicit* solution method.

An alternative iterative approach is to divide the length of the pipe into sufficiently short sections, such that the temperature change over each short section is small. Thus, the changes in U and c_p over each section are also small, furthermore justifying the assumption that an *explicit* solution, or in other terms $U = U(T_{in})$ and $c_p = c_p(T_{in})$, for each short section is a sufficiently accurate approximation. Using this assumption, the fluid temperature over the entire length L of the pipe can be solved explicitly in short increments of the length coordinate, providing a value for T_{out} at the outlet of the final iteration section. The iterative *implicit* solution method can also be combined with the approach of dividing the solution domain into several shorter sections, over which the solution is iterated. This combined approach offers the benefits of both iterative approaches, at the cost of increased computation times. The shorter the solution sections are, the more accurate the solution is, as the temperature-dependent terms in the equation are re-evaluated more often, and each section is closer to the assumption of a *small* temperature change. However, this also leads to increased computation times, as the number of required iteration steps increases.

3.1.2 Explicit and implicit Euler methods

For ordinary differential equations with simple boundary conditions, analytical solutions can be derived, resulting typically in a continuous function as the solution. For more complex boundary conditions, however, deriving such analytical solutions may be difficult or even impossible, and thus, numerical solution methods are used. Thus, in situations where the heat loss problem and its boundary conditions are too complicated to solve using the analytical method discussed in Section 3.1.1, an alternative solution method is required.

For first-order ordinary differential equations, a simple and well-known numerical solution method is the Euler method [5][21]. From the overarching concept of the Euler method, two sub-methods can be identified: the explicit and the implicit Euler method. The basic principle of the Euler method is the discretisation of a differential term into a difference term, such that the gradient of the evaluated function does not significantly change over the small difference [5][21]. An example of this, relevant to evaluating the heat loss of a pipeline, is provided below.

Combining Equations (2.51) and (2.52) gives the expression

$$\dot{m} c_p \Delta T_f = UA(T_{inf} - T_f), \tag{3.4}$$

which links the heat loss in a pipe to the temperature change of the fluid between the inlet and the outlet of the pipe. For a pipe section of an infinitesimally short length dx, the heat transfer area can be expressed as $A = P \cdot dx$, where P is the perimeter $P = 2\pi r_o$ for a cylindrical geometry with the external radius r_o of the pipe or its insulation. For the infinitesimally short pipe section, the temperature change ΔT_f of the fluid becomes an

infinitesimally small temperature change dT_f, and Equation (3.4) becomes

$$\dot{m}c_p dT_f = UPdx(T_{inf} - T_f). \tag{3.5}$$

The Equation (3.5) can be rearranged to form

$$\dot{m}c_p \frac{dT_f}{dx} = UP(T_{inf} - T_f), \tag{3.6}$$

which is a first-order ordinary differential equation featuring the fluid temperature T_f and its gradient along the length of the pipe. From here, the differential term is discretised into a difference term by converting the infinitesimally small terms dT_f and dx into merely small terms ΔT_f and Δx, such that

$$\dot{m}c_p \frac{\Delta T_f}{\Delta x} = UP(T_{inf} - T_f). \tag{3.7}$$

For a sufficiently small Δx, Equation (3.7) is a sufficiently accurate approximation of the differential Equation (3.6). If the fluid temperature $T_{f,x}$ at position x is known, the temperature $T_{f,x+\Delta x}$ at position $x + \Delta x$ can be solved as

$$\begin{aligned}
\dot{m}c_p \frac{\Delta T_f}{\Delta x} &= UP(T_{inf} - T_f) \\
\Leftrightarrow \Delta T_f &= \frac{UP}{\dot{m}c_p}(T_{inf} - T_f)\Delta x \\
\Leftrightarrow T_{f,x+\Delta x} - T_{f,x} &= \frac{UP}{\dot{m}c_p}(T_{inf} - T_f)\Delta x \\
\Leftrightarrow T_{f,x+\Delta x} &= T_{f,x} + \underbrace{\frac{UP}{\dot{m}c_p}(T_{inf} - T_f)}_{f(T_{f,x}) \text{ or } f(T_{f,x}, T_{f,x+\Delta x})} \cdot \Delta x.
\end{aligned} \tag{3.8}$$

As noted in the Equation (3.8), the equation that is supposed to solve T_f features $U = U(T_f)$ and T_f itself as unknowns. If these unknowns are evaluated using the known value $T_{f,x}$, the equation can be solved explicitly, and thus the method is known as the *explicit Euler method*. A more physically accurate method would be to take the value of $T_{f,x+\Delta x}$ into account when evaluating the unknowns, using the mean temperature, for example. This, however, results in an implicit equation that must be solved iteratively, and thus the method is called the *implicit Euler method* [5]. While computationally simpler than its implicit counterpart, the explicit Euler method is not as numerically stable, meaning that the numerical solution may not converge. The implicit Euler method, while more stable, is also slower due to the need for several iterative calculations of the equation [5]. As with the analytical solution discussed in Section 3.1.1, the accuracy of the numerical solution can be improved by shortening the step length Δx [5], at the cost of increased calculation times. Due to the improved stability of the additional iterative element, the implicit solution method is typically stabler even with relatively large step lengths, whereas the explicit form of the solution method often requires a shorter step length, as can be seen in Section 5.1.1, where the methods are compared using different step lengths.

3.2 Economic optimisation of insulation thickness

Using the numerical solution methods discussed in Section 3.1, it is possible to calculate the heat loss for a pipe system, comparing multiple different insulation thicknesses. Based on the price of the insulation and the cost of the energy required to replace the energy loss, it is possible to determine the insulation thickness with which the total cost over the lifetime of the pipe system is the lowest. This section discusses this optimisation, or the process of determining the optimal insulation thickness, first through its underlying economic principles, and finally through the numerical methods with which the optimal solution is determined.

3.2.1 Economic analysis

An economically optimal insulation thickness for a pipeline can be determined by considering and minimising the lifetime total cost of the pipeline. The two most significant aspects of the total lifetime cost to consider are the initial investment cost of the insulation and the total energy cost over the lifetime [31]. Given that the energy cost is related to replacing the energy lost through heat loss, and that heat loss can be reduced by adding insulation, an optimisation problem can be established to find the insulation thickness which gives the lowest total cost over the pipeline lifetime. One approach to analysing and minimising the lifetime costs of the pipeline is to evaluate the total annual costs of the pipeline [31]. Before the initial investment cost and the annual energy costs can be meaningfully compared in a financial context, however, the annual costs and the investment costs must be converted to and evaluated at their value at a common time of reference. The future payments of the annual energy costs can be *discounted* to their value at the time of the investment, or alternatively the investment cost can be divided into annual payments.

When the objective is to make profit from investments, it is common to assume or expect a certain rate of interest i, which states the factor by which the value of an investment increases, or decreases, over time, typically per year when dealing with annual costs. For profitable endeavours, $i > 0$ and the present day value of future payments is less than their value at the time of payment in the future. For a payment C_f, made n years in the future, the present day value C_p with an interest rate i can be calculated from [23]

$$C_p = \frac{C_f}{(1+i)^n}. \tag{3.9}$$

Inversely, an initial investment of C_i can be divided into annual payments of C_a over n years at an interest rate i with the annuity factor $a_{n/i}$, such that

$$C_a = a_{n/i} \cdot C_i, \tag{3.10}$$

where the annuity factor can be calculated from [31]

$$a_{n/i} = \frac{i}{1-(1+i)^{-n}}. \tag{3.11}$$

When optimising the insulation thickness from an economic standpoint, the goal of cost minimisation can be pursued either by evaluating and minimising the present day value of the lifetime costs, or by evaluating and minimising the annual costs. The standard SFS 3977 suggests the latter approach, where the annual energy cost and the annual capital cost, evaluated from the investment cost using an annuity factor, are minimised [31]. The total annual costs can be calculated from

$$C_{tot,a} = a_{n/i} \cdot k \cdot C_{ins} + C_e, \tag{3.12}$$

where $k > 1$ is a dimensionless factor that approximates the additional required insulation for pipe bends, valves and other equipment, C_{ins} is the insulation cost per unit length, and C_e is the annual energy cost per unit length of pipe [31].

The annual energy cost in Equation (3.12) can be calculated from

$$C_e = \dot{Q}_{tot,L} \cdot u \cdot C_{e,th} \cdot \tau_a, \tag{3.13}$$

where $\dot{Q}_{tot,L}$ is the heat loss flow per unit length of pipe, $C_{e,th}$ is the price of thermal energy, τ_a is the number of annual operating hours and the dimensionless factor u approximates the effects of changes in the price of thermal energy [31]. The factor u can be calculated from

$$u = (1+p)^{n/2}, \tag{3.14}$$

where p is a dimensionless factor describing the annual price increase of thermal energy, and n is the number of years in the lifetime of the pipeline [31].

3.2.2 Optimisation methods

The optimal insulation thickness for a given pipe system can be determined using numerical optimisation methods which can be implemented on top of the underlying heat loss calculation model. Many such methods exist, varying in their implementational complexity and computational efficiency. From the perspective of the optimisation method, the objective is to minimise the total cost by varying the insulation thickness. As the insulation thickness increases, the capital cost of the insulation increases, while the energy cost of the heat loss decreases as the increased insulation thickness reduces heat loss. The behaviour of the cost functions is visualised in Figure 3.1.

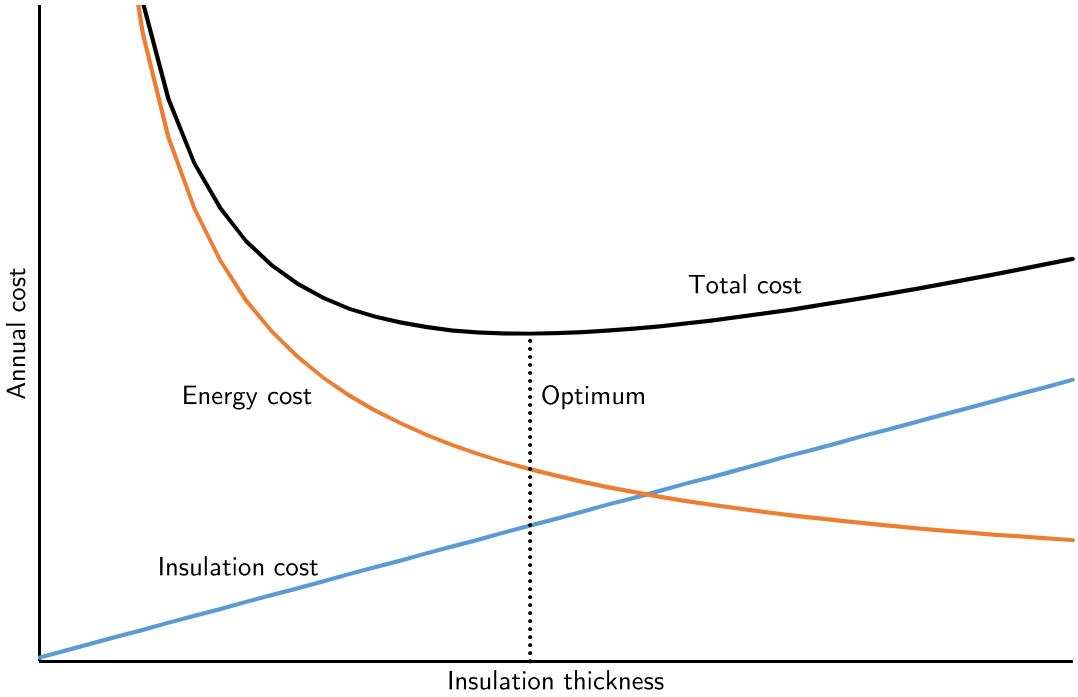

Figure 3.1. *Behaviour of cost functions.*

As can be seen from Figure 3.1, the minimum of the total cost function is found at the insulation thickness with which the derivatives of the energy and insulation cost functions have the same absolute value but different signs. The insulation thickness for which the energy and insulation costs are equal has no special use or meaning for determining the minimum of the total cost function. While it is theoretically possible to analytically determine the optimal insulation thickness by solving the minimum of Equation (3.12), the insulation cost function $C_{ins}(t)$ is not typically known in the form of a mathematical function of insulation thickness t, but rather a price table of discrete values for different insulation thicknesses and pipe sizes. Additionally, evaluating the derivative of the energy loss analytically is not a trivial task.

A considerably simpler solution, although not as computationally efficient and elegant, is to calculate the total costs of the pipe system for numerous different insulation thicknesses, and to select the insulation thickness which produces the lowest total cost. This *brute force* method is reliable, but time-consuming from a computational perspective. This method can be improved upon, given that typically the behaviour of the energy and insulation cost functions produce a total cost function with only a single turning point, which is the global minimum, representing the optimal solution. Thus, a simple numerical *gradient descent* optimisation method can be utilised. For the initial estimated value of insulation thickness, required as the starting point for the gradient descent method, a feasible choice is the insulation thickness suggested by a standard, such as SFS 3977. The efficiency of the optimisation method is discussed further in Sections 4.3, 4.4, and 5.2.2.

4 MATERIALS AND METHODS

In order to provide an easy-to-use method of evaluating heat loss in process industry pipes as well as optimising pipe insulation, a computer program was implemented into Vertex G4Plant, an existing process plant design software product, using the programming language C++. Screenshots of the user interface of an early prototype of the calculation program are presented in Appendix A. This chapter presents how the program was implemented, and discusses the measures which were taken to evaluate the validity of the results provided by the program. The individual steps taken as part of this work are visualised in Figure 4.1. The figure represents the progress of the overall work, advancing from left to right, as well as the transformation of input data into relevant outputs, downwards from the top.

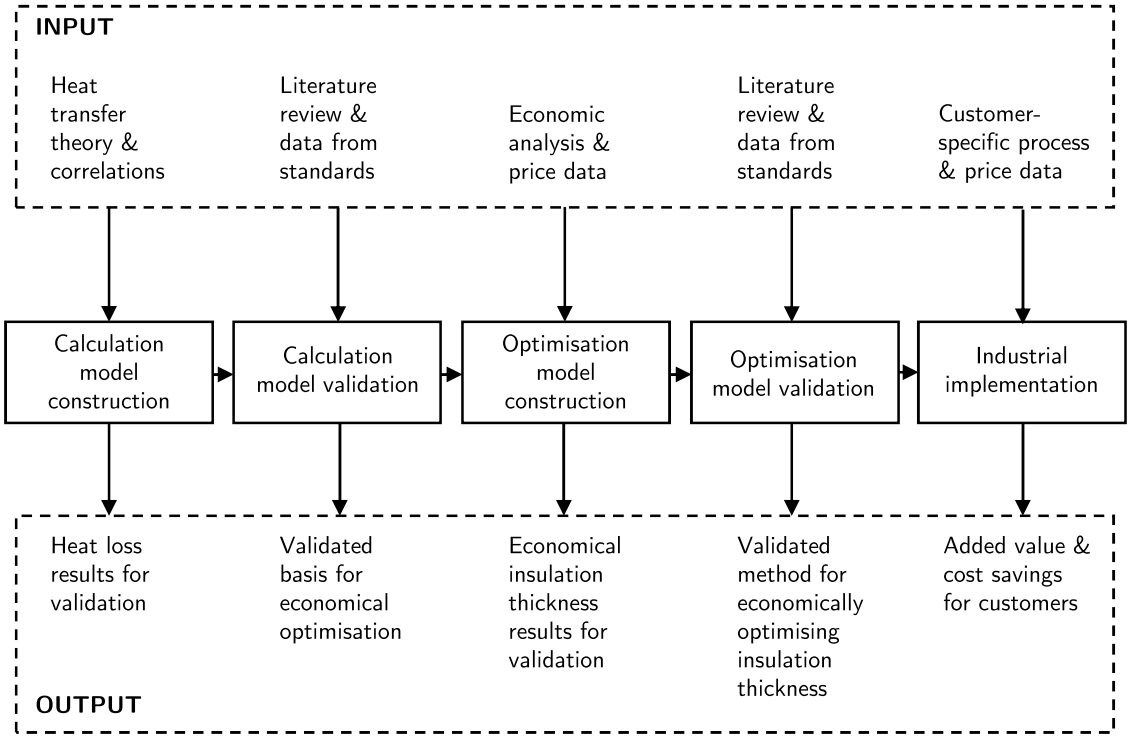

Figure 4.1. *Methodology overview and project workflow.*

In this chapter, the steps leading up to the industrial implementation are discussed. Each section presents how the input data of the step are transformed into relevant outputs, and how each step leads to the next, as presented in Figure 4.1. An overview of the software solution and its benefits to customers in the industry is presented in Figure 4.2.

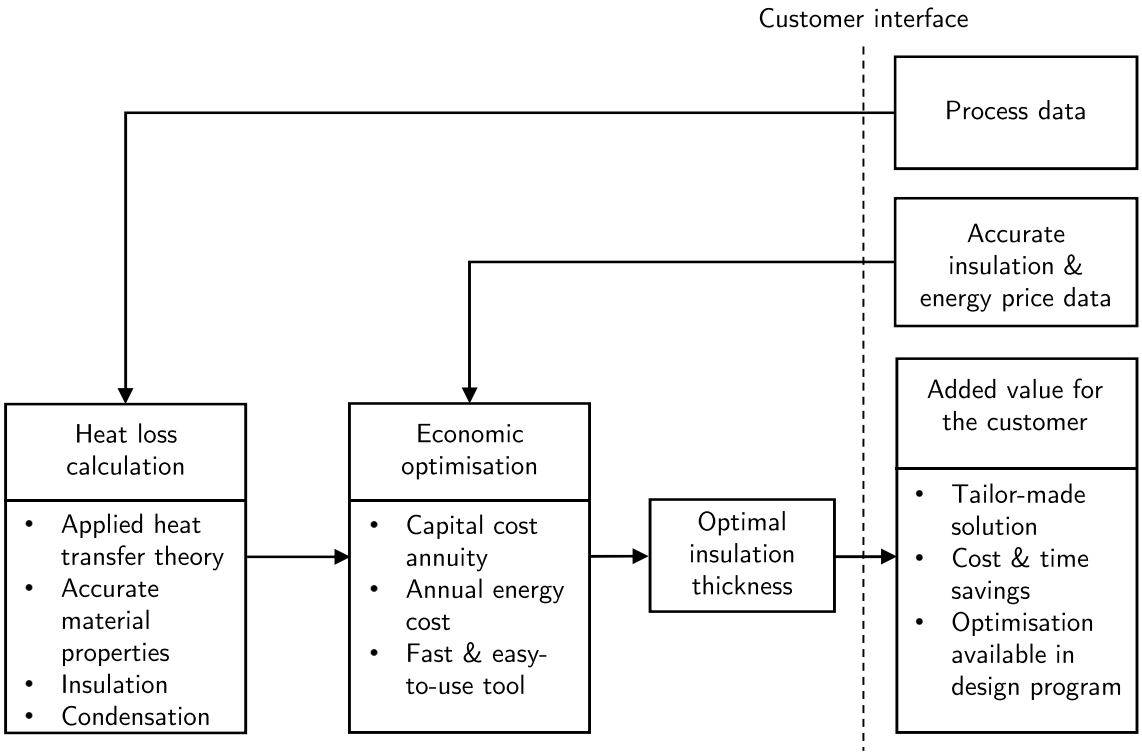

Figure 4.2. *Software solution overview.*

The pipe insulation optimisation method presented in this thesis, as visualised in Figure 4.2, revolves around the interface between the customer and the software solution: what is provided by the customer to the software solution, and vice versa. At the base level, the software solution is built on the heat loss calculation model. In order to accurately predict the heat loss of a pipeline, the software solution requires data on the process and the pipeline, such as pipe length and size, initial fluid temperature, and the temperature of the surroundings. The best source for these data is the customer, who naturally is the most familiar with their own pipelines and processes. Heat transfer theory and numerical solution methods, presented in Chapters 2 and 3, respectively, are applied to the process data, resulting in an analysis of the heat loss in the pipeline as a function of insulation thickness.

In order to optimise the insulation thickness from an economic standpoint, the heat loss analysis needs to be combined with price data, so that the cost of the heat loss can be meaningfully weighed against the cost of insulation. Once again, to make sure that the results are relevant to the customer, the most sensible source for the price data is the customer. The price of energy can vary over time, as well as depending on how the customer acquires the energy, whether producing it on-site or purchasing from a secondary source. Similarly, the price of insulation can vary from provider to provider and from project to project. Using the price data, the results of the heat loss calculation can be economically evaluated to provide an estimation of the optimal insulation thickness for the needs of the customer.

By using the tailor-made solution provided by the program, taking into account the specifics of the process and utilising accurate price data, the customer can achieve cost savings over the lifetime of the pipeline, when compared to relying on the insulation thicknesses provided by a standard. The potential for cost savings is discussed in greater detail in Section 5.2.1. In addition to providing potential cost savings, the optimisation method proposed in this thesis is also time-efficient. Running a heat loss calculation or an insulation thickness optimisation takes seconds to calculate, making the method faster than manually acquiring the proposed insulation thickness from a standard table. Additionally, by being integrated into an existing process plant design software solution, the optimisation method does not create significant extra work for the customer, as the required process data are already available in the design software from the regular plant design workflow. The efficiency and accuracy of the insulation thickness optimisation method is discussed at greater length in Sections 4.3, 4.4, and 5.2.2.

4.1 Calculation model construction

Before the optimal insulation thickness on a process industry pipe can be sensibly discussed, it is imperative to understand and to evaluate the heat transfer phenomena that contribute to the heat loss in the pipe. For this purpose, a tool for calculating the heat loss in a pipe was implemented into the overall calculation program. This section presents the method with which the program solves the heat loss in the pipe, based on the heat transfer theory presented in Chapter 2 and utilising the numerical methods discussed in Chapter 3.

4.1.1 Solution method for heat loss

As evident in the final forms of the derived equations for both the analytical solution and the Eulerian schemes, Equations (3.3) and (3.8) respectively, the numerical methods are built around iteratively solving the temperature of the fluid inside the pipe as a function of length-wise position in the pipe. As both the analytical solution and the Euler schemes are derived from the same starting point, the quantities and properties required for solving the next temperature value are the same. The solution method using the implicit form of the analytical solution is visualised in Figure 4.3.

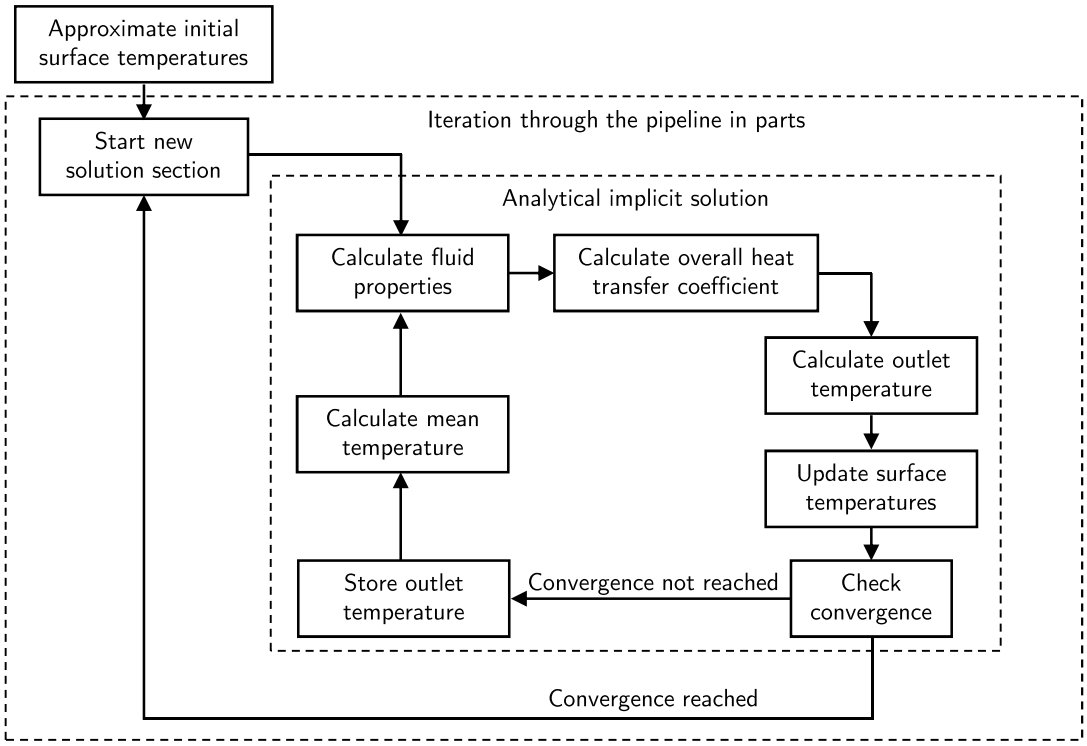

Figure 4.3. *Heat loss solution method overview.*

As presented in Figure 4.3, initially the surface temperatures are approximated. For the first iteration of the first section of the pipeline, the interior and exterior surfaces of the pipe are assumed to be at the inlet temperature of the fluid. If the pipe is insulated, the surface temperature of the insulation is approximated as the average of the temperature of the surroundings and the temperature of the exterior surface of the pipe. These assumptions are based on the relatively high thermal conductivity of the pipe wall material and the relatively low thermal conductivity of the insulation material. Once the initial surface temperatures have been approximated, the solution method begins evaluating the heat loss of the first section of the pipe using the implicit form of the analytical solution.

For the first implicit iteration of each section of pipe, the fluid properties are evaluated at the inlet temperature of the fluid, as initially the outlet temperature is approximated to be equal to the inlet temperature. The fluid properties for both the interior and exterior fluids are evaluated using the CoolProp library [3], which is discussed more in Section 4.2.1. The overall heat transfer coefficient U is calculated using Equation (2.50), where the total heat transfer resistance R_{tot} is solved using Equation (2.49). Once the overall heat transfer coefficient has been calculated, the outlet temperature is solved using Equation (2.52), where the heat loss $\dot{Q}$ is evaluated using Equation (2.51). If the temperature of the fluid would cross the saturation temperature of the fluid, the temperature is capped at the saturation temperature, and a phase change is evaluated. The heat flow required to bring the fluid to the saturation temperature is calculated and reduced from the total heat flow, after which the amount of fluid condensing, or evaporating, is calculated using the latent heat of the fluid and the remainder of the heat flow. The surface temperatures

are then re-evaluated using the relevant individual heat transfer resistances and the heat loss $\dot{Q}$. The calculated outlet temperature is compared with the previous known value of the outlet temperature, which for the first iteration is the initial assumption, being equal to the inlet temperature. If the two values of the outlet temperature differ less than the convergence tolerance, for which a value of $1 \cdot 10^{-5}\ \mathrm{K}$ was used, the outlet temperature is deemed to have converged to a valid result, and the solution method advances to the next section of pipe.

If, however, the difference exceeds the convergence tolerance, the solution method returns to the beginning of the current section of pipe. The interior fluid properties are calculated at the new mean temperature, which is the average of the inlet temperature and the latest calculated value for the outlet temperature. The exterior fluid properties are evaluated at the mean temperature of the temperature of the surroundings and the updated exterior surface temperature of the pipe wall, or insulation if the pipe is insulated. With the new evaluations of the fluid properties, the solution method recalculates the heat loss for the pipe section, and continues to do so with the same steps until the calculated value for the outlet temperature converges, or a maximum number of iterations is reached. Due to the behaviour of the analytical solution and the stability of its implicit form, the maximum number of iterations should not be reached in normal calculation cases. Similarly, the use of an under-relaxation factor for the implicit iteration of the outlet temperature was deemed unnecessary. The two nested iterative loops are continued, until the end of the pipeline is reached, at which point the solution method ends and displays the results in the user interface of the calculation program.

Certain quantities, such as the length L of the pipe section acting as the solution domain, the inlet temperature T_{in} of the fluid, and the temperature of surroundings T_{inf}, can be assumed to be provided by the user as part of the initial calculation problem setup. For the calculation program, it is assumed that the temperature of the surroundings stays constant. Additionally, while the length of each iterative solution domain could be dynamically altered based on the conditions, the calculation program divides the pipe into sections of equal length. Shorter solution section lengths provide more accurate results, as the temperature-dependent heat transfer properties are re-evaluated more often. However, shorter solution section lengths also increase the required number of solution sections, thus increasing calculation times. For solution sections after the first one, the inlet temperature can be taken from the outlet temperature of the previous section. As mentioned before, the program can also detect when the temperature of the fluid reaches the saturation temperature for the given pressure. In this case, the condensing, or alternatively evaporating, mass flow is deducted from the main phase mass flow. For small mass fractions of entrained liquid droplets in a gaseous flow, or small mass fractions of evaporated gas in a liquid flow, the approximation is made that the secondary phase does not significantly affect the fluid properties of the primary phase. Thus, the only effect of condensation or evaporation in the interior flow is a reduction in mass flow.

4.1.2 Assumptions

As mentioned briefly at the end of Section 2.1.2, the correlations by Churchill and Chu for natural convection on the pipe exterior for the laminar regime (Equation (2.26)) and the turbulent regime (Equation (2.27)) do not provide continuous results for the Nusselt number in the transition regime between the two correlations in the vicinity of $\mathrm{Ra} \sim 10^9$. This transition from the comparably lower values for the Nusselt number in the laminar region to the higher values of the Nusselt number in the turbulent region causes an abrupt increase in the heat transfer in the system as the Rayleigh number crosses the threshold between the two correlations. Values of the Nusselt number calculated using Equation (2.26), referred to as *Laminar*, and Equation (2.27), referred to as *Turbulent*, for a range of $1 \cdot 10^1 \leq \mathrm{Ra} \leq 1 \cdot 10^{12}$ are presented below for $\mathrm{Pr} = 7$ in Figure 4.4.

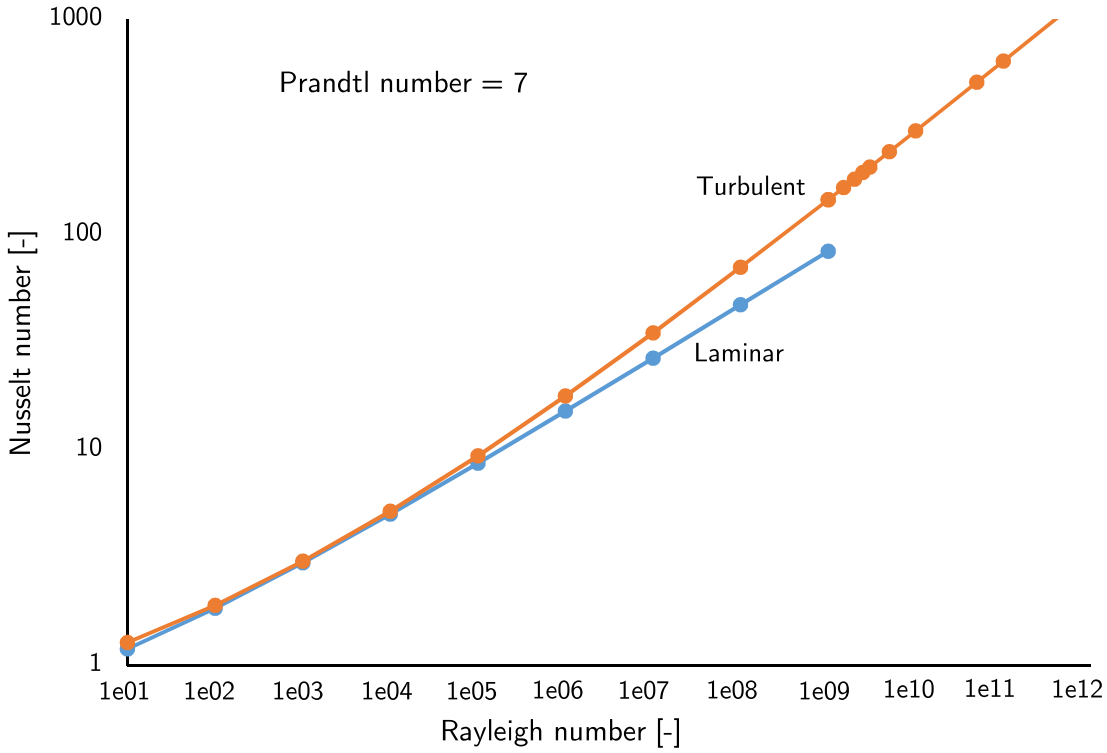

Figure 4.4. *Nusselt number by Churchill and Chu for $Pr = 7$.*

As with all turbulence, it is questionable to claim that laminar fluid flow transitions to full turbulence precisely and predictably at a certain value of a dimensionless group describing the behaviour of the flow. An undisturbed flow may remain laminar for Rayleigh numbers typically describing turbulent flow, while similarly, a laminar flow may transition to turbulence even at relatively low Rayleigh numbers if the flow is disturbed, e.g. by irregularities in the surface geometry. Thus, the sudden discontinuity in values of the Nusselt number in the transitional regime at a specific pre-determined value of the Rayleigh number is not warranted.

As the specific point of transition from laminar to turbulent flow cannot be exactly predicted, a simple interpolation is applied to smooth out the transition from the lower values of the Nusselt number in the laminar regime to the higher values of the Nusselt number in the turbulent regime. The interpolated value of the Nusselt number in the transitional regime is calculated as

$$\mathrm{Nu}_{transitional} = (1 - x) \cdot \mathrm{Nu}_{laminar} + x \cdot \mathrm{Nu}_{turbulent}, \tag{4.1}$$

where $\mathrm{Nu}_{laminar}$ is calculated using Equation (2.26), $\mathrm{Nu}_{turbulent}$ is calculated using Equation (2.27), and the blend factor x is calculated from

$$x = \frac{\mathrm{Ra} - \mathrm{Ra}_{min}}{\mathrm{Ra}_{max} - \mathrm{Ra}_{min}}, \tag{4.2}$$

where Ra_{min} and Ra_{max} are the lower and upper limits, respectively, of the transitional regime. Figure 4.5 presents values of Nusselt number for a range of $1 \cdot 10^1 \leq \mathrm{Ra} \leq 1 \cdot 10^{12}$ using Equation (4.1) for the transitional regime, such that the lower and upper limits of the transitional regime are $\mathrm{Ra}_{min} = 1 \cdot 10^9$ and $\mathrm{Ra}_{max} = 1 \cdot 10^{10}$, respectively.

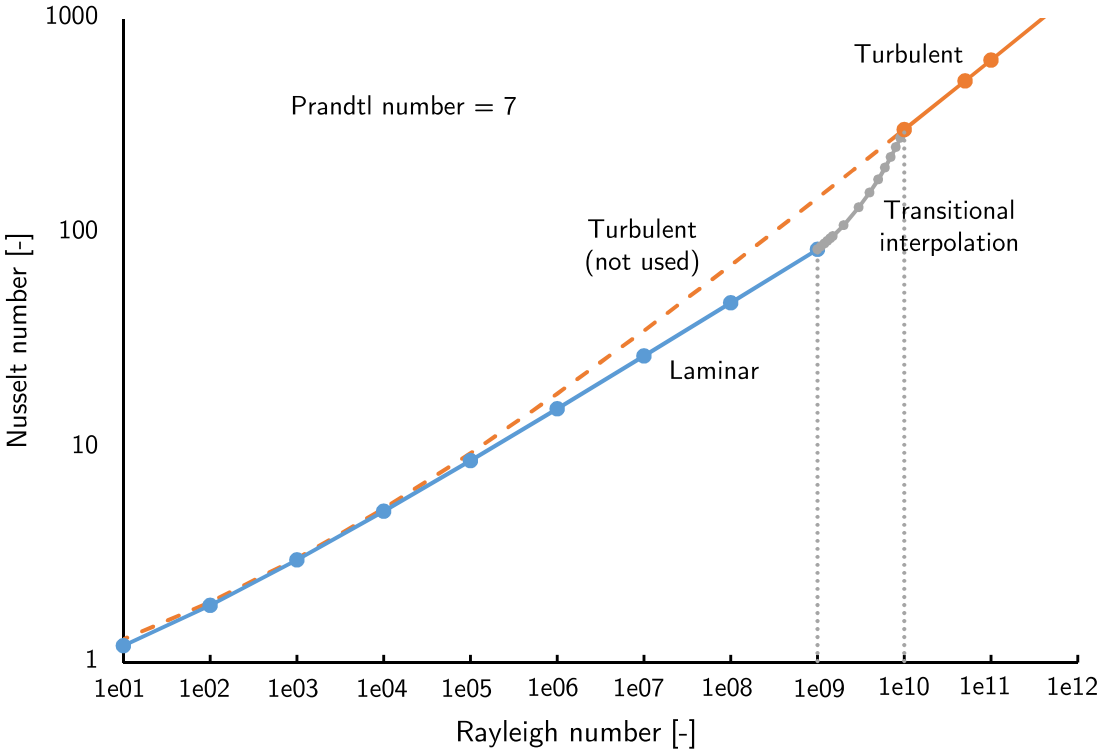

Figure 4.5. *Nusselt number by interpolated Churchill and Chu for* $Pr = 7$.

Typical pipelines in the process industry are mostly horizontal, and especially for long pipelines, for which the evaluation of heat loss is most relevant, it is assumed that the influence of horizontal sections outweighs the influence of vertical sections. Thus the effect of different pipe orientations on phenomena such as natural external convection can be neglected, and the entire length of pipe can be evaluated using the correlations

for natural external convection for horizontal pipes, as presented in Equations (2.26) and (2.27). A similar reasoning can be presented for pipe bends and elbows, which are greatly outweighed by the sections of straight pipe. Thus, the effect of pipe bends and elbows on the heat transfer of the pipe is also neglected.

4.2 Calculation model validation

Ensuring the validity of the results given by the calculation model requires scrutinising both the validity of the numerical solution method used in the model, and also the validity of the underlying correlations used by the solution method. This section discusses the methods with which both of the aforementioned aspects were studied to ensure the reliability and validity of the overall calculation model.

4.2.1 Calculation code

Given the nature of software development, it is necessary to test the calculation program to detect and fix possible issues related to the programming, due to the possibility and probability of human error. From the viewpoint of numerical analysis, it is also sensible to conduct tests to compare the stability and accuracy of the numerical solution methods presented in Chapter 3.

In order to study ways of improving the efficiency of the calculation code without sacrificing accuracy, different numerical solution methods were compared using a series of test calculations. The tests included both the implicit and explicit forms of the analytical solution presented in Section 3.1.1, as well as the implicit and explicit Euler methods discussed in Section 3.1.2. The test cases were formed using three pipe sizes, three fluid inlet temperatures, and three fluid inlet pressures, as presented in Table 4.1, in all 27 unique combinations, as presented in Table 4.2.

Table 4.1. *Test case parameters for numerical method comparison.*

Pipe size	T_{in} [°C]	p [bar]
DN 50	50	1
DN 250	200	10
DN 800	500	100

In all test cases, the fluid was water, with a mass flow of $10\ \mathrm{kg/s}$. The ambient temperature was $T_{inf} = 20\ ^{\circ}\mathrm{C}$, and the pipeline was $100\ \mathrm{m}$ long, with wall thickness of $3.2\ \mathrm{mm}$, thermal conductivity of $k_{pipe} = 14.4\ \mathrm{W/(m \cdot K)}$, and surface emissivity of $\epsilon = 0.8$. In the test cases, the pipeline was calculated in a single part, as well as iteratively in 10 and 100 parts of equal length. As discussed in Section 3.1, the lower step counts

are likely to place the explicit forms of the solution methods at a disadvantage, as they typically require shorter step lengths than their implicit counterparts. However, when the number of steps is as high as 100 for the given pipe length, the temperature gradient is unlikely to be large enough in the cases with lower temperature to cause significant differences in the results of the explicit and the implicit methods. For the cases with a higher temperature, more significant differences may be found. The results of the tests are presented and discussed in Section 5.1.1.

Table 4.2. *All test cases for numerical method comparison.*

	DN	T_{in} [K]	p [bar]		DN	T_{in} [K]	p [bar]		DN	T_{in} [K]	p [bar]
A	50	323.15	1	J	250	323.15	1	S	800	323.15	1
B	50	323.15	10	K	250	323.15	10	T	800	323.15	10
C	50	323.15	100	L	250	323.15	100	U	800	323.15	100
D	50	473.15	1	M	250	473.15	1	V	800	473.15	1
E	50	473.15	10	N	250	473.15	10	W	800	473.15	10
F	50	473.15	100	O	250	473.15	100	X	800	473.15	100
G	50	773.15	1	P	250	773.15	1	Y	800	773.15	1
H	50	773.15	10	Q	250	773.15	10	Z	800	773.15	10
I	50	773.15	100	R	250	773.15	100	+	800	773.15	100

Additionally, to help verify that the calculation program is performing as designed, results from the program were compared to the results presented in the Finnish standard SFS 3977 [31]. Table 1 of the SFS 3977 standard presents values for heat loss per unit length of *uninsulated* pipe for a combination of several different pipe surface temperatures and nominal diameters [31]. The standard provides some additional information on the pipe system in question: the emissivity of the pipe is $\epsilon = 0.8$, the temperature of the surroundings is $T_{inf} = 20\,^{\circ}\mathrm{C}$, and the velocity of the outside air is $V_{ext} = 0\ \mathrm{m/s}$. It is not explicitly stated whether the results neglect external convection entirely, or whether the results assume natural external convection. Through a series of test calculations it was confirmed that the results presented in the standard do include natural exterior convection, using the Equation (2.28) presented in the standard. The results of the comparison are presented in Section 5.1.1.

As the calculation program determines the change in the temperature of the fluid along the length of the pipe, thus also changing the surface temperature of the pipe, test calculations were performed for a pipe length of $1.0\ \mathrm{m}$, so that the change in temperature would be minimal, and thus more in line with the table presented in the standard. Given that the standard presents results based on the surface temperature of the pipe, and the calculation program calculates the surface temperature of the pipe based on internal convection and conduction in the pipe wall, it is to be expected, based on Equation (2.34),

that the calculation results will most closely resemble the results of the standard when the heat transfer resistances of internal convection and pipe wall conduction approach zero. In the calculation tests, sufficiently high mass flows were used, such that the surface temperature closely matched the temperature of the fluid, justifying the comparison with the results presented in the standard. The temperature difference over the metal pipe wall was assumed to be negligible.

The material properties used in the calculation program are evaluated using CoolProp, an open-source C++ library by Bell et al. [3]. The library has been widely accepted, and it is based on a large bibliography of respectable, peer-reviewed papers. Thus, validation of the library and the material properties provided by it is not covered in this work. The library is discussed in length by Bell et al. [3] in their paper.

In order to compare the significance of the different heat transfer modes, the respective heat transfer resistances, presented in Equation (2.49) and Figure 2.1, were compared using several calculation cases of varying parameters, as presented in Table 4.2, the same as with the test comparing different numerical methods. Furthermore, each case was calculated both with and without insulation. For each case, the pipeline was 100 m long with a mass flow of 10 $\mathrm{kg/s}$ of water. Insulation thicknesses of 50 mm, 100 mm, and 200 mm were used for the temperatures 323.15 K, 473.15 K, and 773.15 K, respectively. The thermal conductivity of the insulation was 0.04 $\mathrm{W/(m{\cdot}K)}$. The aim of this part of the study was to find the most and least significant heat transfer modes, so that resources in developing the calculation program could be allocated accordingly. Additionally, information can be gained to determine which input parameters have the most significant effect on the output of the calculation value. This governs the accuracy with which these parameters should be provided to the calculation program.

While heat transfer through heat conduction in the pipe wall and the insulation is calculated using an analytical solution, as presented in Equation (2.36), studying the significance of heat conduction on the overall heat transfer coefficient aids in determining whether or not it is important to accurately evaluate the exact values of thermal conductivity for the pipe wall and insulation materials, or whether a simple approximation is sufficient. Given the relatively small thickness of the pipe walls and the high thermal conductivity of metals, the most common material group in process industry piping, it is to be expected that heat conduction through the pipe wall does not significantly contribute to the overall heat transfer coefficient. In contrast, as the primary purpose of pipe insulation is to decrease the rate of heat transfer, it is to be expected that heat conduction in the pipe insulation has a significant impact on the overall heat transfer coefficient.

As discussed in Section 2.1.3, radiative heat transfer can be modelled with a simple analytical solution, presented in Equation (2.32). However, should the significance of radiative heat transfer dominate, it would be sensible to re-evaluate the assumptions on which the analytical solution is based. Similarly, the accuracy with which the surface emissivity of either the pipe or insulation material is evaluated should be higher, if radiative heat transfer dominates the overall heat transfer coefficient.

The lack of analytical solutions makes the convective heat transfer modes the most important subjects to study in the comparison of heat transfer modes and their significance on the overall heat transfer coefficient. Should the impact of either mode of convective heat transfer be relatively insignificant, it would not be sensible to allocate development and calculation resources in using more intricate correlations and solution methods for that mode of heat transfer. However, should either mode of convective heat transfer dominate the overall heat transfer coefficient, a re-evaluation of base assumptions and the application of more in-depth solution methods and correlations would be beneficial.

The significance of the different heat transfer resistances was studied by calculating the contribution of each heat transfer resistance to the total heat transfer resistance. For the heat transfer resistances of interior convection, conduction in the pipe wall and conduction in the insulation, which are all in series, the contribution of each individual resistance can be calculated simply as R_i/R_{tot}. However, due to the behaviour of resistances in parallel, the same approach cannot be used for the heat transfer resistances of exterior convection and heat radiation. Instead, the contribution for the combination of the two resistances in parallel, $R_{o,tot}$, is calculated, from which the contribution of each individual resistance is calculated with the simple Equation (4.3). The equation, presented here for the contribution x of exterior convection, is

$$x = \frac{R_{conv,o}}{R_{conv,o} + R_{rad,o}} \cdot \frac{R_{o,tot}}{R_{tot}}. \tag{4.3}$$

Thus, the sum of the contributions of each of the five heat transfer resistances is unity, or 100%, and the significance of the heat transfer resistances can be compared easily.

4.2.2 Correlations

Given the complex nature of the phenomena involving turbulent fluid flow, a great deal of effort in the field of academic study has been put into researching and modelling convective heat transfer. While analytical and numerical solutions for heat transfer can be, and have been, derived for laminar flow, heat transfer solutions for turbulent flow largely rely on empirical correlations fitted to experimental data [13]. The transition from laminar to turbulent flow, however, is not very well understood, and as a result, heat transfer correlations for transitional flow are not as readily available and widely accepted as the correlations for laminar and turbulent flow [13].

While widely accepted heat transfer correlations for forced internal convection in cylindrical pipes exist for both the laminar and the turbulent regime, as discussed in Section 2.1.2, the unpredictability of the transitional region between laminar and turbulent flow causes considerable uncertainty for selecting a valid correlation. Building upon earlier work of their own and also by others, Gnielinski has proposed a linear interpolation between the forced internal convection heat transfer solutions for laminar flow and the correlation for turbulent flow modified by Gnielinski, as shown in Equation (2.23) [13]. The interpolation

method connects the gap at $2300 \leq \mathrm{Re}_d \leq 4000$ between the laminar case given by Equation (2.17) and the turbulent case given by Equation (2.23). Due to a lack of relevant experimental data for the region $2300 \leq \mathrm{Re}_d \leq 4000$, Gnielinski has regrettably not been able to provide much in terms of validation for the interpolation method [13].

For natural external convection for horizontal cylindrical geometries, a well-established and widely accepted correlation for the Nusselt number is the correlation by Churchill and Chu [7, see 26 and 36]. While certain sources cite only one correlation for natural convection [36], Equation (2.27), the original work by Churchill and Chu presents a different form of the correlation for laminar natural convection [7, see 26], as presented in Equation (2.26).

The VDI Heat Atlas presents Equation (2.27) without explicitly stating a range of the Rayleigh number for which the correlation is valid [36]. VDI Heat Atlas does, however, present the correlation as an analogy to a similar correlation for natural convection near a vertical surface, for which a valid range of $10^{-1} \leq \mathrm{Ra} \leq 10^{12}$ is presented, covering both laminar and turbulent flows [36]. This implies a contradiction with the separate correlations for laminar and turbulent natural convection as presented by Mills [26], where the laminar correlation (2.26) is stated to be valid for $10^{-6} < \mathrm{Ra} \lesssim 10^{9}$, and the turbulent correlation (2.27) is stated to be valid for $\mathrm{Ra} \gtrsim 10^{9}$. Both sources cite the same work [7] by Churchill and Chu without much further explanation on the validity of the correlations.

The cited work by Churchill and Chu presents Equation (2.26) for the laminar regime $\mathrm{Ra} < 10^{9}$, except for the range $\mathrm{Ra} < 10^{-6}$ based on poor performance of the correlation when compared with experimental data on small wires [7]. Equation (2.27) is presented in the cited work by Churchill and Chu as valid for all values of $0 < \mathrm{Ra} < \infty$, with the acknowledgements that the equation fails to represent the discrete transitions from laminar to turbulent flow, and that Equation (2.26) better represents the values based on experimental data on uniform surface temperatures in the laminar regime, or $\mathrm{Ra} < 10^{9}$ [7].

4.3 Optimisation model construction

The objective of the economic optimisation of pipe insulation is minimising cost over the lifetime of the pipeline. As mentioned earlier, this can be achieved through evaluating and minimising the annual costs of the pipeline. This section discusses the numerical method used for optimising insulation thickness, and the insulation cost function used in the optimisation analysis.

4.3.1 Minimising cost over pipeline lifetime

Initially in the development of the optimisation tool, a *brute force* approach was deemed sufficient for determining the optimal insulation thickness. Thus, the heat loss for the same pipeline was evaluated up to 41 times, using different insulation thicknesses ranging from no insulation to $400\ \mathrm{mm}$ of insulation, in increments of $10\ \mathrm{mm}$. The total annual costs for each case were evaluated using Equation (3.12), and the insulation thickness corresponding with the lowest total annual costs was chosen as the economically optimal insulation thickness. While this method spends noticeably more time than what is needed to find the optimal insulation thickness, it is very robust and reliable.

For the economical insulation thickness optimisation analyses presented in this thesis, a continuous cost function was used for the insulation price. The function is fitted to price data tables from a commercial pipe insulation provider, referenced in December 2019. The correlation function for insulation cost per unit length of pipe, C_{ins}, resembles a linear function of insulation thickness t,

$$C_{ins} = k \cdot t + b, \tag{4.4}$$

where k is the slope of the linear function and b is a constant. However, to ensure a better fit to the data, both the slope k and pseudo-constant b are functions of pipe outer diameter D. The function for slope k is a linear function of pipe outer diameter D, such that

$$k = k' \cdot D + b', \tag{4.5}$$

where k' and b' are constants which were fitted to the price data. The function for the pseudo-constant b,

$$b = \frac{D^a}{d^a} + c, \tag{4.6}$$

similarly contained fitted constants a, c, and d. The values for the fitted constants are presented in Table 4.3. The full price correlation function can be acquired by substituting Equations (4.5) and (4.6) into Equation (4.4), resulting in

$$C_{ins} = (k' \cdot D + b') \cdot t + \left(\frac{D^a}{d^a} + c\right). \tag{4.7}$$

Table 4.3. *Insulation cost function parameters.*

Constant	Value
k'	0.001321
b'	0.168832
a	3.489456
c	1.523564
d	283.5772

Insulation prices as a function of insulation thickness for pipes of different sizes are presented in Figure 4.6, comparing prices obtained from the tables with prices acquired using Equation (4.7).

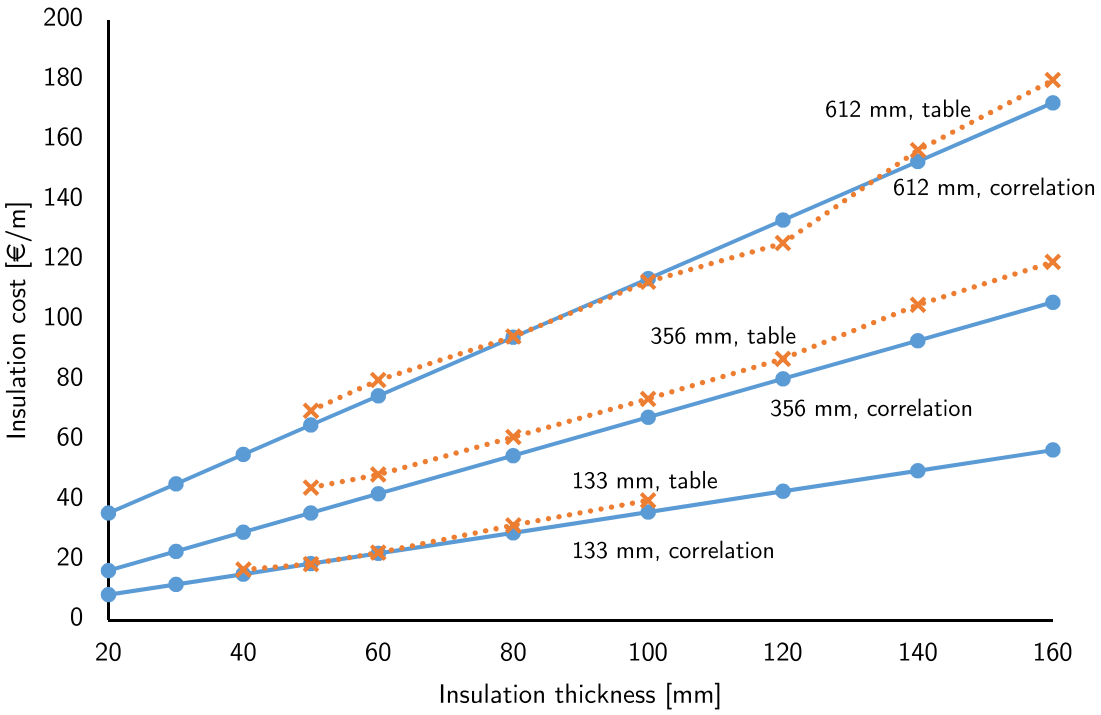

Figure 4.6. *Comparing the insulation price correlation with commercial price tables for different pipe sizes.*

Three different pipe sizes have been selected for the comparison in Figure 4.6, as presented by the labels. Overall, the prices acquired from the correlation are in sufficiently good agreement with the prices in the commercial table. While a more perfect match could likely be achieved using a more intricate correlation, the objective here is not to perfectly model the particular price table, but rather model it with enough accuracy to decently represent the market price level as a whole. Naturally, for utilising the full software solution, the end user is encouraged to provide, via the user interface, price data that most accurately represents the current market situation for the end user.

4.4 Optimisation model validation

The Finnish standard SFS 3977 provides pre-calculated tables of suggested insulation thickness to minimise total costs from heat loss and insulation investment. In the standard, a selection diagram guides the user to reference the correct table, ranging from Table B.1 to B.6. The diagram bases the selection of the table on five parameters: the lifetime of the pipeline, the rate of interest, the price of thermal energy, the annual operating hours of the pipeline, and the type of application. The three application types are power plant piping, process piping, and vessel and pipe bridges. [31] The insulation prices are averaged from several insulation providers, based on prices in November 2005 [31]. The standard suggests the use of an index that describes the market cost level of insulation, with which the insulation tables can be updated to the price levels of present day. The index I is calculated as the average of two additional indices, an installation cost index I_a and an insulation material cost index I_e [31]. The indices can be acquired from the building cost index, published by Statistics Finland [4].

The optimal insulation thicknesses suggested by the calculation program were compared with the insulation thicknesses suggested by SFS 3977 by producing a set of tables, equivalent to Tables B.1–B.6 in the standard, using the same parameters. The economic parameters used in the calculations are presented in Table 4.4.

Table 4.4. *Insulation thickness table comparison parameters.*

Table	t_{oper} [h]	C_{en} [€/MWh]	n [a]	i [-]
B.1	8000	20	5	0.04
B.2	8000	20	7	0.04
B.3	8000	20	10	0.04
B.4	8000	30	8	0.04
B.5	8000	30	12	0.04
B.6	8000	30	15	0.04

In Table 4.4, the energy cost C_{en} is equivalent to the index-modified energy cost e_L/I in SFS 3977. All the calculations related to Table 4.4 featured a $100\ \mathrm{m}$ long pipe of water or steam, based on the conditions, with a mass flow of $\dot{m} = 10\ \mathrm{kg/s}$ at a pressure of $p = 100\ \mathrm{bar}$. The insulation cost per unit length was acquired using Equation (4.7) as discussed in Section 4.3.1. As the correction factor u, which is calculated using Equation (3.14) based on the factor p describing the annual price increase of energy, is not mentioned in the context of the insulation tables in SFS 3977, the effect of u was neglected by assuming $p = 0$, which gives $u = 1$ for the purposes of Equation (3.13).

Due to the differences in the method for optimising insulation and the differences in the methods for evaluating the heat loss, it was expected that the calculation program

would not exactly replicate the insulation tables presented in SFS 3977. The insulation tables of the standard could still be used as an approximate benchmark to ensure that the optimisation tool suggested insulation thicknesses in a sensible range. Once it was established that the optimisation tool performed as intended, the results could be compared with the standard. The results are discussed in Section 5.2.1, and an example comparison of suggested insulation thicknesses between the calculation program and Tables B.1–B.6 in SFS 3977 is presented in Figure 5.11. The comparison tables were produced twice with different methods, to study how efficiently sufficient results could be acquired. Using the implicit form of the analytical solution, discussed in Section 3.1.1, the calculations were performed by calculating the entire pipeline as one part in the first series of tests, and in the second series of tests the pipeline was divided into 100 parts of equal length. The latter method takes considerably longer to calculate the optimal insulation thickness for a single case, but is inherently more accurate in its evaluation. Thus, if the different methods produced significantly different results, the additional time required for the calculations by the latter method would be justified. However, should the results of the methods be identical or only slightly different, it would be sensible to use the faster method to acquire the optimal insulation thickness. The results of the comparison are discussed in Section 5.2.2.

Based on the results of the comparison of suggested insulation thicknesses, two case examples were formed, showcasing the potential cost savings brought by optimising the insulation thickness with the calculation program instead of using the tables in the standard. The case examples were selected to demonstrate different situations in which the calculation program could provide cost savings. The main parameters of the two case examples are presented in Table 4.5.

Table 4.5. *Case example parameters for determining the economically optimal insulation thickness.*

	Case A	Case B
Annual operating hours [$\mathrm{h/a}$]	8000	8000
Cost of energy [€$/\mathrm{MWh}$]	30	20
Lifetime [a]	12	7
Rate of interest [–]	0.04	0.04
Fluid temperature [$^\circ\mathrm{C}$]	250	410
Nominal diameter (DN)	300	800
Compared with standard SFS 3977 table	B.5	B.2

The technical parameters used in the heat loss calculation for both case examples are presented in Table 4.6. While all of the parameters presented in Table 4.5 are required when using the standard Tables B.1–B.6, the values of the parameters presented in Table 4.6 cannot be customised by the user when using the standard tables.

Table 4.6. *Case example common technical parameters.*

	Cases A & B
Fluid	Water
Mass flow [$\mathrm{kg/s}$]	10
Pressure [bar]	125
Pipe length [m]	100
Pipe wall thickness [mm]	3.2
Pipe wall thermal conductivity [$\mathrm{W/(m{\cdot}K)}$]	14.4
Insulation thermal conductivity [$\mathrm{W/(m{\cdot}K)}$]	0.04
Insulation surface emissivity [–]	0.95

In case A the fluid is liquid water, whereas at the high temperature of case B the water is steam. In both the standard tables and the case examples presented here, the ambient temperature was $20\ ^{\circ}\mathrm{C}$. The results of the case examples are discussed in Section 5.2.1 and presented in Figures 5.12 and 5.13 for cases A and B, respectively.

5 RESULTS AND DISCUSSION

The results of the construction and validation steps of the software solution outlined in Chapter 4 are presented and discussed in this chapter, along with case examples which demonstrate the potential benefits of using the software solution over standardised insulation tables.

5.1 Accuracy of the heat loss calculation model

This section focuses on discussing the heat loss calculation model on top of which the insulation thickness optimisation tool is built. Results of the tests discussed in Section 4.2.1 are presented and discussed, with the purpose of evaluating the applicability of the calculation program as the basis for economic optimisation of insulation thickness.

5.1.1 Calculation code

As part of the tests designed and carried out for the calculation code, four different numerical methods for calculating the heat loss were compared, as discussed in Section 4.2.1. The test cases are labelled and their parameters are presented in Table 4.2. The different numerical methods have distinct advantages and disadvantages, the effects of which were evaluated with the tests. The main objective of the heat loss calculation tool is to provide accurate results. Based on its nature, as discussed in Section 3.1.1, the implicit form of the analytical solution is the most likely to be the most accurate numerical method compared to the other three. Characteristically, implicit methods allow the use of fewer calculation steps, leading to relatively quick calculation times despite the additional iteration brought by the implicit form. However, if the pipe is divided into fewer calculation sections, the calculation program will not be able to predict the starting location of condensation in the pipe as accurately. If the calculation with only a single calculation step would predict the heat loss with sufficient accuracy, the calculation could make no statement on where in the pipeline the possible condensation is taking place. Thus, the user may have a valid motivation to evaluate the heat loss of the pipe in shorter calculation sections, leading to more calculation steps. For this reason, the calculation tests evaluated whether computationally cheaper explicit methods could be utilised if a shorter calculation step length was already required by other factors. Between the implicit

and explicit solution methods, there is a possibility of a significant difference in the number of calculation iterations required per calculation case, as is to be expected given the nature of the implicit solution, discussed in Sections 3.1.1 and 3.1.2. Thus, if the explicit form of the solution method provides results with sufficient accuracy, the solution can be acquired more efficiently using the explicit method than with the implicit method. As long as the primary objective of providing accurate results is achieved, a secondary objective of fast performance may be pursued.

While the Euler methods are general-purpose solution methods for solving simple differential equations, the analytical method is built for the exact purpose of solving heat transfer problems in pipes. The analytical method can be acquired and applied as the solution method due to the simple boundary conditions of the heat loss problems discussed in this thesis. Regarding computational cost, there is very little difference between the analytical method and the Euler method, and thus there is little incentive to utilise the Euler method over the analytical solution, as long as the boundary conditions remain simple. However, should the need arise to evaluate the heat loss in pipes with more complex boundary conditions for which an analytical solution cannot be acquired, the Euler methods are a possible solution, and thus included in the calculation tests. In order to compare the numerical methods, results of the calculation cases described in Table 4.2 are discussed below.

As discussed in Section 3.1.2, the step length of the iterative calculation significantly affects the accuracy of the calculation. For explicit methods, a larger step length generally leads to a larger error in the approximation of the difference term. In implicit methods, this error is mitigated to some degree with the additional iteration of each calculation section until convergence is reached, thus allowing implicit methods to achieve greater accuracy even with large step lengths. In Figure 5.1, a comparison of the four methods is presented with two different step lengths. In one set of calculations, the $100\ \mathrm{m}$ long pipe was divided into 100 parts, and in the other set, the pipe was calculated in a single part, giving a considerably larger step length.

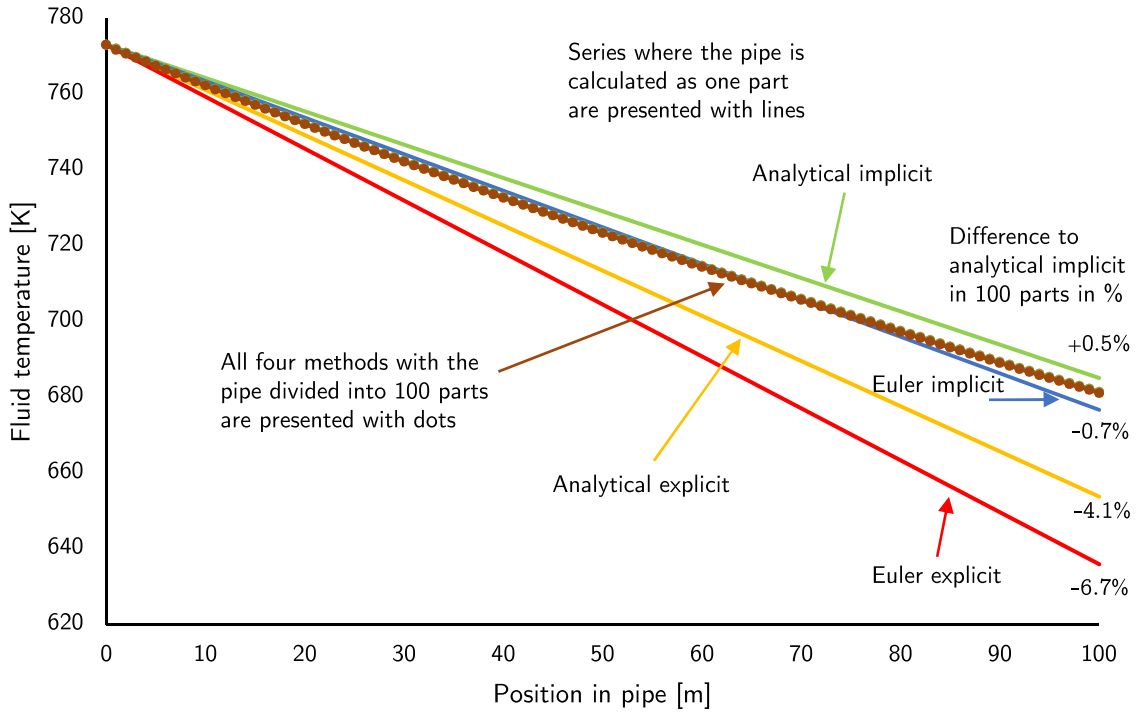

Figure 5.1. *Comparison of numerical methods and the effect of step length for a DN 800 pipe with high fluid temperature.*

As can be seen in Figure 5.1, when the pipe is divided into 100 parts, the difference between the four numerical methods is negligible, as the fluid temperatures calculated with the different methods agree to within 0.1%. When the step size is increased, differences between the methods emerge, as can be seen in the results where the pipe was calculated in a single part. As presented in Figure 5.1, both implicit methods are within 1% of the results calculated in 100 parts even when the entire pipe is calculated in just one part. The explicit methods, however, give a more significant error, over-predicting the temperature drop in the fluid. For further comparison, the calculation methods are compared in Figure 5.2, where the calculation case of Figure 5.1 is repeated with the pipe divided into 10 parts.

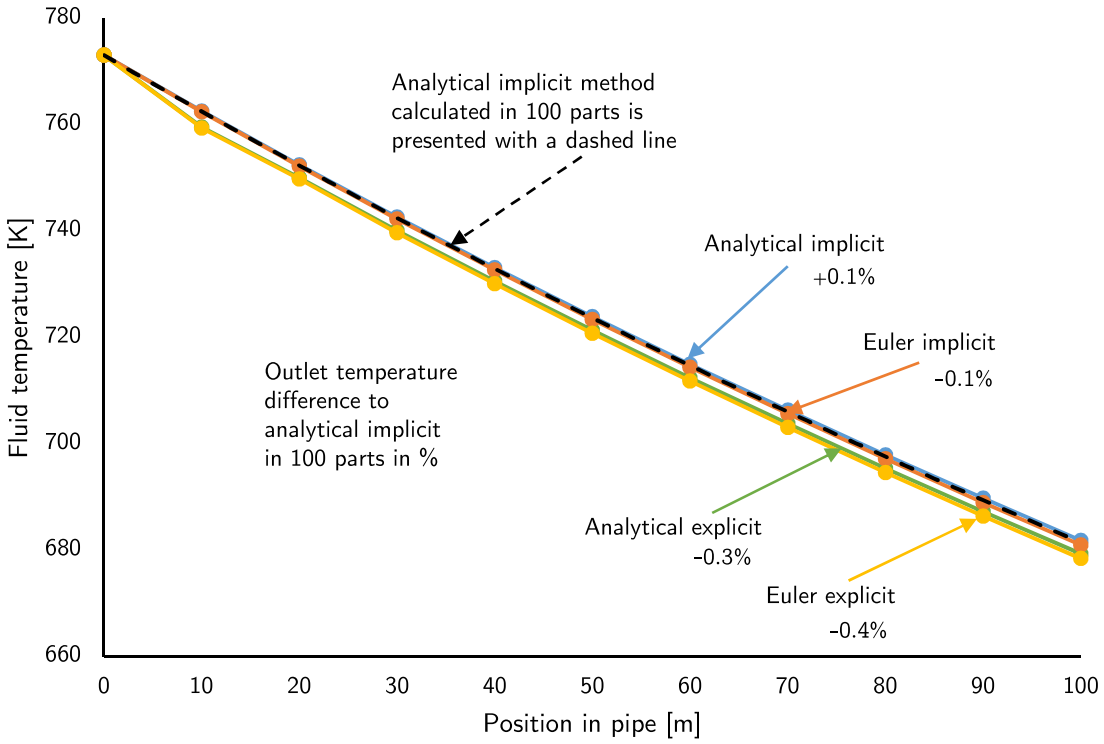

Figure 5.2. *Comparison of numerical methods for high fluid temperature in a DN 800 pipe divided into* 10 *parts.*

The differences between the four methods are present, although not very significant, in Figure 5.2. As with the single-step cases presented in Figure 5.1, the explicit forms over-predict the temperature drop. However, both explicit forms still predict the outlet temperature to within 1% of the results calculated using the analytical implicit solution in 100 parts. In cases with lower temperature, the gradient of the outlet temperature is smaller, as the lower fluid temperature leads to a diminished rate of heat transfer. As the error of the approximated gradient in the explicit forms is greater when the gradient itself is greater, the accuracy of the explicit forms is improved further in cases with lower fluid temperature.

Thus, from the results presented in Figures 5.1 and 5.2, a conclusion can be made that decently accurate approximations of the heat loss can be acquired even with low calculation step counts with either of the implicit methods. If the step count is increased beyond what is otherwise necessary, for example to provide more accurate information on the location of condensation, the explicit methods provide results with essentially the same degree of accuracy as the implicit methods. In this case the use of explicit methods can lead to shorter calculation times. However, as the longest total calculation times observed in the test with the implicit methods were in the range of a few seconds for the entire pipeline, the time savings brought by explicit methods are ultimately negligible for individual calculations.

In the test calculations studying the significance of the different modes of heat transfer and the corresponding heat transfer resistances, clear trends can be seen. In uninsulated

cases, as presented in Table 4.2, the two most dominant modes of heat transfer in all cases were the natural convection and radiative heat transfer on the exterior of the pipe, together contributing typically between 75% and 99% of the total heat transfer resistance. Figure 5.3 presents two comparisons of the heat transfer resistances for different sizes of uninsulated pipe with the lowest fluid inlet temperature of $323.15\ \mathrm{K}$.

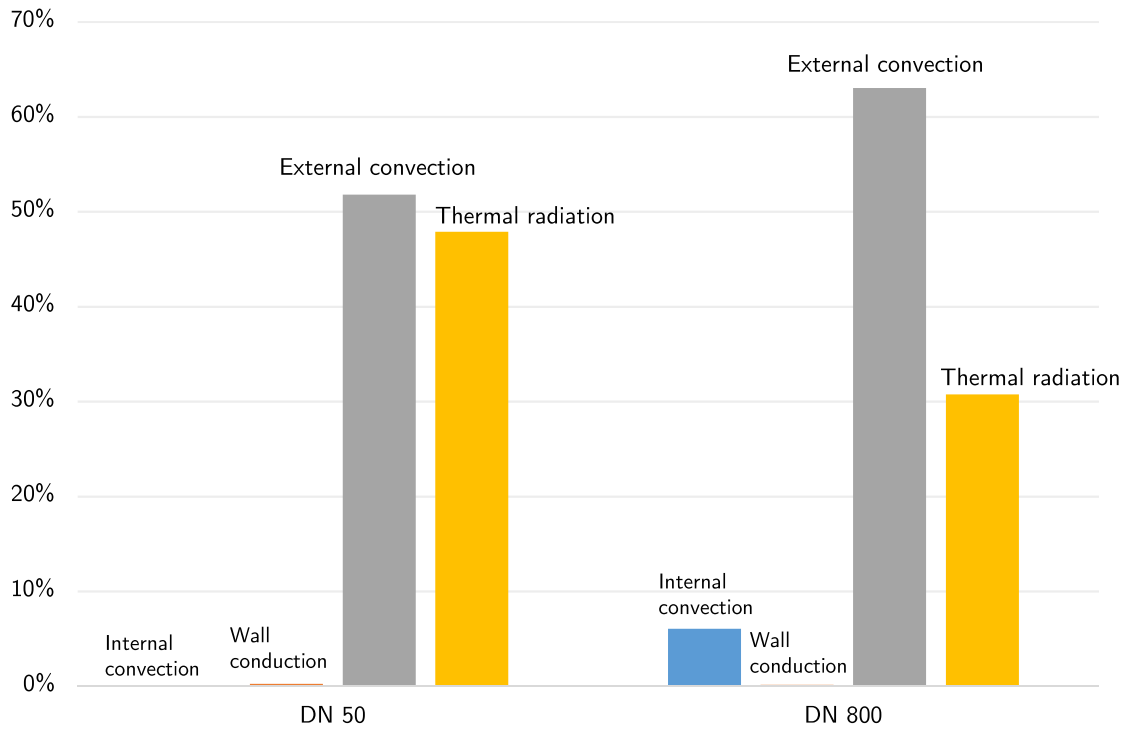

Figure 5.3. *Comparison of heat transfer resistances for an uninsulated pipe with internal fluid temperature of* $323.15\ K$.

The cases presented in Figure 5.3, corresponding with cases B and T in Table 4.2, showcase the phenomena which were observed in the test calculations. At low temperatures and small pipe sizes, the significance of the external convection and heat radiation are roughly equal. However, for larger pipe sizes, the heat transfer resistance of exterior convection becomes considerably more significant. The increased heat transfer surface area in a larger pipe affects both the heat transfer resistance of exterior convection and radiative heat transfer similarly, as can be seen in Equations (2.38) and (2.42), respectively. The heat transfer resistance of radiative heat transfer is a function of the pipe diameter only through the effect of the heat transfer surface area. In contrast, the heat transfer resistance of external convection has an additional dependence on the pipe diameter through the convective heat transfer coefficient, which is a more complicated function of pipe diameter, as discussed in section 2.1.2. Thus, the behaviour of the heat transfer resistances of external convection and radiative heat transfer differ as the pipe diameter is altered. A minor increase in the heat transfer resistance of interior convection can also be seen as the pipe size increases. This is due to the constant mass flow flowing through a larger pipe, causing a lower flow velocity, thus decreasing the

heat transfer coefficient of internal convection. Despite the increase, the significance of internal convection is negligible compared to external convection and radiation. Similarly, heat conduction through the thin metal pipe wall is insignificant in comparison.

Figure 5.4 presents heat transfer resistances from cases H and Z, otherwise corresponding with the cases of Figure 5.3, but at a higher temperature of $773.15\ \mathrm{K}$.

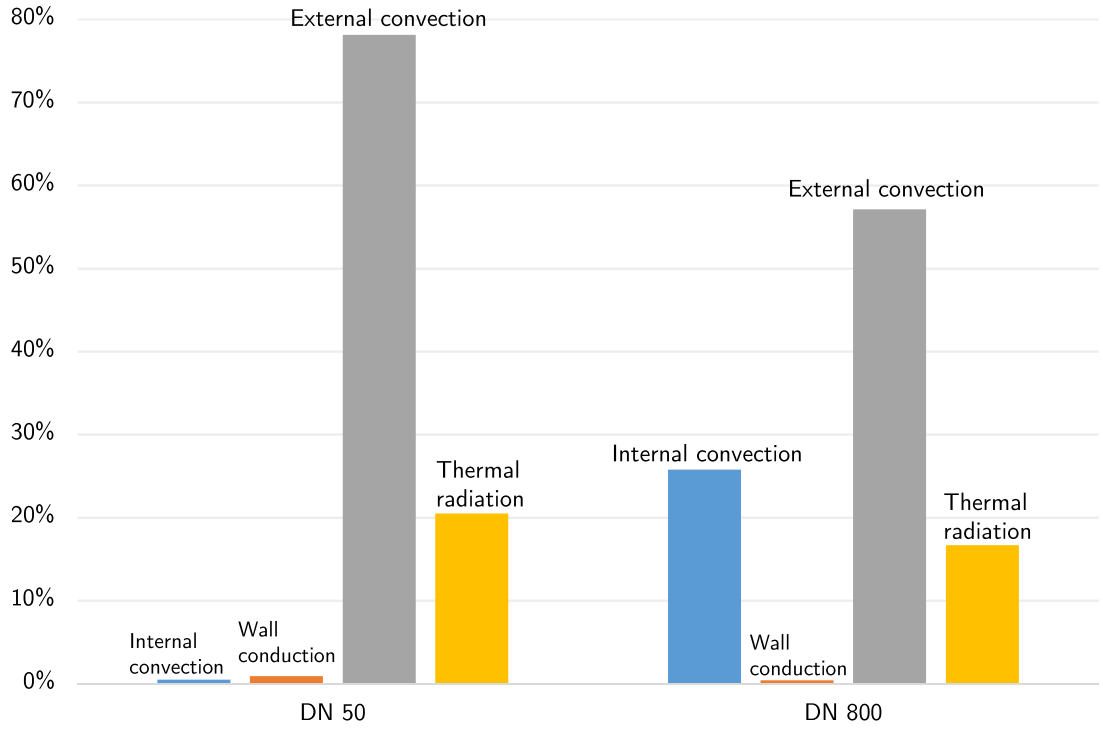

Figure 5.4. *Comparison of heat transfer resistances for an uninsulated pipe with internal fluid temperature of* $773.15\ K$.

As can be seen from Figure 5.4, the contribution of radiative heat transfer to the total heat transfer resistance is considerably smaller at higher temperatures than in the cases presented in Figure 5.3. This is largely due to the fourth-power temperature dependence of radiative heat transfer, presented in Equation (2.32), leading to a third-power inverted dependence on temperature in radiative heat transfer resistance, as presented in Equation (2.42). As the temperature of the fluid increases, the surface temperature of the uninsulated pipe very closely matches the fluid temperature, resulting in a significant decrease in radiative heat transfer resistance, increasing the radiative heat transfer.

Due to the fluid in the test cases being water, the actual value of heat transfer resistance of interior convection increases dramatically as the fluid temperature increases above the saturation temperature. At the high temperature of $773.15\ \mathrm{K}$, the fluid is no longer liquid in either of the cases presented in Figure 5.4. A further comparison of internal convection heat transfer resistance between cases with liquid water and steam is presented in Figure 5.5.

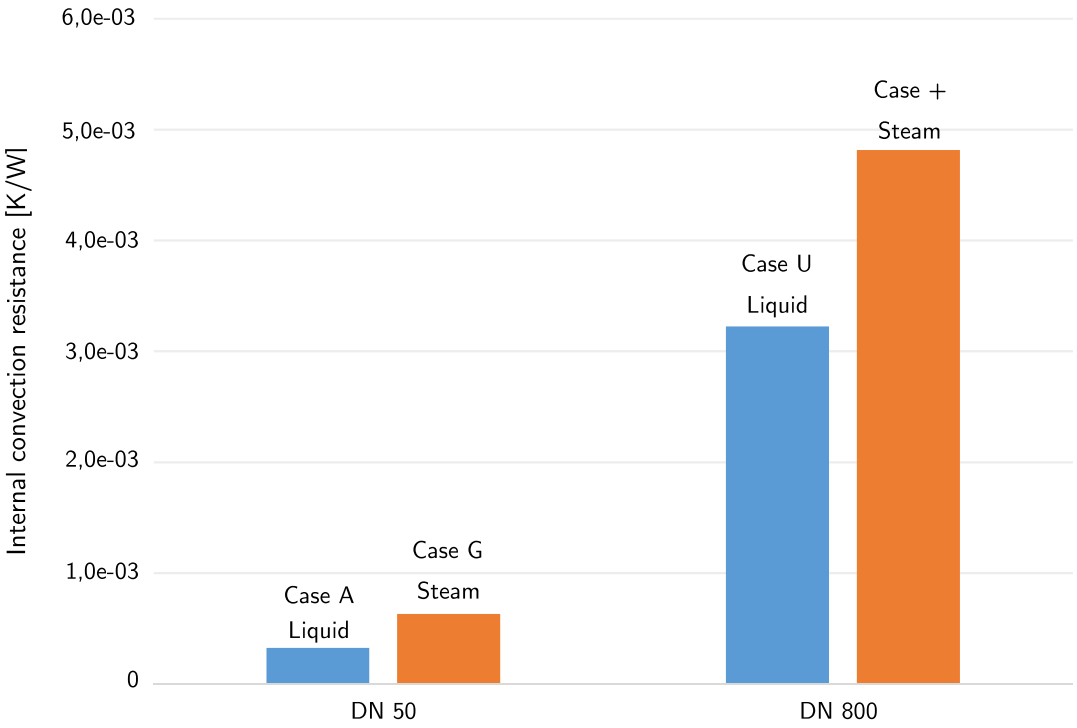

Figure 5.5. *Comparison of internal convection heat transfer resistances for uninsulated pipes with liquid water and steam.*

The increase in internal convection heat transfer resistance is approximately $+94\%$ in case G compared to case A, and $+49\%$ in case + compared to case U. The constant mass flow across the test cases results in the cases with steam having a considerably higher flow velocity, and a significantly higher Reynolds number despite the lower density, leading to a larger Nusselt number. However, the drastically lower thermal conductivity of steam causes the internal convection heat transfer coefficient to be ultimately smaller in the cases with steam than the cases with water. Thus, the value of heat transfer resistance of internal convection is increased in pipe flows featuring steam, or other fluids of low thermal conductivity.

To further demonstrate the effect of the phase of the fluid, and more specifically the thermal conductivity of the fluid, three cases at a fluid temperature of $473.15\ \mathrm{K}$ are presented in Figure 5.6. At the temperature of $473.15\ \mathrm{K}$, the saturation pressure for water is approximately $15.5\ \mathrm{bar}$, and as such, the fluid in the low-pressure cases V and W is steam, and liquid water in the high-pressure case X. The significance of the heat transfer resistance of internal convection is considerable smaller in case X with liquid water than with the other two cases with steam, as can be seen in Figure 5.6.

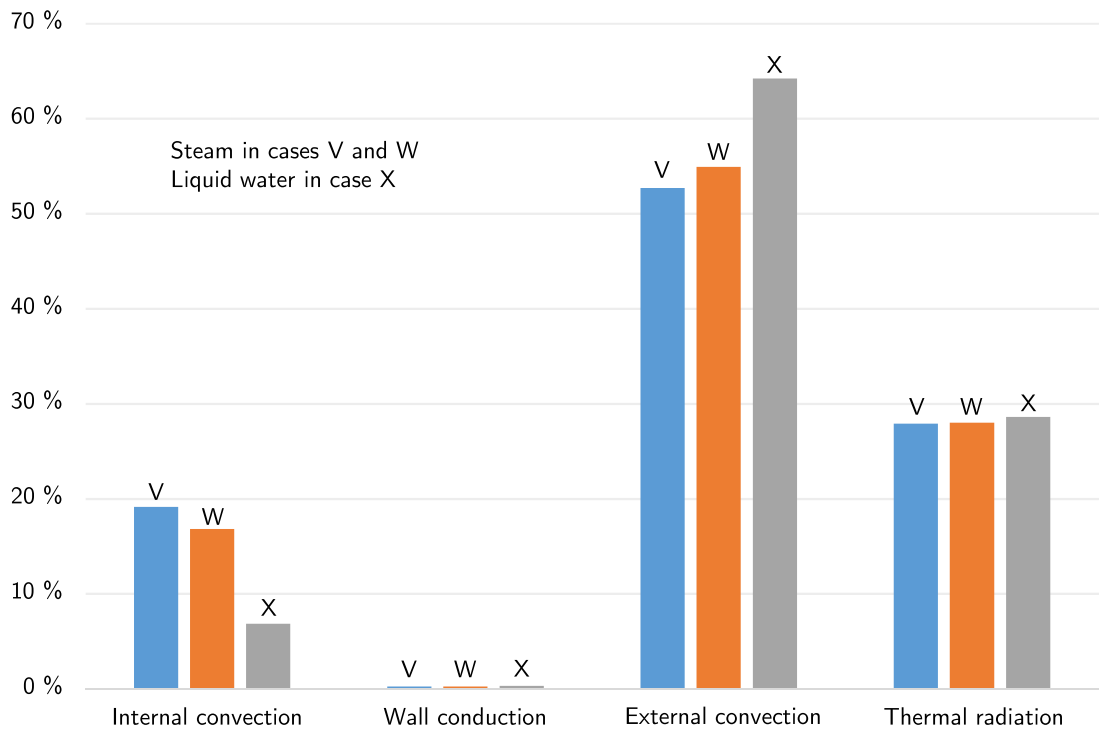

Figure 5.6. *Comparison of heat transfer resistances for uninsulated DN 800 pipes with steam and liquid water at* $473.15\ K$.

In Figure 5.6, an increase in the external convection heat transfer resistance can be seen as well in case X with liquid water, compared to case W with steam. While the internal convection does not directly affect the external convection, the change in internal convection heat transfer resistance alters the surface temperature of the pipe. The change in surface temperature affects the external convection and radiative heat transfer according to the behaviours of the equations of the heat transfer modes, as discussed in Section 2.1. The behaviour of external convection as a function of surface temperature is complicated due to the external fluid properties, which are evaluated as a function of both the surface temperature and the ambient temperature.

From the results of the calculations, examples of which are presented in Figures 5.3, 5.4, 5.5, and 5.6, a conclusion can be drawn that for fluids with relatively high thermal conductivity, such as liquid water, internal convection can largely be neglected, along with heat conduction through metal pipe walls. The most significant modes for the evaluation of heat transfer are thus convective and radiative heat transfer on the exterior of the pipe. At high temperatures the heat transfer resistance of radiative heat transfer diminishes, leaving external convective heat transfer as the most significant factor, providing as much as 60–80% of the total heat transfer resistance. For fluids of low thermal conductivity, such as steam, the contribution of internal convection to the total heat transfer resistance is greater, but still ultimately considerably less significant than the contribution of external convection.

As mentioned in Section 4.2.1, the test cases for comparing the significance of heat transfer resistances were also calculated with insulation. As is to be expected, the effect of pipe insulation dominates the total heat transfer resistance, as it is designed to do. A comparison of heat transfer resistances for selected test cases with $50\ \mathrm{mm}$ of insulation, separated from the corresponding uninsulated cases with an asterisk, is presented in Figure 5.7.

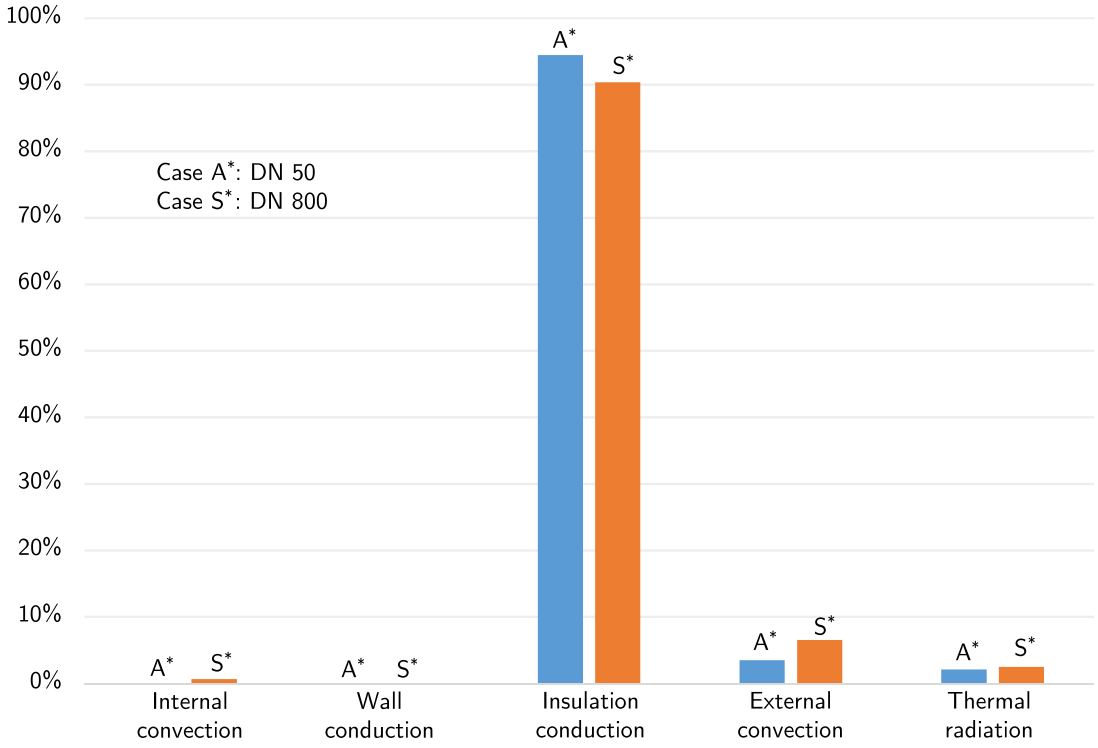

Figure 5.7. *Comparison of heat transfer resistances for insulated pipes with* $50\ mm$ *of insulation and fluid temperature of* $323.15\ K$.

As can be seen in Figure 5.7, the heat transfer resistance of heat conduction through the insulation dominates the total heat transfer resistance of an insulated pipe. For larger insulation thicknesses, the dominance of the insulation is even more prevalent, consistently providing upwards of 90% of the total heat transfer resistance in the calculated test cases. Due to the overwhelming domination of the heat transfer resistance of the pipe insulation, any error in the evaluation of the thermal conductivity of the insulation can have a significant impact on the evaluated value of the heat loss. As discussed in Section 2.2.2, the thermal conductivity of the insulation material typically is a function of the temperature difference between the interior and exterior of the insulation, as well as the mean temperature of the material. In the results presented in this thesis, a constant value for the thermal conductivity of pipe insulation material is used. As shown here, the accuracy of the results could likely be improved by implementing a temperature dependence for the thermal conductivity of the insulation material.

The Finnish standard SFS 3977 presents values of heat losses of uninsulated pipes in Table 1 in the standard, to serve as an example, for pipes of different nominal diameter and surface temperature. As starting values for the calculation, the standard reports a surface emissivity of $\epsilon = 0.8$, ambient temperature of $T_{inf} = 20\ ^{\circ}\mathrm{C}$, and air velocity of $V_{ext} = 0\ \mathrm{m/s}$ [31]. To provide validation for the heat loss calculation model used in this work, heat losses for the same combinations of starting values were calculated and compared with the values presented by the standard. Results from the validation calculation cases are presented in Figure 5.8, as heat loss per unit length of pipe as a function of the outer diameter of the pipe. The different surface temperatures are presented as separate data point series. As with the table in the standard, the temperatures in the full set of calculations ranged from $50\ ^{\circ}\mathrm{C}$ to $500\ ^{\circ}\mathrm{C}$, for nominal diameters ranging from DN 50 to DN 800.

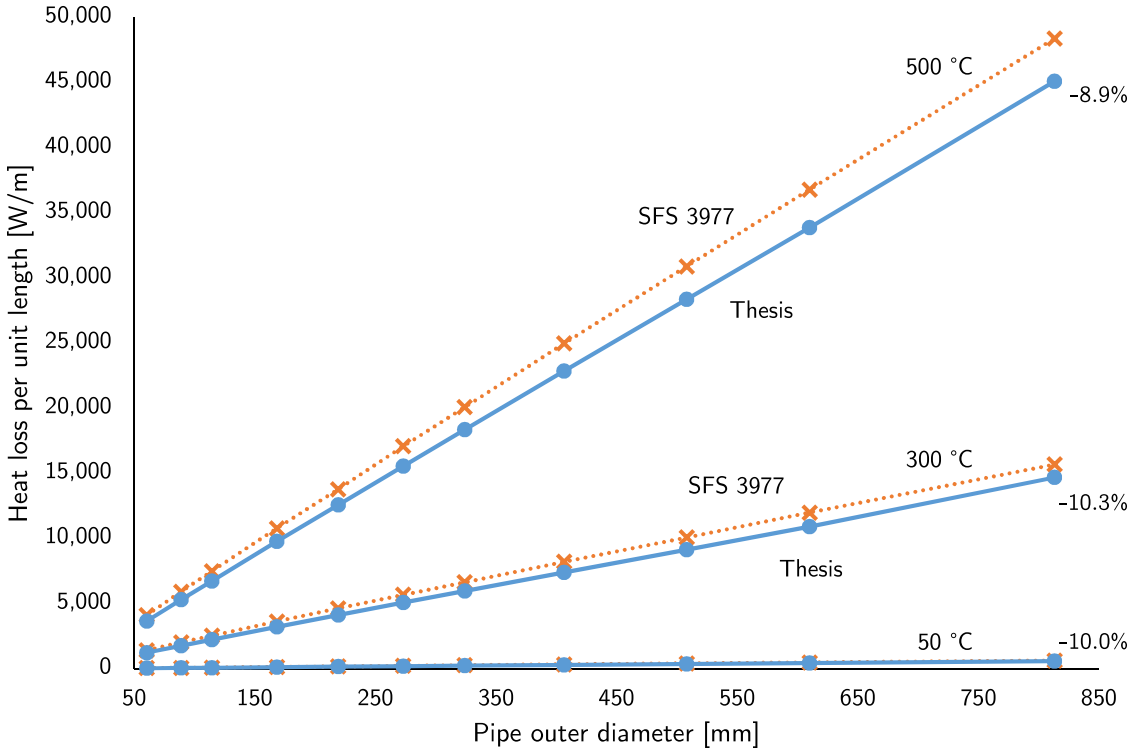

Figure 5.8. *Heat loss of an uninsulated pipe as a function of pipe outer diameter.*

The series in Figure 5.8 show a strong linear behaviour, similarly to the results presented in the standard. The results of the validation calculations are in close agreement with the results of the standard, giving results of approximately 10% less than the standard, across all cases. The difference between the results given by the calculation program and the results presented in the standard is presumably largely due to the different correlation used for external natural convection, as the solution method used for radiative thermal radiation is the same for both sets of results, and the other modes of heat transfer can largely be neglected, as discussed earlier. The solution for natural external convection used in the standard, Equation (2.28), is considerably simpler to implement than the Equation (2.27) suggested by Churchill and Chu, and provides approximately 30% higher

heat transfer coefficients than the coefficients acquired in this thesis using Equations (2.26) and (2.27). In Figure 5.9, the data points from the comparison of the heat loss of an uninsulated pipe are presented instead as a function of pipe surface temperature, such that the data points are grouped into series corresponding with the different pipe sizes.

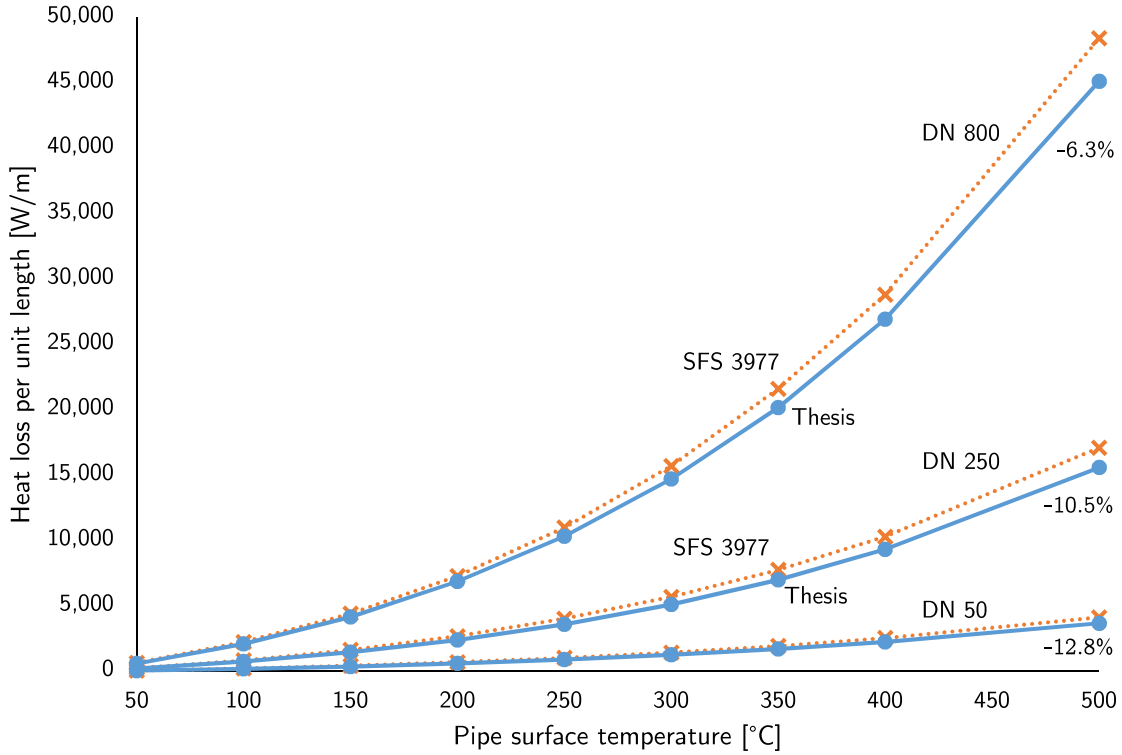

Figure 5.9. *Heat loss of an uninsulated pipe as a function of pipe surface temperature.*

When plotted as a function of temperature in Figure 5.9, the heat losses of an uninsulated pipe grow at an increasing rate as the surface temperature increases. This is to be expected, given that the nonlinear fourth-power temperature dependence of heat loss through thermal radiation, as presented in Equation (2.32), becomes more prevalent as the temperature is increased. Additionally, as can be predicted from Equation (2.32), the effect is more pronounced in larger pipe sizes, as the heat transfer surface area increases as the outer diameter of the pipe is increased.

5.1.2 Correlations

As discussed in Section 5.1.1, external convection is typically the most significant contributor in the total heat transfer resistance of an uninsulated pipeline. As discussed in Sections 2.1.2 and 4.2.2, well-established correlations by Churchill and Chu [7] for natural external convection exist for laminar and turbulent flow, with Equations (2.26) and (2.27), respectively. Due to Equation (2.27) being technically valid for both the laminar and turbulent regimes, sometimes Equation (2.26) is omitted in the literature

[36]. Here, the results of both equations are compared for the laminar regime, to study whether significant benefit can be gained by implementing both equations and transitioning between them depending on the Rayleigh number. The results of the two equations are visualised in Figure 5.10.

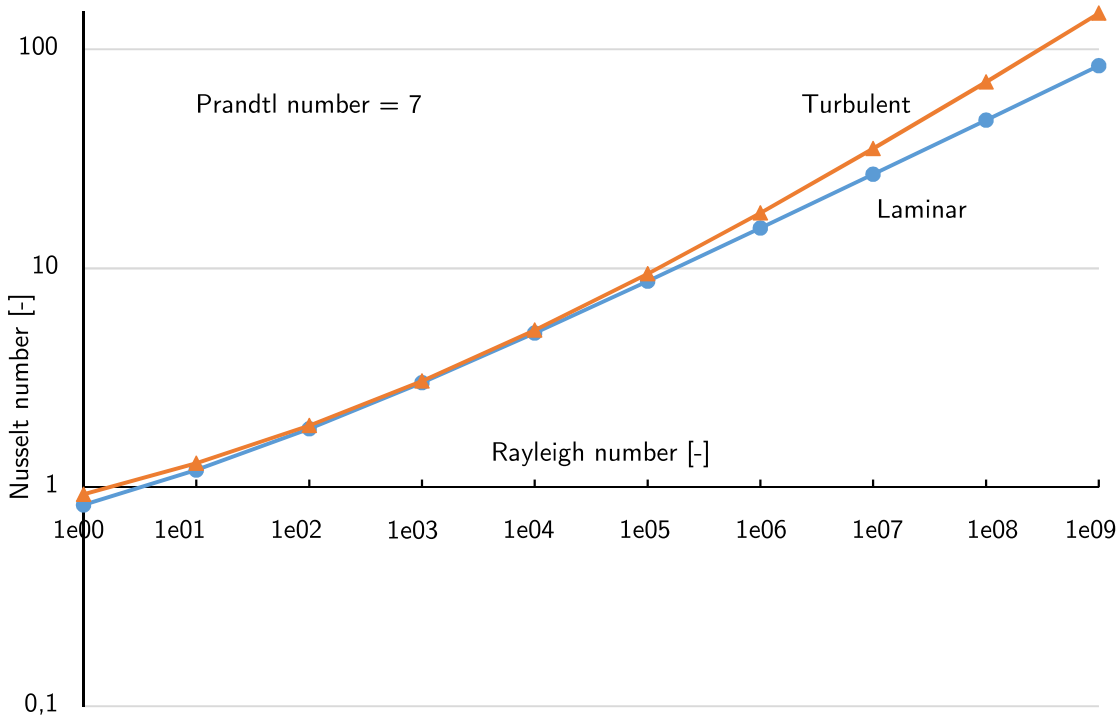

Figure 5.10. *Comparison of two correlations by Churchill and Chu for the laminar regime of external natural convection.*

Figure 5.10 shows that while the two correlations closely agree in certain ranges of relatively small Rayleigh numbers, the results diverge as the Rayleigh number grows. A further comparison of the results of Equations (2.26) and (2.27) for a range of different Prandtl numbers is presented in Table 5.1. The values in the table are calculated simply as the relative difference between the results of the two equations, normalised with the result of the laminar equation, or

$$x = \frac{\mathrm{Nu}_{turbulent}(\mathrm{Ra},\,\mathrm{Pr}) - \mathrm{Nu}_{laminar}(\mathrm{Ra},\,\mathrm{Pr})}{\mathrm{Nu}_{laminar}(\mathrm{Ra},\,\mathrm{Pr})} \cdot 100\%. \tag{5.1}$$

The equations are compared for the laminar regime in the range of $1 \cdot 10^0 \leq \mathrm{Ra} \leq 1 \cdot 10^9$, and for different values of the Prandtl number ranging from 0.33 to 7. The data series presented in Figure 5.10 are also represented in Table 5.1.

Table 5.1. *Error of the turbulent correlation compared to the laminar correlation for the laminar regime of external natural convection by Churchill and Chu.*

Ra [-] \ Pr [-]	0.33	0.7	1.3	3	7
$1 \cdot 10^0$	+13.50%	+12.90%	+12.48%	+12.01%	+11.65%
$1 \cdot 10^1$	+9.44%	+8.67%	+8.15%	+7.61%	+7.22%
$1 \cdot 10^2$	+5.08%	+4.43%	+4.02%	+3.63%	+3.36%
$1 \cdot 10^3$	+2.13%	+1.88%	+1.75%	+1.66%	+1.63%
$1 \cdot 10^4$	+1.92%	+2.22%	+2.47%	+2.80%	+3.06%
$1 \cdot 10^5$	+5.19%	+6.12%	+6.82%	+7.60%	+8.20%
$1 \cdot 10^6$	+12.35%	+13.99%	+15.15%	+16.44%	+17.40%
$1 \cdot 10^7$	+23.75%	+26.14%	+27.82%	+29.65%	+31.02%
$1 \cdot 10^8$	+39.79%	+43.02%	+45.28%	+47.72%	+49.54%
$1 \cdot 10^9$	+61.04%	+65.23%	+68.14%	+71.29%	+73.61%

As can be seen from Table 5.1, the error of the turbulent equation compared to the laminar equation behaves quite similarly for the different values of the Prandtl number presented. The two correlation equations are closest to each other in the range of $1 \cdot 10^3 \leq \mathrm{Ra} \leq 1 \cdot 10^4$, where the error is relatively small. For smaller and larger values of the Rayleigh number, however, the error grows significantly, especially closer to the transitional regime.

In Section 5.1.1 it was discussed that the significance of internal convection on the total heat transfer resistance is typically negligible in a pipeline. Only in the rare case of a high fluid temperature in a very large pipe did the effect of internal convection become significant, as presented in Figures 5.4 and 5.6. Thus, it was not deemed worthwhile or necessary to implement the internal convection interpolation method for the transition between laminar and turbulent flow by Gnielinski, which was discussed in Section 4.2.2. Instead, the simpler correlation Equation (2.21), also proposed by Gnielinski, was used. Additionally, the effect of development length on the internal convection, presented in Equation (2.25), was neglected. In future work, should the need for improved accuracy for the evaluation of internal convection arise, these aspects should be reconsidered. As discussed earlier, the need for a more rigorous analysis of internal convection would most likely be related to fluids with low thermal conductivity, such as steam.

5.2 Economic optimisation of insulation thickness

In this section, the results of the insulation optimisation tool are discussed. Section 5.2.1 compares the economically optimal insulation thicknesses suggested by the optimisation tool with the insulation tables of the Finnish standard SFS 3977. In Section 5.2.2, the efficiency and accuracy of the optimisation tool are discussed.

5.2.1 Comparison to existing insulation optimisation methods

As discussed before, a common method of choosing the insulation thickness for a pipeline in the industry is by using tables of suggested insulation thicknesses presented in standards, such as the Finnish standard SFS 3977 [31]. In SFS 3977, a selection diagram guides the user to select the correct insulation table based on parameters which affect the economical optimum of insulation thickness [31]. In Figure 5.11, optimal insulation thicknesses for a DN 300 pipe as a function of fluid temperature are presented, comparing the insulation thicknesses suggested by the calculation program created in this thesis against the insulation thicknesses suggested by SFS 3977. The economic parameters for the selection diagram are presented in Table 4.4. While test calculation runs were performed using different pipe sizes ranging from DN 15 to DN 800, results based on a DN 300 pipe are presented as an example.

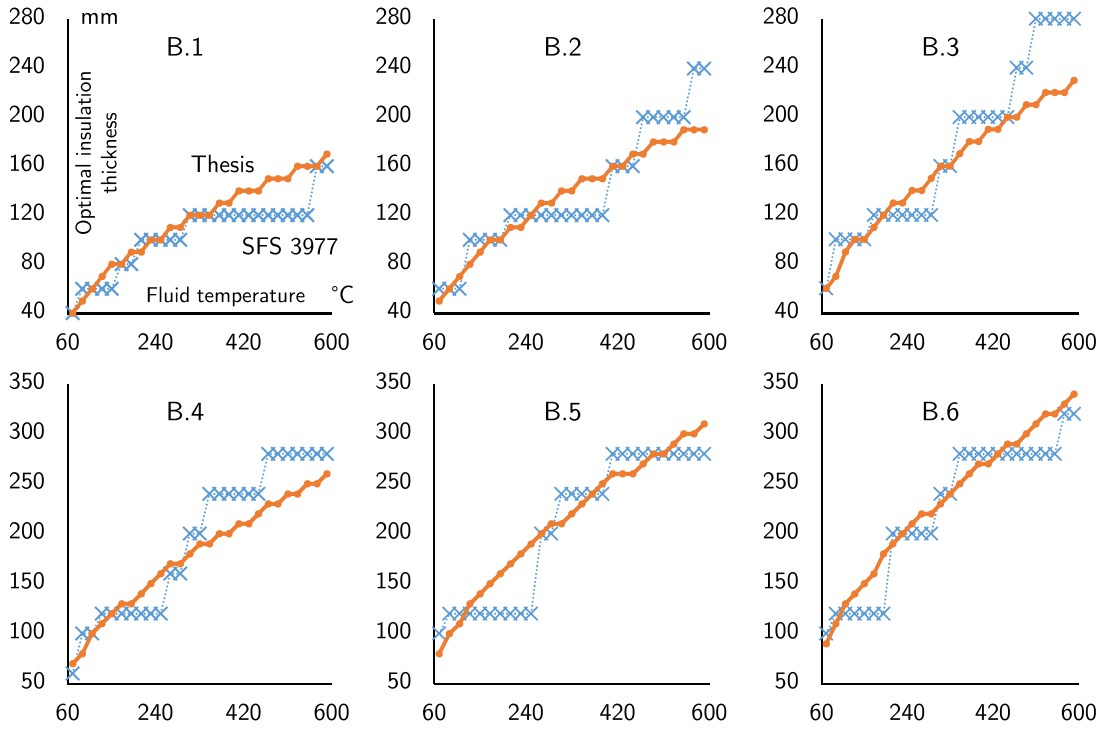

Figure 5.11. *Comparison of optimal insulation thicknesses for DN 300 pipes suggested by the calculation program of this thesis and SFS 3977.*

On a general level, the insulation thicknesses suggested by the calculation program resemble the insulation thicknesses suggested by SFS 3977. A key difference between the two methods is that SFS 3977 limits insulation thicknesses to a small set of discrete common insulation thicknesses, whereas the calculation program outputs insulation thicknesses at a resolution of $10\ \mathrm{mm}$. This can lead to significant differences between the insulation thicknesses suggested by the different methods near the thresholds where

the standard moves on to a different discrete level of insulation thickness. However, this does not explain all the cases where the methods differ, such as in the comparison with the standard Table B.3 at high temperatures. In this case, the insulation thicknesses suggested by the calculation program would not warrant the use of the higher discrete insulation thickness, $280\ \mathrm{mm}$, even at the highest temperatures. This suggests that according to the insulation optimisation method suggested in this thesis, in certain cases cost savings could be achieved compared to the insulation thicknesses suggested by SFS 3977, even if the optimum given by the calculation program is rounded to the same set of discrete insulation thicknesses used by the standard.

As a large number of test cases were calculated to compare the calculation program and SFS 3977, and to provide data for Figure 5.11, it was discovered that a significant portion of the time taken by each calculation iteration was consumed in evaluating the material properties with the *PropsSI* function in CoolProp. In order to improve the performance of the calculation program and decrease calculation times, measures were taken, such as calling the *PropsSI* function using temperature and *density*, instead of temperature and *pressure*, as suggested by the authors of CoolProp [3]. In addition, tests were performed where the material properties would only be re-evaluated if the fluid temperature had changed significantly from the previous evaluation. Different values of the temperature change threshold were experimented with, acknowledging that a larger threshold would decrease the number of times when the material properties would be re-evaluated, thus decreasing the time elapsed, at the cost of lowered accuracy.

While noticeable improvements in performance were achieved with threshold values of $1\ \mathrm{K}$ and $0.5\ \mathrm{K}$, the accuracy of the calculation program appeared questionable while the threshold was in use. One phenomenon brought by using the threshold was such that the optimal insulation thickness for a certain pipe size would be smaller at certain individual temperatures than at the previous data point with lower temperature. After closer investigation, this phenomenon was found to relate to the behaviour of the natural convection on the exterior of the pipe, when operating near the threshold of whether or not to re-evaluate the material properties. When the material properties were re-evaluated for each iteration step, such behaviour did not occur. Thus, it was deemed that the improvement in calculation times could not justify the use of the method of reusing material properties, as the method would jeopardise the accuracy of the results provided by the calculation program.

The insulation thickness optimisation method proposed in this work can provide cost savings compared to relying on the insulation thickness tables of a standard in two scenarios: by suggesting a greater insulation thickness when insulation is cheaper than energy, or by suggesting a smaller insulation thickness when energy is cheaper than insulation. The two case examples described in Table 4.5 showcase both scenarios, and suggest potential cost savings compared to the use of the Finnish standard SFS 3977. The cases are parametrised using the quantities related to economic optimisation, as discussed in Section 3.2.1 and as used in SFS 3977. The price of insulation was

evaluated using price data from a Finnish process industry pipe insulation provider, as discussed in Section 4.3.1. The insulation and energy cost, as well as the total cost, for case A, as a function of insulation thickness are presented in Figure 5.12. The figure also indicates the optimal insulation thicknesses as suggested by the insulation optimisation method proposed in this work, and by the Finnish standard SFS 3977.

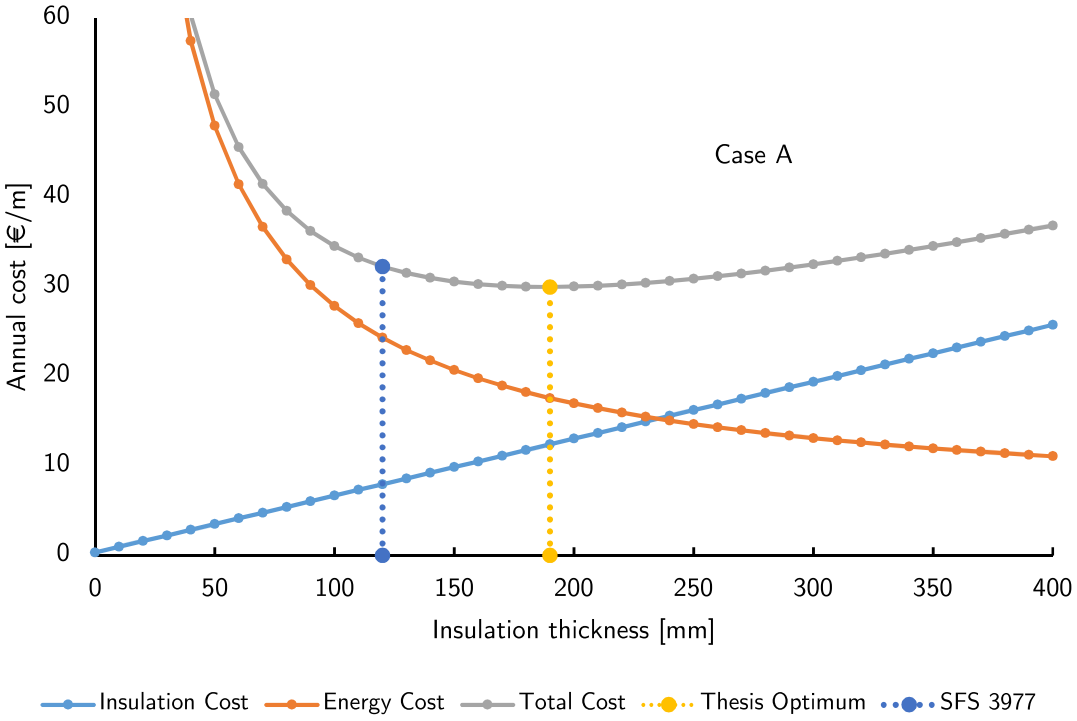

Figure 5.12. *Case A cost comparison.*

In case A, the high cost of energy justifies the investment cost of thicker insulation, which decreases the heat loss and drives down the cost brought by heat loss. Due to diminishing returns from increasing insulation thickness, an optimum can be found where increasing the insulation thickness would increase insulation cost more than it would decrease the cost of heat loss. According to the optimisation method proposed in this work, the optimal insulation thickness for case A would be 190 mm, whereas the Finnish standard SFS 3977 would suggest an insulation thickness of 120 mm, as read from Table B.5 [31]. An economic comparison of the two insulation thicknesses is presented in Table 5.2. The cost functions for case B are presented in Figure 5.13.

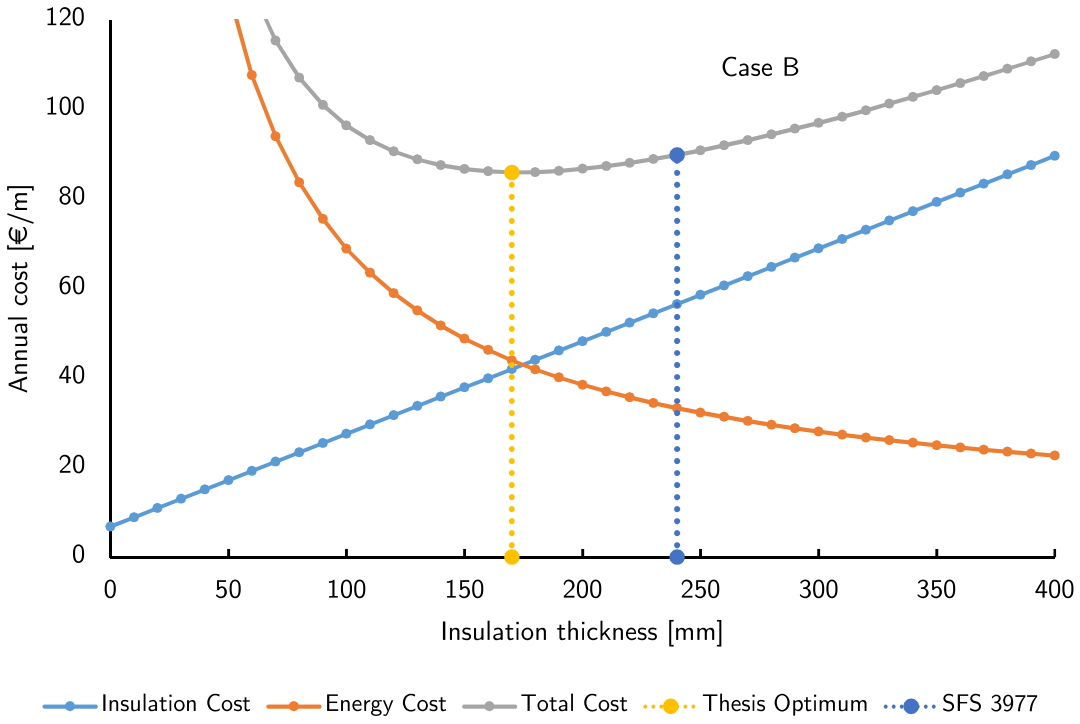

Figure 5.13. *Case B cost comparison.*

As the cost of energy is low in comparison to the cost of insulation, in case B the insulation optimisation method proposed in this work suggests an insulation thickness of 170 mm, which is considerably smaller than the insulation thickness of 240 mm proposed by SFS 3977 in Table B.2 [31]. The potential cost savings brought by the smaller insulation thickness in case B are presented in Table 5.2. Figure 5.14 visualises the insulation thicknesses suggested by the calculation program and by SFS 3977, and the difference in the suggested insulation thicknesses, which was used as a guide for the initial selection of the case examples.

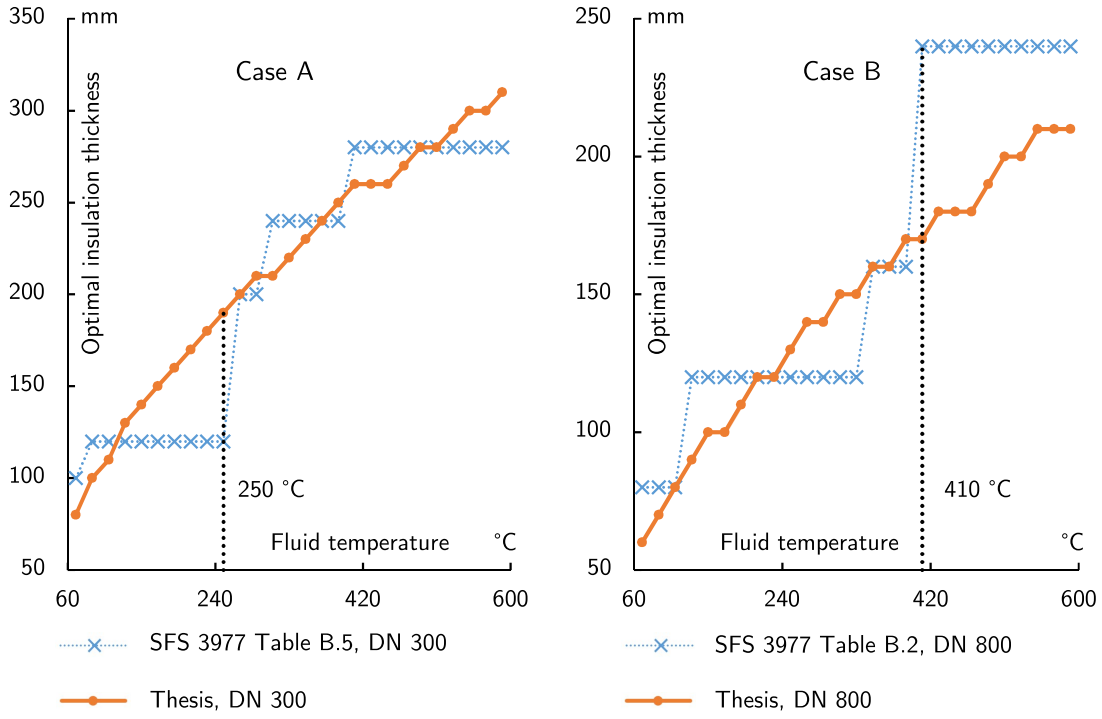

Figure 5.14. *Visualisation of case examples A and B.*

As Figure 5.14 shows, the largest differences between the insulation thicknesses suggested by the calculation program and SFS 3977 can be found in the vicinity of temperatures where the insulation thickness suggested by SFS 3977 transitions to a new discrete insulation thickness. Thus, the most significant potential cost savings brought by using the insulation thickness suggested by the calculation program rely on the availability of insulation with varying or customisable thickness. However, as discussed earlier in relation to Figure 5.11, even if the selection of insulation thicknesses is limited to the ones suggested by SFS 3977, cost savings can be achieved when the calculation program proposed in this thesis is used to guide at which temperature the transition to a new discrete insulation thickness should be made. Table 5.2, where it is assumed that insulation thicknesses are available at increments of $10\ \mathrm{mm}$, presents the potential cost savings of using the insulation thickness suggested by the calculation program instead of the insulation thickness suggested by SFS 3977.

Table 5.2. *Cost savings in the case examples.*

	Case A		Case B	
	Thesis	SFS 3977	Thesis	SFS 3977
Insulation thickness [mm]	190	120	170	240
Annual insulation cost [€/m]	12.41	7.96	42.03	56.52
Annual energy cost [€/m]	17.58	24.32	43.91	33.30
Annual total cost [€/m]	29.99	32.28	85.93	89.82
Annual total cost [€]	2998.70	3227.62	8593.19	8982.08
Annual cost difference [€]	-228.92	–	-388.89	–
Lifetime cost [€]	35984.42	38731.46	60152.34	62875.57
Lifetime cost difference [€]	-2747.04	–	-2722.22	–
Lifetime cost difference [€/m]	-27.47	–	-27.22	–
Cost difference	-7.1%	–	-4.3%	–

Both cases show potential cost savings in the lifetime cost of the pipeline: by suggesting a larger insulation thickness than the standard in case A, and by suggesting a smaller insulation thickness than the standard in case B. While the annual and lifetime cost savings may appear meagre by themselves, their effects are multiplied in a process plant featuring dozens of similar pipelines.

5.2.2 Efficiency and accuracy of the optimisation

The calculation time for a single iteration of the heat loss, solving the outlet temperature for the entire pipeline in a non-iterative method, or for one part of the pipeline in an iterative method, is in the range of 25 milliseconds for the calculation program. By itself, such a short calculation time is negligible. However, as the number of required iterations is increased, the calculation times begin to compound noticeably. In a majority of the test calculations performed as part of this work, an iterative method was used, where the heat loss was solved by dividing the pipeline into 100 sections, which were calculated in succession. This naturally increases the calculation time consumption by a factor of 100, bringing the typical calculation time from 25 milliseconds to 2.5 seconds, which is a very noticeable duration for the user. The required calculation time is further increased when an implicit solution method is used. For the test calculations in this work, the implicit methods used a tolerance of $1 \cdot 10^{-5}$ K for the difference in the value of the outlet temperature between iterations.

As the optimisation method for optimising the insulation thickness relies on comparing the heat loss for several different insulation thicknesses, several full calculations of the

heat loss in a pipeline are required for a single optimisation calculation. This naturally increases the total time consumption even further. Two methods for improving the performance of the overall calculation method can be identified. The first method is to decrease the calculation time of the heat loss calculation, which is likely to involve sacrificing the accuracy of the calculation to some degree. The second method is to decrease the number of different insulation thicknesses which need to be compared, thus decreasing the number of times a full heat loss calculation is required. The latter method involves implementing a more sophisticated optimisation method than *brute force*.

A series of test calculations was performed to compare the results of the insulation thickness optimisation, where the pipeline was calculated either as a single part, or divided into 100 parts of equal length. In the tests, the implicit form of the analytical solution, which is discussed in Section 3.1.1, was used as the numerical solution method. A series of tables equivalent to Tables B.1–B.6 from SFS 3977 was produced, as was done in Section 5.2.1, where the results were obtained with the calculation in 100 parts. For the majority of the values in the tables, the suggested optimal insulation thicknesses were the same, regardless of whether the pipeline was calculated in a single part or 100 parts. In individual cases, the suggested insulation thicknesses differed by 10 mm or 20 mm, where 10 mm was the smallest increment used in the optimisation calculations. The differences in the insulation thicknesses suggested by the calculations in 100 parts are compared to the results of the calculations in one part in Table 5.3.

Table 5.3. *Differences in the suggested insulation thickness between calculation in one part and calculation in* 100 *parts.*

Table	Diff. ± 10 mm	Diff. ± 20 mm	Total cases	Diff. %
B.1	5	0	540	0.93
B.2	19	0	540	3.52
B.3	28	0	540	5.19
B.4	31	0	540	5.74
B.5	27	0	540	5.00
B.6	33	4	540	6.85
Total	143	4	3240	4.54

This suggests that the optimisation of insulation thickness can be performed using the simpler method, with only a negligible impact on the accuracy of the results. By using the simpler method, the required calculation times are shortened drastically.

In the brute force optimisation method, the heat loss and the total annual costs are evaluated for all possible insulation thicknesses, up to 41 times, corresponding with the uninsulated case and the range of up to 400 mm insulation divided into 10 mm increments. While by no means an elegant solution method, the use of brute force provides a full

set of data, which can be used for visualisations such as Figures 5.12 and 5.13. As the calculation cases with different insulation thicknesses are independent, the time consumption of the brute force method could be improved by running the calculation cases in parallel, at least partially. However, as discussed earlier, the total cost function for this particular type of optimisation problem characteristically has only a single local minimum, which therefore is also the global minimum. Thus, for the purpose of finding the optimal insulation thickness, if discrete insulation thicknesses are calculated by increasing the insulation thickness in discrete increments, the calculation process can be stopped as soon as a total cost higher than the previous one is found. This method eliminates the unnecessary calculations of insulation thicknesses that are larger than the optimum, and works best for cases where the optimal insulation thickness is small. For large optimal insulation thicknesses, the method is less effective, as it does nothing to decrease the number of times insulation thicknesses smaller than the optimum are calculated.

One approach to decrease the number of unnecessary calculations with a nonoptimal insulation thickness is to improve the initial guess to some other value than zero, an uninsulated case, and to search for the optimum by means of *gradient descent*. A simple implementation of a gradient descent method would start by calculating the total cost for the initial guess and the adjacent values of insulation thickness. From there, the method would either increase or decrease the insulation thickness, depending on the direction in which the total cost is decreasing. Due to the characteristics of the total cost function, the gradient descent method will always find the minimum of the function, regardless of the initial guess. However, the closer to the optimum the initial guess is, the fewer iterations the method requires. The insulation thicknesses suggested by the tables of the Finnish standard SFS 3977 would perform well as initial guesses for the gradient descent method, as they are either already optimal or at least near the optimum. The number of unnecessary iterations could further be decreased by altering the step size of moving the guess depending on how steep the gradient of the cost function is. This, however, introduces the possibility of overshooting the optimum, and requires additional modifications to the implementation of the method.

5.3 Discussion

The case examples presented in Section 5.2.1 suggest that cost savings of up to 7% of the total heating and insulation costs can be achieved by optimising the insulation thickness of process industry pipelines using the calculation program described in this thesis, instead of using the insulation thicknesses suggested by standards such as the Finnish standard SFS 3977. While the calculation program is accessible through Vertex G4Plant, which is a commercial plant design software product, the cost savings made available by the use of the insulation thickness optimisation can compensate the price of acquiring the commercial software package. Regardless, the results of this thesis show that while the insulation thicknesses suggested by SFS 3977 are often close to

optimal, overall better results, tailored for each specific case and set of conditions, can be achieved by a proper evaluation of heat loss through iterative computer-aided calculations. Additionally, the use of the calculation program allows the user to customise the insulation price data, instead of relying on insulation price data from November 2005, as SFS 3977 does.

In the literature, it is typical that the methods presented for the economic optimisation of insulation thickness severely simplify the evaluation of heat loss, as can be seen in the work of Kaynakli [18]. Several works, such as those by Bahadori and Vuthaluru [1][2] and Čarnogurská et al. [6], suggest calculation methods that replace the traditional evaluation of heat transfer theory with other models, such as correlations fitted to empirical data [1][2], or more complex models such as the Buckingham π theorem [6]. Some authors, such as Genić and Jaćimović [11] argue that mathematically rigorous methods are time-consuming due to the use of iterative calculation methods. However, with modern software implementations, such as the calculation program presented in this thesis, the time consumption of the iteration process is largely negligible. The calculation program is capable of optimising the insulation thickness for a given pipeline in a matter of seconds, which does not add a significant delay to the process of optimising insulation. Any calculation method where a human user must input values to the calculation solution via a user interface will take several seconds, if not a few minutes, even before the calculation can even be begun. Thus, the calculation times of the calculation program presented in this work are negligible in any larger context.

As the calculation program evaluates fluid material properties using the CoolProp library, the calculation program supports over 100 different fluids [3]. Due to the diversity of fluids used in the process industry, the use of the library significantly improves the usability of the calculation program, as the user does not need to manually evaluate the material properties. This in turn enables the automated iterative calculation process which is used in the heat loss calculation method described in this thesis.

As discussed in Section 5.1.1, the conductive heat transfer resistance of pipe insulation typically contributes over 90% of the total heat transfer resistance of an insulated pipeline. Due to the dominant effect of insulation on the total heat transfer resistance, it would be beneficial to evaluate the thermal conductivity of the insulation material with improved accuracy, taking into account the mean temperature of the insulation material. However, as the pipe insulation typically limits the temperature change of the interior fluid considerably, it is unlikely that the mean temperature of the insulation material would change over the course of the pipeline enough to significantly alter the thermal conductivity of the insulation. Thus, the assumption of a constant thermal conductivity of the insulation material is likely to be sufficient, assuming that the thermal conductivity is initially evaluated as a function of the mean temperature of the insulation.

For uninsulated pipes, typically the most dominant mode of heat transfer, according to the results presented in Section 5.1.1, is convective heat transfer on the exterior of the pipe. The correlations for external convection used in this thesis assume that the

convection is natural and free. This assumption is valid for pipes which are surrounded by mostly still air, which is typically true for pipes indoors. However, pipes which are located outdoors may be subjected to forced external convection as the result of wind. Similarly, if a pipe indoors is subjected to strong air conditioning, the exterior convection may exhibit properties of forced convection. In these cases, the external natural convection correlations must be replaced with correlations for external forced convection, which can be found in the literature. Similarly, the external convection correlations used in this thesis assume that the pipes are horizontal. As the external convection contributes such a large portion of the total heat transfer resistance, if significant portions of the pipeline are vertical, those sections of the pipeline should be evaluated using external convection correlations for vertical pipes for improved accuracy. The findings on the significance of the different modes of heat transfer were mainly in agreement with the standard SFS 3977, where the effect of internal convection and conduction through the metal pipe wall are typically neglected [31]. However, the results presented in Section 5.1.1 showed that for fluids with low thermal conductivity, the effect of internal convection can be nearly as significant as radiative heat transfer. While the standard does suggest that the effect of internal convection is not neglected for low-pressure gases [31], the effect of internal convection was found in this work to be significant even for high-pressure cases with fluids of low thermal conductivity. Thus, for steam pipes, it would be advisable to evaluate the effect of internal convection. Across all tests, however, the effect of external convection was dominant in the total heat transfer resistance.

Although flanges, valves and other pipe equipment do contribute to the heat loss in a pipeline, their effects are neglected in the calculation method discussed in this thesis. This is a valid assumption for long pipelines, especially with insulation. For shorter pipelines and pipes with more equipment per unit length, the significance of pipe equipment on the heat loss is greater. In these circumstances, the effect of equipment can be evaluated using approximated equivalent lengths of pipe corresponding to the different types of equipment, as suggested in SFS 3977 [31]. However, unless accurate empirical data for the types and models of equipment used are available, the use of equivalent lengths to evaluate the heat loss caused by pipe equipment is a significant potential source of error.

As discussed in Section 5.1.1, the significance of internal convection in the evaluation of the total heat transfer resistance could largely be neglected, except for fluids of low thermal conductivity, such as steam. In this thesis, only pipes surrounded by air were studied. For underground pipes, where the external convective and radiative modes of heat transfer are replaced by heat conduction to the surroundings, the assumption of the negligibility of the internal heat convection should be revisited. This applies especially to underground steam pipes, due to the low thermal conductivity of the fluid. However, should the pipes be insulated, the effect of internal convection is still likely to be insignificant. For cases where a more in-depth analysis of internal convection is required, it would be advisable to include the effect of the development length of the flow, using models such as Equation (2.19). Additionally, an interpolation method capable of

handling the transition from laminar to turbulent flow can be applied, such as the method suggested by Gnielinski [13], discussed in Section 4.2.2. However, given the relative rarity of transitional flows in practical applications, such a method is likely to have limited use for the majority of users.

Similarly, for the majority of use cases, the boundary conditions for the heat loss problem of the pipeline are likely to be simple, such as the assumption of constant ambient temperature, which is used in the calculation program presented in this thesis. For pipes with discrete transitions between sections of different constant ambient temperature, such as a pipeline that exists partially indoors and partially outdoors, the heat loss of the pipeline can be evaluated with sufficient accuracy by calculating the sections separately, such that the assumption of constant ambient temperature can be applied to each section separately. However, should a situation arise where the boundary conditions are complex enough that they cannot be circumvented in a similar manner, and that an analytical solution cannot be acquired, the implicit Euler method, discussed in Section 3.1.2, should provide sufficiently accurate results, as discussed in the comparison of numerical methods in Section 5.1.1.

The comparison of numerical methods in Section 5.1.1 was performed to locate a balance between the accuracy and the performance of the heat loss evaluation. The accuracy of the methods was compared to results acquired with the implicit form of the analytical solution by dividing the pipe into 1, 10, and 100 sections. For the highest step count, all four methods gave essentially identical results even for high-temperature cases, and thus the implicit analytical solution in 100 parts was treated as a reliable base case. The main findings of the tests were that the implicit methods, both the analytical and the Eulerian, gave sufficiently accurate results for the outlet temperature at low step counts, within 1% of the base case, even for calculation with just a single section. When the step count was increased, the accuracy of the explicit methods increased significantly, due to the decreased step length. For a high-temperature case, both the explicit methods provided outlet temperatures within 1% of the base case, even at the relatively low step count of 10. Based on the findings, the implicit analytical solution with a low step count is suggested, when only the outlet temperature of the interior fluid is evaluated. For determining the location of condensation in a pipeline, the step count must be increased, and thus the explicit analytical solution becomes valid. For optimising insulation thickness, the implicit analytical solution with a low step count is suggested, as discussed in Section 5.2.2.

In many cases discussed in Section 5.1.1, the significance of radiative heat transfer resistance was comparable to the significance of external convective heat transfer. Similarly to the temperature dependence of the thermal conductivity of insulation materials, the emissivity of pipe and insulation materials depends on the temperature, as discussed in Section 2.1.3. In cases where the significance of radiative heat transfer on the total heat transfer resistance is notable, the surface emissivity should be evaluated with care, as a function of surface temperature. Once the initial value of surface emissivity is evaluated, sufficient accuracy should be achieved by using the constant value of

surface emissivity for the remainder of the calculation, unless the surface temperature significantly changes along the length of the pipe, as is possible especially for uninsulated pipes.

The insulation tables in SFS 3977 suggest a selection of discrete insulation thicknesses, with increments of up to $40\ \mathrm{mm}$ for the larger insulation thicknesses. As shown in Section 5.2.1, transitions between these discrete insulation thicknesses can lead to cases with sub-optimal insulation thicknesses, merely due to the limited selection of insulation thicknesses. While it is understandable from the point of view of a manufacturer or provider of insulation that pipe insulation products are not available in all possible variations of insulation thickness, this practise can result in economically and ecologically sub-optimal decisions in process industry pipe design. A modular way of increasing the insulation thickness per customer requirements could be beneficial in allowing for economic optimisation of insulation thickness without negatively impacting the logistics and finances of insulation manufacturers and providers.

While the outdated insulation price data from November 2005 used in SFS 3977 can be updated using indices acquired from Statistics Finland, as instructed in the standard, the non-customisable method of determining the price of insulation is detrimental to the economic optimisation of insulation thickness for individual users and cases. With the standard, the user is bound to the averaged and index-corrected prices, instead of being flexibly able to study the optimal insulation thickness with the insulation prices actually available to them. As of December 2019, Statistics Finland suggests the indices for insulation prices and the cost of work as 0.981 and 1.042 [4], respectively. Using the equation presented in SFS 3977, a total index of 1.012 can be acquired as the average of the two indices [31]. This index is used in modifying the cost of energy, guiding the selection of the proper insulation thickness table in the standard. In this work, the value of the index was essentially neglected, as the energy prices were manually selected to simplify the comparison with the tables of the standard. With the value of the index at the time of the calculations, even if the energy prices were modified with the index, the results would not be altered enough to close the gap between the insulation thicknesses suggested by SFS 3977 and the insulation thicknesses optimised using the calculation program.

6 SUMMARY AND CONCLUSION

This thesis provides an alternative method for optimising insulation thickness in process industry pipelines, enabling savings of cost and time compared to utilising insulation thickness tables presented in standards. The computer program constructed as a part of this thesis is capable of evaluating the heat loss of a pipeline based on user input and optimising the insulation thickness for the pipeline based on customisable financial parameters. By performing the heat loss calculation and insulation thickness optimisation in a computer program which can be operated through a simple user interface, the end product of this thesis saves time in the plant design process. Additionally, the optimised insulation thickness saves costs over the lifetime of the pipeline, and the process industry plant as a whole.

The potential cost savings are demonstrated through case examples, which compare the insulation thickness suggested by the Finnish standard SFS 3977 with the insulation thickness optimised using the calculation program developed as part of this thesis. In the case examples, cost savings of upwards of $2{,}000$ €, or 20 €$/\mathrm{m}$, corresponding to approximately 7% of the total insulation and heating costs, could be achieved per pipeline, over the lifetime of the pipeline. The economically optimised insulation thicknesses suggested by the calculation program were also compared on a larger scale with the insulation tables of SFS 3977. On a general level, the insulation thicknesses suggested by the two methods were in a similar range, although significant differences were also found in certain cases. Some differences between the insulation thicknesses suggested by the two methods could be explained by the standard suggesting only certain discrete insulation thicknesses with large gaps between the possible choices, whereas the calculation program suggests insulation thicknesses with a resolution of $10\ \mathrm{mm}$. While the use of the limited discrete insulation thicknesses in the standard is likely due to the common availability of the particular insulation thicknesses from insulation providers, it is still beneficial to study the optimal insulation thickness with greater precision, to help guide the process of selecting the insulation thickness.

All differences between the insulation thicknesses suggested by the calculation program and those suggested by the standard SFS 3977 could not be explained by the difference in available insulation thicknesses, however. In the comparison of the suggested insulation thicknesses, cases could be identified where the results of the calculation program would not justify the transition to a larger discrete insulation thickness suggested by the insulation tables of SFS 3977. Thus, using the calculation program would achieve

cost savings in certain cases, even if only the discrete insulation thickness options used in SFS 3977 were available.

The significance of the different modes of heat transfer was evaluated for both uninsulated and insulated pipes. For uninsulated pipes, the overwhelming majority of the total heat transfer resistance, typically between 75% and 99%, was due to the external convection and radiative heat transfer. For small pipe sizes and low temperatures, the significance of the two modes of heat transfer was nearly equal. With larger pipe sizes and higher temperatures, the rate of radiative heat transfer increased more than the rate of external convective heat transfer, corresponding with a diminished significance of radiative heat transfer resistance. Additionally for larger pipe sizes, the contribution of internal convection to the total heat transfer resistance became more significant. However, this was at least in part due to the lower flow velocity, as all the test cases had the same mass flow. For fluids with low thermal conductivity, such as steam, the effect of internal convection was also found to be more significant. For insulated pipes, the heat transfer resistance of the heat conduction through the insulation contributed upwards of 90% of the total heat transfer resistance. Thus, the evaluation of the thermal conductivity of the insulation material is a large potential source of error. It is advisable to evaluate the thermal conductivity of the insulation material as a function of its mean temperature.

The numerical methods used in evaluating the heat loss in a pipeline were compared in terms of accuracy and computational cost. An analytical solution for the heat loss was compared with a simpler Euler scheme equation, and both equations were evaluated in their explicit and implicit forms. The difference between the results of the analytical solution and the Euler scheme equation were found to be negligible when both equations were either explicit or implicit. A more significant difference was found between the explicit and implicit forms of the equations, with both implicit methods performing well even with low step counts. Thus, the implicit form of the analytical solution was chosen when only evaluating the heat loss, despite its potentially higher computational cost.

The increased calculation times of the implicit equation significantly impacted the calculation times of the optimisation of insulation thickness, where initially a brute force approach was used, evaluating the heat loss of the pipeline for several different insulation thicknesses. Thus, the step count of the implicit analytical heat loss solution was decreased when optimising insulation thickness, and the calculation program was improved so that the evaluation of insulation thickness options was stopped when the global minimum of the total cost function at the optimal insulation thickness was passed. The implementation of an improved gradient descent optimisation method is planned as part of future work. As additional potential future work, the Euler methods can be utilised if a need arises to evaluate the heat loss in pipes with more complex boundary conditions. The explicit methods studied in this work can also prove useful and time-efficient when a high calculation step count is required, for example to accurately evaluate the location of condensation in a pipeline.

To summarise, the main contributions of the thesis are:

- Providing a fast method for optimising economical insulation thickness in process industry pipelines as an alternative to using insulation tables in standards.
- Implementing the optimisation method as a computer program as part of an existing plant design software solution.
- Enabling cost and time savings compared to using standard insulation thickness tables by:
  - Minimising the investment cost of insulation and the operational costs of heat loss using numerical optimisation based on a numerical heat loss solution method, enabling savings of up to 7% in the total heating and insulation costs of a pipeline.
  - Saving time in the engineering design process by using data from the plant design software solution and by utilising fast computational methods.
- Determining the modes of heat transfer that are the most significant in the use cases of the calculation program, allowing the program to guide the user to evaluate the most important input parameters with sufficient accuracy.

REFERENCES

[1] A. Bahadori and H. B. Vuthaluru. A simple correlation for estimation of economic thickness of thermal insulation for process piping and equipment. *Applied Thermal Engineering* 30 (2010), 254–259.

[2] A. Bahadori and H. B. Vuthaluru. A simple method for the estimation of thermal insulation thickness. *Applied Energy* 87 (2010), 613–619.

[3] I. H. Bell, J. Wronski, S. Quoilin and V. Lemort. Pure and Pseudo-pure Fluid Thermophysical Property Evaluation and the Open-Source Thermophysical Property Library CoolProp. *Industrial & Engineering Chemistry Research* 53.6 (2014), 2498–2508. DOI: 10.1021/ie4033999. eprint: http://pubs.acs.org/doi/pdf/10.1021/ie4033999. URL: http://pubs.acs.org/doi/abs/10.1021/ie4033999.

[4] *Building cost index, December 2019*. Statistics Finland, 2020.

[5] J. C. Butcher. *Numerical Methods for Ordinary Differential Equations, Second Edition*. John Wiley & Sons, Ltd, 2008.

[6] M. Čarnogurská, M. Příhoda, M. Puškar, M. Fabian, R. Dobáková and M. Kubík. Measurement and mathematical modelling of heat loss in the pipe systems of a central heat distribution network. *Measurement* 94 (2016), 806–811.

[7] S. W. Churchill and H. H. S. Chu. Correlating equations for laminar and turbulent free convection from a horizontal cylinder. *International Journal of Heat and Mass Transfer* 18.9 (1975), 1049–1053.

[8] A. Daşdemir, T. Ural, M. Ertürk and A. Keçebaş. Optimal economic thickness of pipe insulation considering different pipe materials for HVAC pipe applications. *Applied Thermal Engineering* 121 (2017), 242–254.

[9] Directorate-General for Research and Innovation (European Commission). *Sustainable process industry*. Publications Office of the European Union, 2017.

[10] Energy Resources Conservation Board ERCB. *ERCB Investigation Report: MEG Energy Corp. Steam Pipeline Failure, May 5, 2007*. Energy Resources Conservation Board ERCB, 2008.

[11] S. Genić and B. Jaćimović. A Shortcut to Determine Optimal Steam Pipe Diameter. *Chemical Engineering Progress* 114.8 (2018), 22–27.

[12] V. Gnielinski. New equations for heat and mass transfer in turbulent pipe and channel flow. *International Chemical Engineering* 16 (1976), 359–368.

[13] V. Gnielinski. On heat transfer in tubes. *International Journal of Heat and Mass Transfer* 63 (2013), 134–140.

[14] V. Gnielinski, Verein Deutscher Ingenieure and VDI-Gesellschaft Verfahrenstechnik und Chemieingenieurwesen. *VDI Heat Atlas, 2nd Edition. Forced Convection*. Springer, 2010.

[15] GPSA Editorial Review Board. *Engineering Data Book, Twelfth Edition*. Gas Processing Suppliers Association, 2004.

[16] J. A. Hesketh and P. J. Walker. Effects of wetness in steam turbines. *Proceedings of the Institution of Mechanical Engineers: Journal of Mechanical Engineering Science, Part C* 219.C12 (2005), 1301–1314.

[17] S. Kabelac, D. Vortmeyer, Verein Deutscher Ingenieure and VDI-Gesellschaft Verfahrenstechnik und Chemieingenieurwesen. *VDI Heat Atlas, 2nd Edition. Radiation*. Springer, 2010.

[18] O. Kaynakli. Economic thermal insulation thickness for pipes and ducts: A review study. *Renewable and Sustainable Energy Reviews* 30 (2014), 184–194.

[19] P. K. Konakov. A new correlation for the friction factor coefficient in smooth tubes. *Berichte der Akademie der Wissenschaften der UdSSR* Band LI 51 (1946), 503–506.

[20] J. H. Lienhard IV and J. H. Lienhard V. *A Heat Transfer Textbook, 4th Edition*. Phlogiston Press, 2017.

[21] G. R. Lindfield and J. E. T. Penny. *Numerical Methods Using MATLAB, Third Edition*. Elsevier Inc., 2012.

[22] S. Lips and J. P. Meyer. Two-phase flow in inclined tubes with specific reference to condensation: A review. *International Journal of Multiphase Flow* 37 (2011), 845–859.

[23] R. P. McAfee. *Introduction to Economic Analysis*. California Institute of Technology, 2005.

[24] Mechanical Engineering and Metals Industry Standardization in Finland. *SFS-EN 10216-5 – Seamless steel tubes for pressure purposes. Technical delivery conditions. Part 5: Stainless steel tubes, 2nd edition*. Finnish Standards Association SFS, 2014.

[25] S. Milivojevic, V. D. Stevanovic and B. Maslovaric. Condensation induced water hammer: Numerical prediction. *Journal of Fluids and Structures* 50 (2014), 416–436.

[26] A. F. Mills. *Basic Heat & Mass Transfer, 2nd Edition*. Prentice Hall, Inc., 1999.

[27] P. J. Mohr, D. B. Newell and B. N. Taylor. *CODATA Recommended Values of the Fundamental Physical Constants: 2014*. National Institute of Standards and Technology, 2015.

[28] T. N. Narasimhan. Fourier's Heat Conduction Equation: History, Influence, and Connections. *Reviews of Geophysics* 37.1 (1999), 151–172.

[29] W. Nusselt. Das Grundgesetz des Wärmeübergangs. *Gesundheits-Ingenieur* 38 (1915), 477–482.

[30] T̃. Öztürk, H. Karabay and E. Bilgen. Thermo-economic optimization of hot water piping systems: A comparison study. *Energy* 31 (2006), 2094–2107.

[31] PSK Standards Association. *SFS 3977 – Insulation of pipes, vessels and equipment. Dimensioning, 6th edition*. Finnish Standards Association SFS, 2008.

[32] PSK Standards Association. *SFS 3914 – Insulation of pipes. Vessels and equipment. Covering materials and support structures, 2nd edition*. Finnish Standards Association SFS, 2016.

[33] PSK Standards Association. *SFS 3976 – Insulation of pipes, vessels and equipment. Insulating materials and elements, 6th edition*. Finnish Standards Association SFS, 2016.

[34] P. Smith. *Piping materials selection and applications*. Elsevier, 2005.

[35] P. Stephan, Verein Deutscher Ingenieure and VDI-Gesellschaft Verfahrenstechnik und Chemieingenieurwesen. *VDI Heat Atlas, 2nd Edition. Fundamentals of Heat Transfer*. Springer, 2010.

[36] A. Thess, Verein Deutscher Ingenieure and VDI-Gesellschaft Verfahrenstechnik und Chemieingenieurwesen. *VDI Heat Atlas, 2nd Edition. Free Convection*. Springer, 2010.

[37] Uni-Bell PVC Pipe Association. *Handbook of PVC pipe design and construction, Fifth edition*. Industrial Press, 2013.

[38] L. Wang, X. Yue, D. Chong, W. Chen and J. Yan. Experimental investigation on the phenomenon of steam condensation induced water hammer in a horizontal pipe. *Experimental Thermal and Fluid Science* 91 (2018), 451–458.

A SCREENSHOTS FROM THE USER INTERFACE OF AN EARLY CALCULATION PROGRAM PROTOTYPE